# The strong AJ conjecture for hyperbolic prime knots is false

RJ Acuña

**Abstract**

Let $K$ be a knot in $S^3$. The strong AJ conjecture relates two of its invariants. The first is the minimal-order annihilator $\widehat{A}$ of the $n$th colored Jones polynomial $J(n)$. The second is the two-variable $A$-polynomial of Cooper, Culler, Gillet, Long, and Shalen. The conjecture says that after specialization $\varepsilon^*(\widehat{A}) \asymp A$. Zhang gave the first family of composite-knot counterexamples. For $8_{11}$ the specialization of $\widehat{A}$ carries an extra trefoil factor $L + M^6$. We prove this by verifying Lê's $\widehat{P} = \widehat{A}$ conjecture. Zhang's corrected formulation of the AJ conjecture agrees with Lê's weak AJ conjecture, which we prove for $8_{11}$. Li, Li, and Sun have since reported counterexamples of the weak AJ conjecture among non-hyperbolic prime knots. This work was AI assisted, and parts of it have been formalized in Lean.

hexagon:2611.00686v2

## 1 Introduction

Let $K$ be a knot in $S^3$, we take it to be understood, and suppress it from the notation. Let $J\colon \mathbb{N} \to \mathbb{Q}[q^{\pm 1}]$ be its colored Jones function. Set $EJ(n) = J(n+1)$ and $QJ(n) = q^n J(n)$, so $EQ = qQE$. The annihilator left ideal $\mathrm{Ann}(J)$ becomes principal after localization to $\mathbb{Q}(q,Q)[E;\sigma]$. We use $\mathrm{Ann}(J)$ for the ideal both before and after localization. The order of an operator is its degree as a polynomial in $E$. A nonzero annihilator is minimal if it has least order. After localization, $\mathrm{Ann}(J)$ has a unique monic minimal generator; clearing its denominators gives $\widehat{A}$. The specialization map is $\varepsilon(q,E,Q) = (1,L,M^2)$.

Let $M = S^3 \setminus N(K)$, where $N(K)$ is an open tubular neighborhood of $K$.[1] Thus $\partial M \cong S^1 \times S^1$, with $\pi_1(\partial M) = \langle \lambda, \mu \rangle \cong \mathbb{Z}^2$. Write $X(M)$ for its $\mathrm{SL}_2(\mathbb{C})$-character variety. The character variety of the boundary, $X(\partial M)$, has coordinate ring $\mathbb{C}[M^{\pm 1}, L^{\pm 1}]^{\eta}$, where $\eta(M,L) = (M^{-1}, L^{-1})$. For a representation $\rho\colon \pi_1(M) \to \mathrm{SL}_2(\mathbb{C})$, the commuting matrices $\rho(\mu)$ and $\rho(\lambda)$ have a common eigenline, with eigenvalues $M, L$ [DG, §1, p. 1145]. These pairs lift the image of the restriction map $X(M) \to X(\partial M)$ to eigenvalue coordinates. Let $D \subset \mathbb{C}^2$ be the plane curve obtained by taking the Zariski closure of the image.[2] Its ideal $I(D)$ is principal, and its generator $A$ is the $A$-polynomial[3] [CCGLS, §§2.2–2.3].

For nonzero $f, g \in \mathbb{C}[M,L]$, we say that $f$ and $g$ are $M$-essentially equal, written $f \asymp g$, if $f/g \in \mathbb{C}(M)^\times$. We say that $f$ is $M$-essentially divisible by $g$ if $g$ divides $h(M)f$ for some nonzero $h(M) \in \mathbb{C}[M]$. Two algebraic subsets of $(\mathbb{C}^*)^2$ are $M$-essentially equal if they become equal after adding finitely many lines parallel to the $L$-axis. A set is $M$-essentially contained in another if it is contained after adding such lines to the latter [L, §§0.2, 3]. We write $\mathfrak{r}(f)$ for the product of the distinct irreducible factors of $f$.

**Conjecture 1** (Strong AJ [Gb, L])**.** *For every knot, $\varepsilon^*(\widehat{A}) \asymp A$.*

**Conjecture 2** (Weak AJ [L])**.** *The zero sets of $\varepsilon^*(\widehat{A})$ and $A$ are $M$-essentially equal.*

Equivalently, weak AJ asserts $\mathfrak{r}(\varepsilon^*(\widehat{A})) \asymp A$, which is Zhang's reformulation of the AJ conjecture [Z].

A framing of a knot is a continuous, nowhere-zero normal vector field along it, considered up to homotopy. We say that a framed knot in $S^3$ has zero framing if the disjoint parallel copy obtained by pushing it in the framing direction has linking number zero with the original knot. We use this framing for $K$. Put $R = \mathbb{C}[t^{\pm 1}]$,[4]

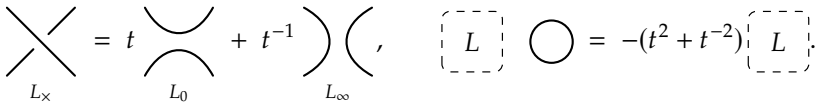
[1] We assume the reader can distinguish the meaning of letters from context. E.g. here $M$ is the 3-manifold, and an eigenvalue of $\rho(\mu)$.

[2] Points of the Zariski closure are discarded, as in [CCGLS, §§2.2–2.3].

[3] Lê denotes this polynomial by $A'_K = (L-1)A_K$ [L, §3.2]. This is a standard normalization, since $L-1$ divides $A$ for a knot in a homology sphere [CCGLS, §2.5].

[4] We use $q = t^{-4}$ throughout. Here $t$ is the Kauffman bracket parameter and $q$ is the Jones variable. Thus $t = -1$ gives $q = 1$. With this substitution, we write $\widehat{A}$ in the operators $LJ(n) = J(n+1)$ and $MJ(n) = t^{-2n}J(n)$, and the specialization in the AJ conjecture is $\varepsilon(t,L,M) = (1,L,M)$.

and for an oriented 3-manifold $M$, let the Kauffman bracket skein module $\mathcal{S}_t(M)$ be the quotient of the free $R$-module on isotopy classes of framed unoriented links by $L_\times = tL_0 + t^{-1}L_\infty$ and $L \sqcup \bigcirc = -(t^2 + t^{-2})L$. Its elements are called skeins.




$L_\times$ $L_0$ $L_\infty$

The first relation replaces a crossing by its two smoothings, with the links unchanged outside a ball. In the second, the dashed box denotes $L$, and $\bigcirc$ is a zero-framed unknot in a ball disjoint from $L$ [L, §1.1]. Every framed link in $S^3$ has a blackboard-framed diagram. Therefore $\mathcal{S}_t(S^3) = R\langle\varnothing\rangle$ by resolving its crossings and removing trivial circles [L, §1.2]. For a framed link $L$ in $S^3$, write $\langle L\rangle$ for the coefficient of $\varnothing$ in its skein class. Gluing $N(K)$ to $M$ gives the pairing $\mathcal{S}_t(N(K)) \otimes_R \mathcal{S}_t(M) \longrightarrow R$, with $\langle x, y\rangle = \langle x \cup y\rangle$ [L, §§1.2, 4.4].

The boundary skein algebra $\mathcal{S}_t(\partial M \times I)$ acts on $\mathcal{S}_t(M)$. For $a \in \mathcal{S}_t(\partial M \times I)$, put $\Theta(a) = a \cdot \varnothing$. The cyclic submodule generated by $\varnothing$ is $\mathcal{S}_t(\partial M \times I)\varnothing \cong \mathcal{S}_t(\partial M \times I)/\mathrm{Ann}(\varnothing)$ by the first isomorphism theorem for left $R$-modules. Since a boundary skein can be glued on either side, the pairing factors through the map $\mathcal{S}_t(N(K)) \otimes_{\mathcal{S}_t(\partial M\times I)} \mathcal{S}_t(M) \longrightarrow \mathcal{S}_t(S^3)$. The peripheral ideal of Frohman–Gelca–Lofaro is $\ker\Theta = \mathrm{Ann}(\varnothing)$. Following Lê, define the orthogonal ideal $\mathcal{O}$ to consist of $a \in \mathcal{S}_t(\partial M \times I)$ such that $\langle u, \Theta(a)\rangle = 0$ for every $u \in \mathcal{S}_t(N(K))$ [L, §4.4]. Their construction gives the following [FGL, §3.3].

$$\begin{array}{ccccc} \mathrm{Ann}(\varnothing) & \hookrightarrow & \mathcal{S}_t(\partial M \times I) & \xrightarrow{\Theta} & \mathcal{S}_t(M) \\ \downarrow{\scriptstyle\Phi} & & \downarrow{\scriptstyle\Phi} & & \\ \mathcal{O} & \hookrightarrow & \mathcal{T}. & & \end{array}$$

Here $\Phi$ identifies the boundary skein algebra with the invariant subalgebra $\mathcal{T}^\eta$ of the quantum torus $\mathcal{T}$. We regard $\mathcal{O}$ as a subideal of $\mathcal{T}^\eta$ via $\Phi$. Therefore peripheral relations annihilate the colored Jones function.[5]

Let $\mathrm{Ч}_n$ be the sequence of orthogonal polynomials defined by $\mathrm{Ч}_{n+1}(z) = z\mathrm{Ч}_n(z) - \mathrm{Ч}_{n-1}(z)$, with initial conditions $\mathrm{Ч}_0(z) = 1$ and $\mathrm{Ч}_1(z) = z$. For $j \geq 0$, let $K^j$ be $j$ parallel copies of $K$ in this framing, with $K^0 = \varnothing$. For a polynomial $f(z) = \sum_j a_j z^j$, its cabling is the skein $f(K) = \sum_j a_j K^j \in \mathcal{S}_t(N(K))$. For this framing, we use the normalization $J(n+1) = (-1)^n\langle \mathrm{Ч}_n(K)\rangle/[n+1]$, where $[m] = (t^{2m} - t^{-2m})/(t^2 - t^{-2})$. Thus $J_\bigcirc(n) = 1$ [L, §1.3]. Gelca proves that a nonzero peripheral relation and finitely many initial values determine the sequence [Ga].

At $t = -1$, the Kauffman bracket skein module $\mathcal{S}_{-1}(M)$ has a natural commutative algebra structure, and its quotient by the nilradical is $\mathbb{C}[X(M)]$, the coordinate ring of the character variety [B, PS]. A choice of spin structure on $M$ gives an algebra isomorphism $\mathcal{S}_1(M) \cong \mathcal{S}_{-1}(M)$ by changing the signs of framed links, so the same quotient description holds at $t = 1$ [PS, Theorem 2.2, Proposition 2.4].

The specialization diagram is

$$\begin{array}{ccc} \mathcal{S}_t(\partial M \times I) & \xrightarrow{\Theta} & \mathcal{S}_t(M) \\ \downarrow{\scriptstyle\varepsilon} & & \downarrow{\scriptstyle\varepsilon} \\ \mathbb{C}[X(\partial M)] & \xrightarrow[\theta]{} & \mathbb{C}[X(M)]. \end{array}$$

Here $\theta$ is induced by restriction of characters [L, §4.2].

The left ideal of $\mathcal{T}$ generated by $\Phi(\mathrm{Ann}(\varnothing))$ becomes principal upon localization of the coefficient ring to $\mathbb{C}(t, M)$, its unique monic minimal generator is $\widehat{P}$ [L, §4.3]. A relation that kills $\varnothing$ pairs to zero with every

[5] They kill the colored Kauffman brackets, which equal the colored Jones function after $t \mapsto it$, where $i = \sqrt{-1}$ [Ga, p. 1235].

$\mathcal{H}_n(K)$, so $\widehat{P} \in \mathrm{Ann}(J)$. Therefore $\widehat{P} = C\widehat{A}$ for some operator $C$ [L, §§4.4–4.5]. Lê defines $B$ as a generator of the extension of $\ker(\mathbb{C}[M^{\pm1}, L^{\pm1}]^{\eta} \longrightarrow \mathbb{C}[X(M)])$ to $\mathbb{C}(M)[L^{\pm1}]$ [L, §§3.3–3.4]. Lê–Tran show that $B$ is obtained from $A$ by removing its maximal factor depending only on $M$. For two-bridge knots, $B = A$ [LT, Corollary 2.3, Proposition 2.4].

**Conjecture 3** (Lê's conjecture [L, Conjecture 3])**.** *For every knot $K \subset S^3$, this pairing has trivial right kernel. If $y \in \mathcal{S}_t(M)$ satisfies $\langle x, y\rangle = 0$ for every $x \in \mathcal{S}_t(N(K))$, then $y = 0$.*

Nondegeneracy identifies the peripheral and orthogonal ideals. The latter is the invariant part of the recurrence ideal, so localization gives the following formulation, which we attribute to Lê [L, §§4.4–4.5].

**Conjecture 4.** *For every knot $K \subset S^3$, $\widehat{P} = \widehat{A}$.*

Zhang gave the first family of composite-knot counterexamples to strong AJ, while establishing weak AJ for the same family [Z].

**Theorem 1** (Zhang [Z, Theorem 1.1])**.** *Let $K = T(a,b) \# T(c,d)$, where the pairs are coprime, $|a| > b \geq 2$, $|c| > d \geq 2$, and $a, c$ have the same sign. Then Conjecture 2 holds for $K$, but repeated factors of $A$ occur in $\varepsilon^*(\widehat{A})$ precisely when $ab = cd$ and $a \neq c$.*

His proposed correction is precisely the weak AJ conjecture. We give the first prime-knot counterexample to the strong AJ conjecture.

**Theorem 2.** *The strong AJ conjecture for hyperbolic prime knots is false.*

pf. Let $K = 8_{11}$, we check $\widehat{P} = \widehat{A}$ by showing it has minimal order. The specialization satisfies $\varepsilon^*(\widehat{A}) \asymp (L + M^6)A$. ∎

The same computation disproves Lê's assertion that $\varepsilon^*(\widehat{P}) \asymp B$ for every two-bridge knot [L, Theorem 3]. We explain the gap in his proof in § 4. Since $L + M^6$ divides $A$, the factorization also proves weak AJ for $8_{11}$.

After we uploaded our initial preprint to GitHub on November 13, 2026, Li, Li, and Sun found a family of counterexamples to the weak AJ conjecture, namely marked Whitehead doubles of torus knots $T(r,s)$ with coprime parameters $2 \leq r < s$ [LLS]. Such knots are prime but not hyperbolic, so the weak AJ conjecture remains open for hyperbolic knots. Beyond disproving Conjectures 1 and 2, they find a rather peculiar and geometrically interesting result: $\pi$ times the logarithmic Mahler measure of the extra factor equals the hyperbolic volume of the Whitehead link complement.

Their work suggests that the specialization carries information about the hyperbolic pieces in the JSJ decomposition of knot complements. Recall that the Jaco–Shalen–Johannson decomposition cuts a knot exterior along a canonical minimal collection of essential tori into Seifert-fibered and atoroidal pieces [JS, J]; by geometrization, the non-Seifert pieces have finite-volume hyperbolic interiors. For the Li–Li–Sun family of Whitehead doubles, the pieces are the Seifert-fibered torus-knot exterior and the hyperbolic Whitehead link exterior.

Lê proved the strong AJ conjecture for a two-bridge knot $\mathfrak{b}(p,q)$ when its normalized $A$-polynomial is irreducible over $\mathbb{Z}$ and has $L$-degree $(p-1)/2$ [L, Theorem 1(c)]. Lê–Zhang subsequently proved it whenever the Riley polynomial is irreducible over $\mathbb{Q}$, in particular when $p$ is prime [LZ, Corollaries 1.8–1.9]. Following the work of Lê, Garoufalidis and Koutschan were aware that the recurrence could have factors with extra multiplicities, so they verified the conjecture explicitly for $7_4 = \mathfrak{b}(15,11)$ [GK, §§1.2–1.4]. Lê's theorem doesn't apply here because 15 is not prime. They developed a method to prove minimality using exterior powers. We repeatedly use the Chinese remainder theorem and interpolation to compute annihilators of the $k$th Casoratians of solutions of $\widehat{P} \in \mathrm{Ann}(J)$, thus computing the exterior powers of $\widehat{P}$. An order-$k$ right

factor of $\widehat{P}$ gives an order-one right factor of its $k$th exterior power [GK, Theorem 4.8]. We use Petkovšek's $q$-hypergeometric algorithm to find these order-one right factors [GK, §6], and the evaluation exclusion criterion to rule out most remaining orders $k$.

Besides $8_{11}$, the 2-bridge knots in the Rolfsen table through eight crossings not covered by the Lê–Zhang irreducibility criterion are $7_4$ and $7_7$ [LZ, p. 162][LM].

What usually happens in mathematical discovery is that one first guesses something might be true, and then proves it. This is what happened here. We developed an efficient algorithm to compute $J$, and used it to produce Habiro's cyclotomic coefficients $C\colon \mathbb{N} \to \mathbb{Z}[q^{\pm 1}]$. We then developed an efficient algorithm to guess $q$-holonomic recurrences, and used it to guess $\widehat{H} \in \mathrm{Ann}(C)$.[6] Once an operator and sufficiently many initial values are known, extending the sequence is computationally trivial. We used $\widehat{H}$ to extend $C$, and hence $J$, then applied the same solver to the extended $J$ to guess $\widehat{A}$. This gave candidates for all prime knots through seven crossings, $8_1, \dots, 8_9, 8_{11}, 8_{12}, 8_{13}, 9_1, 9_2, 9_4, 9_5$, and $10_1$. The observation that the AJ conjecture failed for $8_{11}$'s guessed operator led to Theorem 2.

We develop the algorithm to compute $\widehat{P}$ for 2-bridge knots. The completed peripheral calculations agree with the guessed operators for $3_1, 4_1, 5_1, 5_2, 6_1, 6_3$, and $8_{11}$. We initially thought that $8_5$ gave a counterexample to the weak AJ conjecture. Using Culler's tabulated $A$-polynomial [C], we found $\varepsilon^*(\widehat{A}) \asymp (LM^{12} - 1)A$, with $LM^{12} - 1$ not a factor of $A$. However, a surjection $\pi_1(S^3 \setminus 8_5) \twoheadrightarrow \pi_1(S^3 \setminus 3_1)$, together with its effect on the peripheral curves, shows that $LM^{12} - 1$ is a missing factor of the $A$-polynomial in Culler's table.

The knots $8_5$ and $8_{10}$ are 3-bridge knots, so Lê's basis for $\mathcal{S}_t(M)$ is not available and we cannot presently compute $\widehat{P}$. We do not compute $\widehat{P}$ for the intervening 2-bridge knots before $8_{11}$, because these computations are too expensive. For $8_{10}$, our solver detects a candidate Habiro recurrence of order 19 and $Q$-degree 35, but its reconstruction is unfinished. The $8_{11}$ operator already has order 13, $Q$-degree 144 and 457,100 nonzero monomials after clearing denominators, so we'll leave the full calculation of $\widehat{A}$ for $8_{10}$ to future mathematicians.

## 2 Computing $\widehat{P}$ for 2-bridge knots

A knot $K \subset S^3$ is **2-bridge** if there exists a smoothly embedded 2-sphere $S^2 \subset S^3$ meeting $K$ transversely in four points and dividing $S^3$ into two balls $B, B'$, each meeting $K$ in two trivial arcs. Here trivial means that each arc, together with an arc in the boundary of the ball, forms the boundary of an embedded disk. The two disks can be chosen disjoint.

The double cover of a ball branched over two trivial arcs is a solid torus. Thus the bridge decomposition lifts to a decomposition of the double cover of $S^3$ branched over $K$ into two solid tori. Identifying their boundaries gives a **lens space** $L(p, q)$, with coprime integers $p, q$ specifying this identification. These are the parameters in the notation $K = \mathfrak{b}(p, q)$. We use Lê's convention with $p > q \geq 1$ both odd [L, §5.1].

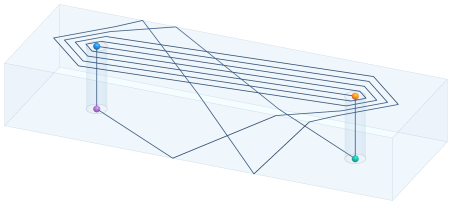


**Figure 1.** The genus 2 handlebody for $4_1$.

Place the two arcs in $B$ vertically, with endpoints $0, \infty$ and $0', \infty'$. Push the two arcs in $B'$ onto $S^2 = \partial B$, so that they join $0$ to $0'$ and $\infty$ to $\infty'$. Removing open tube neighborhoods of the vertical arcs from $B$ gives the genus 2 handlebody $H \cong \Sigma \times I$, where $\Sigma$ is a disk with two holes.

In Lê's box presentation, $B = [0, 6] \times [0, 2] \times [0, 1]$, with spatial coordinates $(x, y, z)$. The points $0 = (1, 1, 1)$ and $0' = (5, 1, 1)$ lie on the top face. The points $\infty = (1, 1, 0)$ and $\infty' = (5, 1, 0)$ lie directly below them. The

[6] $\widehat{H}$ is for Habiro. Garoufalidis and Sun call this operator the noncommutative $C$-polynomial [GS, Definition 1.2].

vertical segments are the arcs of $K$ inside $B$. Lê's construction specifies the boundary arcs from $p, q$ [L, §5.3, Proposition 5.1].

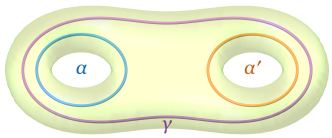



**Figure 2.** The loops $\alpha$, $\alpha'$, and $\gamma$.

For $4_1 = \mathfrak{b}(5,3)$, Figure 1 shows $H$ with the original knot retained as a reference. Its vertical segments run through the removed tubes. The remaining arcs lie on $S^2$. Let $F := \mathbb{Q}(t)$. The skein module of $H$ is $F[\alpha, \alpha', \gamma]$. The loops $\alpha, \alpha'$ surround the individual holes and $\gamma$ surrounds both. Figure 2 shows them in a middle slice $\Sigma \times \{\frac{1}{2}\}$.

To recover the knot exterior $M = S^3 \setminus N(K)$, we must attach one 2-handle to $H$. Its location is determined by the boundary arc $\overline{00'}$ of $K$. Take a narrow neighborhood of this arc in the original sphere $S^2$, including its endpoints, and call its boundary $\omega$. After the tubes have been removed, $\omega$ lies on $\partial H$. Let $D$ be a disk. The 2-handle is $D \times I$, whose side annulus $\partial D \times I$ is glued to an annular neighborhood of $\omega$. We identify $D$ with the core disk $D \times \{\frac{1}{2}\}$ and depict it as the ribbon bounded by $\omega$ in Figure 3 [L, §§5.2–5.4].

**The slide relations.** Lê uses four relative arcs, all with endpoints $P, Q'$. The points $P, Q, Q', P'$ lie on $\omega$ at $x = 3$ on the top face $z = 1$. The direction up the page in Figure 4 is the $y$-direction. We write $\overline{AB}$ for the depicted unoriented segment with endpoints $A, B$. A longer point word lists successive marked points without repeating junctions. The segment $\overline{PQ}$ follows $\omega$ around 0, and $\overline{P'Q'}$ follows $\omega$ around 0′. The other segments lie inside $H$, below the top face. The four arcs are $a_1 := \overline{PQ'}$, $a_2 := \overline{PQQ'}$, $a_3 := \overline{PP'Q'}$, and $a_4 := \overline{PQP'Q'}$. Lê chooses framing vectors normal to the boundary sphere $\partial B$ on these arcs and on the closing arcs of $\omega \subset \partial B$. We use this convention, extending the vectors over the small inward push into $H$. When joining the arcs, we match the endpoint framings and carry the resulting framing through the disk slide [L, §§5.5–5.6.2].

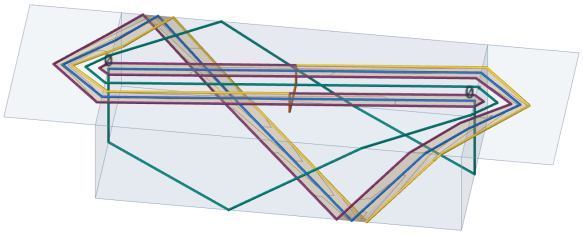


**Figure 3.** The core disk $D$ depicted as a ribbon in the trefoil box. The blue arc $\overline{00'}$ runs along its center. The left slide arc is yellow. The teal arc $\overline{0'0}$ returns through $\infty'$ and $\infty$. Juxtaposition denotes concatenation, so $\overline{00'}\,\overline{0'0} = K$.

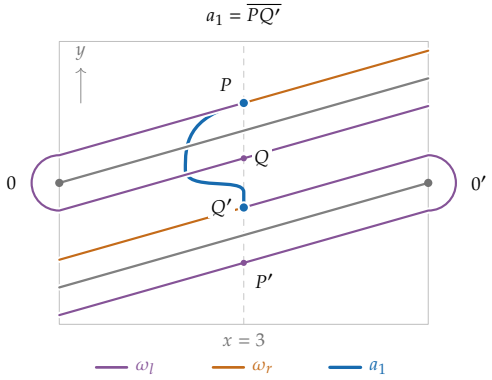



**Figure 4.** Top view of the handlebody.

We use $a_1$, shown in blue in Figure 4. Its endpoints divide $\omega$ into two arcs. Call the one passing around 0 by $\omega_l$ and the other by $\omega_r$. The visible portions of $\omega_l$ include the turns around both 0 and 0′ and are purple. The orange portions belong to $\omega_r$. They leave the strip to the right of $P$ and to the left of $Q'$. The omitted portions continue outside the strip. Closing $a_1$ along $\omega_l$ gives $\mathcal{L}_0$. Closing it along $\omega_r$ gives $\mathcal{R}_0$.

In $M$, the closing arc can move across $D$ from $\omega_l$ to $\omega_r$, while $a_1$ stays fixed. Thus $\mathcal{L}_0$ and $\mathcal{R}_0$ are isotopic as framed links in $M$, and $\langle \mathcal{R}_0 \rangle = \langle \mathcal{L}_0 \rangle$ in $\mathcal{S}_t(M)$. Their skein polynomials in $H$ can nevertheless be different. This difference is the slide relation we compute.

For $k \geq 0$, place $k$ parallel copies of $\gamma$ in a fixed interior collar, disjoint from the boundary collar in which the slide occurs. The link $\mathcal{R}_k$ is $a_1$ closed along $\omega_r$, together with these copies of $\gamma$. The link $\mathcal{L}_k$ uses $\omega_l$ and the same copies in the same positions. The same disk move shows $\langle \mathcal{R}_k \rangle = \langle \mathcal{L}_k \rangle$ in $\mathcal{S}_t(M)$. Figure 5 shows three stages of this move. The box keeps the common tangle, including the copies of $\gamma$, unchanged throughout.

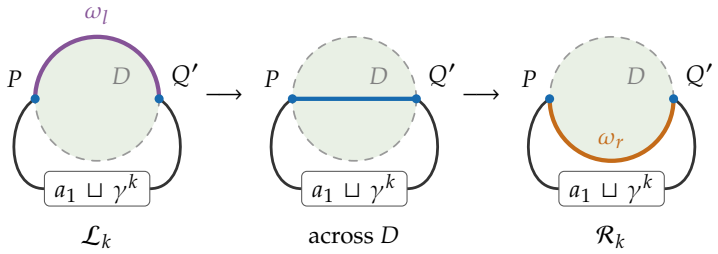



**Figure 5.** A slide across the attached disk $D$, shown in three stills. The closing arc moves from $\omega_l$ (purple) across $D$ to $\omega_r$ (orange). The boxed tangle is fixed. The first and last links are $\mathcal{L}_k$ and $\mathcal{R}_k$.

### 2.1 From diagrams to exact polynomial relations

Let $D \subset H$ be a framed link. Represent $D$ by a planar diagram on the disk with two holes. Its skein is $P = \langle D \rangle \in \mathcal{S}_t(H) = F[\alpha, \alpha', \gamma]$.

A **state** is a choice of one of the two smoothings at every crossing. This leaves disjoint simple circles. Remove each contractible circle with a factor $-t^2 - t^{-2}$, and assign $\alpha$, $\alpha'$, or $\gamma$ to each remaining circle according to which holes it surrounds.

Each smoothing contributes $t$ or $t^{-1}$. The contribution of a state is the product of its smoothing factors, circle factors, and loop variables. The **state sum** adds these contributions over all choices of smoothings. It uses only finitely many additions and multiplications of integer Laurent polynomials, so $P \in \mathbb{Z}[t^{\pm 1}][\alpha, \alpha', \gamma]$. This applies in particular to $\langle \mathcal{L}_k \rangle$ and $\langle \mathcal{R}_k \rangle$.

We compute $\langle \mathcal{L}_k \rangle$ and $\langle \mathcal{R}_k \rangle$ using the recoupling rules of Appendix A. We apply these rules to diagrams on the disk with two holes, with each local move supported in a disk disjoint from the holes. The crossing, fusion, and bubble identities are unchanged. The circle relation removes only a circle bounding such a disk, with factor $\delta = -t^2 - t^{-2}$. A circle surrounding either hole or both is an **essential loop**. It cannot be contracted to a point within the disk with two holes. Such a loop does not bound a disk in this surface, so the circle relation does not remove it.

To use the TL calculus, fill the two removed tubes back into the ball $B$ and mark their cores by fixed strands. The link remains disjoint from these strands. A circle surrounding a hole now encircles the corresponding core, so keeping the cores marked retains the obstruction to contracting that circle. This represents the handlebody diagram as an ordinary tangle with two additional strands whose endpoints remain fixed.

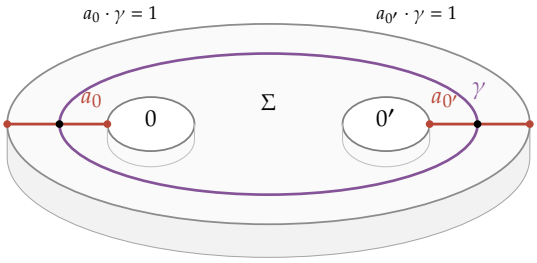



**Figure 6.** The arcs $a_0$ and $a_{0'}$ (red) in a middle slice of $H \cong \Sigma \times I$. The displayed $\gamma$-loop meets each arc once.

Write $a \cdot D$ for the unsigned intersection number of an arc $a$ with a diagram $D$ in $\Sigma$. Choose disjoint arcs $a_0, a_{0'}$ from the boundaries of holes $0, 0'$ to the outer boundary, transverse to $D$ and avoiding its crossings. Figure 6 shows an example with $a_0 \cdot \gamma = a_{0'} \cdot \gamma = 1$, but the arcs need not meet $\gamma$ only once.

**Theorem 3** (Diagrammatic degree bound)**.** *For a diagram $D$ in $\Sigma$,*

$$\deg_\gamma \langle D \rangle \le \min\{a_0 \cdot D, a_{0'} \cdot D\}.$$

*The bound also holds after setting $\alpha' = \alpha$.*

pf. Smooth crossings in disks disjoint from the arcs, so every state retains the same intersection counts. Each state circle representing $\gamma$ separates both inner boundary circles from the outer boundary and therefore meets each arc. Thus each state has at most $\min\{a_0 \cdot D, a_{0'} \cdot D\}$ $\gamma$-circles. Removing contractible circles and summing the states cannot increase this degree, nor can the substitution $\alpha' = \alpha$. ∎

Color the two fixed core strands $a$ and $b$, and choose an admissible total color $c$ for the pair. The colors let us evaluate the tangle by the fusion rules of Appendix A. Keep the auxiliary strands throughout the calculation and close only the strands belonging to the link. The resulting diagram is an endomorphism of $f_a \otimes f_b$. Its restriction to the $c$-channel is a scalar multiple of the identity.

An uncolored circle encircling a strand colored $c$ acts by $\chi_c = -\left(t^{2c+2} + t^{-2c-2}\right)$. This is the encircling identity (16), proved in Appendix A. In particular, $\chi_0 = \delta$. Therefore, the scalar computed for $D$ in the $c$-channel is $P(\chi_a, \chi_b, \chi_c)$. A loop surrounding both holes encircles their fused $c$-strand, which explains the third argument.

**Theorem 4** (Symbolic recovery)**.** *Let $P = \langle D \rangle$ be the skein of a framed link $D \subset H$. With formal color variables $x = t^{2a+2}$, $x' = t^{2b+2}$, and $y = t^{2c+2}$, the characters $\chi_a = -(x + x^{-1})$, $\chi_b = -(x' + (x')^{-1})$, and $\chi_c = -(y + y^{-1})$ are Laurent polynomials fixed by inversion. Expressing the channel evaluation in these three characters and replacing them by $\alpha$, $\alpha'$, and $\gamma$ recovers $P$ uniquely.*

pf. The state sum gives $P \in \mathbb{Z}[t^{\pm 1}][\alpha, \alpha', \gamma]$, so its channel evaluation has the stated form and all intermediate recoupling denominators cancel. Let $v(z) = z^{-1}$ denote inversion. The Laurent polynomial subring invariant under inversion is $F[z^{\pm 1}]^v = F[z + z^{-1}]$. Applying the preceding identity to each variable proves uniqueness. ∎

Put $d = (p+1)/2$. Attaching the 2-handle identifies $\alpha'$ with $\alpha$, so define

$$S_{d+k} := \left(\langle \mathcal{R}_k \rangle - \langle \mathcal{L}_k \rangle\right)\Big|_{\alpha'=\alpha} \in F[\alpha, \gamma]. \tag{1}$$

Lê proves that $\alpha' = \alpha$ and the relations $S_m = 0$, $m \ge d$, generate the kernel of $\mathcal{S}_t(H) \to \mathcal{S}_t(M)$. Moreover, $S_m$ has degree $m$ in $\gamma$ and can be written $S_m = s_m \gamma^m + \sum_{i=0}^{m-1} s_{m,i}(\alpha)\gamma^i$. Here $s_m$ is the leading coefficient and $s_{m,i}(\alpha) \in F[\alpha]$ is the coefficient of $\gamma^i$.

The fact that $s_m$ is a signed power of $t$ comes from the braid closures. Lê's box diagram represents $\mathcal{R}_k$ and $\mathcal{L}_k$ as closures of braids on $2m = (p+1) + 2k$ and $2(m-1) = (p-1) + 2k$ strands, respectively, where $m = d + k$. For a closure on $2m$ strands, exactly one state has $m$ circles surrounding both holes. This state uses the horizontal smoothing at every crossing, which keeps the strands running across the braid. Its coefficient is a product of $t$ and $t^{-1}$, and every other state has lower $\gamma$-degree.

This state sum uses the blackboard framing of the braid diagram. To apply it to $\mathcal{R}_k$ and $\mathcal{L}_k$, we compare that framing with Lê's chosen framings, whose vectors are normal to the boundary sphere $\partial B$ containing $\omega$, and which are carried through the slide. Different choices when matching the endpoint framings can introduce twists, but any difference from the braid diagram's blackboard framing is represented by curls [L, §5.6.2]. One smoothing of a curl produces a contractible circle, and the other straightens the strand. The two curl types therefore multiply the skein by $t\delta + t^{-1} = -t^3$ and $t^{-1}\delta + t = -t^{-3}$, respectively, as shown in Figure 7.

Thus any required framing correction multiplies the leading coefficient by a power of $-t^3$. It remains $\pm t^\ell$ for some integer $\ell$ [L, Lemma 1.1]. Thus $\langle \mathcal{R}_k \rangle$ has $\gamma$-degree $m$, while $\langle \mathcal{L}_k \rangle$ has $\gamma$-degree $m-1$. Subtracting the latter cannot cancel the highest term of the former. The substitution $\alpha' = \alpha$ leaves that coefficient unchanged because it contains neither puncture variable [L, §5.7]. Hence $s_m = \pm t^\ell$ is invertible, and the relation replaces $\gamma^m$ by lower powers of $\gamma$. We explain below why these relations suffice.

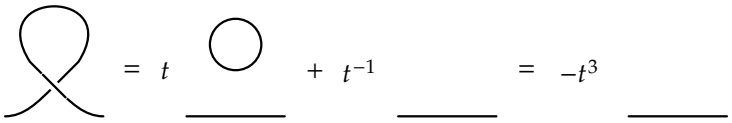



**Figure 7.** Resolving a framing curl gives $t\delta + t^{-1} = -t^3$.

The four arcs $a_1, a_2, a_3, a_4$ from $P$ to $Q'$, defined above, use neither boundary detour, the detour around 0, the detour around 0′, or both detours, respectively. The endpoint framings are normal to the boundary. Resolving crossings expresses every relative skein with these endpoints as a linear combination of the four arcs with additional closed components.

For each arc $a_i$, the two complementary arcs of $\omega$ give two closures. Lê denotes their difference by $\mathrm{sl}(a_i)$. The kernel of $\mathcal{S}_t(H) \to \mathcal{S}_t(M)$ is spanned by these differences and those formed after adding closed components to the relative tangles. These are relations of type $i$, where $i$ specifies the arc.

Lê's Lemmas 5.4–5.6 reduce these four families to the slides of $a_1$ together with $\alpha' = \alpha$. After making that substitution, the kernel is generated over $F[\alpha]$ by the slides of $a_1$ with $k$ parallel copies of $\gamma$, for $k \geq 0$. The generator with $k$ copies is $S_{d+k}$, up to sign, by (1). Setting $m = d + k$ identifies these generators with the family $S_m$, $m \geq d$, stated above.

The degree calculation above gives $\deg_\gamma S_{d+k} = d + k$, with an invertible leading coefficient. Successive reduction therefore leaves degree less than $d$. Conversely, a nonzero finite $F[\alpha]$-linear combination of these slides has degree at least $d$. The largest degree present occurs in exactly one slide and has a nonzero leading coefficient. Thus no nonzero combination of $1, \gamma, \ldots, \gamma^{d-1}$ vanishes in $\mathcal{S}_t(M)$, proving the basis theorem.

Starting with the highest power and repeating this reduction gives coordinates in $1, \gamma, \ldots, \gamma^{d-1}$. These coordinates are unique by Lê's basis theorem.

**Theorem 5** (Lê [L, Theorem 2])**.** *Let $K = \mathfrak{b}(p, q)$ be a 2-bridge knot, let $M = S^3 \setminus N(K)$ be its exterior, and put $d = (p+1)/2$. Then the skein module $\mathcal{S}_t(M)$ is free over $F[\alpha]$ with basis $1, \gamma, \ldots, \gamma^{d-1}$.*

For $m \geq d$, set $\widetilde{s}_{m,i}(\alpha) := s_{m,i}(\alpha)/s_m$. We define the **slide relations** by

$$\widetilde{S}_m := \gamma^m + \sum_{i=0}^{m-1} \widetilde{s}_{m,i}(\alpha)\gamma^i. \tag{2}$$

All coefficients still lie in $F[\alpha]$, since $s_m$ is a signed power of $t$.

**Theorem 6** (Reduction)**.** *Every polynomial $P \in F[\alpha, \gamma]$ has a unique representative $P^\sharp \in F[\alpha, \gamma]$ of $\gamma$-degree less than $d$ in $\mathcal{S}_t(M)$. There are finitely many non-zero polynomials $h_m(\alpha) \in F[\alpha]$ such that*

$$P = P^\sharp + \sum_{m \geq d} h_m(\alpha)\widetilde{S}_m \qquad \text{in } F[\alpha, \gamma]. \tag{3}$$

*The coefficients of $P^\sharp$ are the unique coordinates of the class of $P$ in Lê's basis.*

pf. If $P$ has highest term $b(\alpha)\gamma^m$ with $m \geq d$, replace $P$ by $P - b(\alpha)\widetilde{S}_m$. The highest term cancels exactly. Repeating in decreasing degree terminates at a polynomial $P^\sharp$ of $\gamma$-degree less than $d$. Collecting the subtracted terms gives (3). Each degree $m$ uses its own evaluated slide relation $\widetilde{S}_m$. The slide relations vanish in $\mathcal{S}_t(M)$, so $P$ and $P^\sharp$ represent the same element. Uniqueness follows from Theorem 5. ∎

### 2.2 Constructing the peripheral matrices

Let $\lambda \subset \partial M$ be the parallel copy of $K$ determined by its zero framing, and let $\mu$ be the meridian. We equip these curves with the framings induced by $\partial M$. The notation $\lambda + \mu$ denotes the simple boundary curve with that homology class.

We compute the actions of $\lambda$ and $\lambda + \mu$ on $\mathcal{S}_t(M)$ as matrices $U, V \in \mathrm{Mat}_d(F[\alpha])$. Their columns in Lê's basis satisfy

$$\langle \lambda + \gamma^j \rangle^\sharp = \sum_{i=0}^{d-1} U_{ij}(\alpha)\gamma^i, \qquad \langle (\lambda + \mu) + \gamma^j \rangle^\sharp = \sum_{i=0}^{d-1} V_{ij}(\alpha)\gamma^i. \tag{4}$$

The meridian alone gives $\langle \mu + \gamma^j \rangle^\sharp = \alpha\gamma^j$, so its matrix is just $\alpha I_d$. The mixed slope $\lambda + \mu$ supplies the additional information needed to separate the two longitude orientations and recover the forward action in Section 2.3.

#### 2.2.1 Left-right recombination

A **regular cut** in a Morse diagram is a slice transverse to the strands which contains no crossing, cup, or cap. Let $X$ be the ordered tensor product of the boundary projectors of a colored tangle $D\colon X \to X$, and let $W$ be the corresponding tensor product at the cut. The two halves are $L\colon X \to W$ and $R\colon W \to X$, with $D = R \circ L$.

**Theorem 7** (Left-right recombination)**.** *At a regular cut of a colored framed Morse tangle $D = R \circ L\colon X \to X$, let $i_{c,k}\colon f_c \to W$ be labelled fusion trees with $i^*_{c,k} i_{d,\ell} = \delta_{cd}\delta_{k\ell} n_{c,k} f_c$. Write $L = \sum_{c,k} i_{c,k} \circ L_{c,k}$ and $R^* = \sum_{c,k} i_{c,k} \circ R_{c,k}$, where $L_{c,k}, R_{c,k}\colon X \to f_c$.*

*For a half $A = L$ or $R$, choose fusion trees $i'_{c,\eta}\colon f_c \to W$, $\eta \in \mathbf{L}_c$, and define $C_c$ by $i_{c,k} = \sum_{\eta\in\mathbf{L}_c} (C_c)_{\eta k} i'_{c,\eta}$, using successive applications of (12). An insertion acting on coefficient $\eta$ by a scalar $v_{c,\eta}$ changes $A_c = (A_{c,k})$ to $\widetilde{A}_c = C_c^{-1}\,\mathrm{diag}(v_{c,\eta}) C_c A_c$. The modified tangle is $\widetilde{D} = \sum_{c,k} n_{c,k} \widetilde{R}^*_{c,k} \circ \widetilde{L}_{c,k}$, with the unaffected half unchanged. The sums run over admissible total colors and internal labels. Without scalar insertions, the changes of basis cancel.*

pf. The fusion resolution of $\mathbb{1}_W$ in Appendix A gives the expansions. Recoupling takes either coefficient vector to $C_c A_c$; scalar multiplication in that tree and conversion back give the stated conjugation. Substituting the modified expansions into $\widetilde{R} \circ \widetilde{L}$ and applying orthogonality gives the recombination formula, with the original norms $n_{c,k}$. ∎

For a closed link, $X = f_0$ and only $c = 0$ contributes. The coefficients are then scalars, and reflection fixes scalars in $F$, so the formula reduces to $\langle D \rangle = \sum_\ell L_{0,\ell} R_{0,\ell} n_{0,\ell}$.

Evaluate $L$ and $R^*$ by the Morse-word algorithm of Appendix A, reading the right half backwards with cups and caps interchanged. Express their outputs in the same fusion-tree basis at the cut, using recoupling when necessary.

#### 2.2.2 Algebraic insertions

Write the base longitude diagram as $R \circ L$ at a regular cut. The ribbon between $K$ and its parallel $\lambda$ lets us move the extra meridional turn to the cut. To compute both insertions from the same halves, use the cut constructed in Theorem 10.

**Theorem 8** (Algebraic meridian insertion)**.** *Use the notation and coefficient maps of Theorem 7 for $D = R \circ L$. For two adjacent strands of colors $a, b$ at the cut, let $\tau = B_{b,a} \circ B_{a,b}$ be their full twist, acting as the identity on the remaining strands.*

*Choose a fusion tree that first joins this pair, and let $C_c$ and $\mathbf{L}_c$ be as in Theorem 7. Write $e(\eta)$ for the label on the output edge of the subtree with leaves $a, b$. For $\epsilon = \pm 1$, compute $R \circ \tau^\epsilon \circ L$ by Theorem 7 with $A = L$ and $v_{c,\eta} = (R^{ab}_{e(\eta)} R^{ba}_{e(\eta)})^\epsilon$. For the extra meridional turn, the pair has colors $a, 1$ and $\epsilon$ is fixed by the crossing convention.*

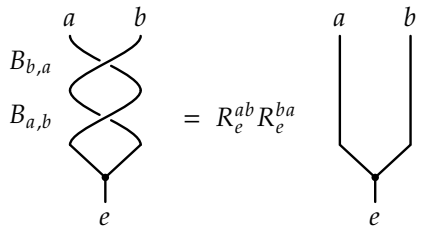



**Figure 8.** The full twist $\tau = B_{b,a} \circ B_{a,b}$ on the fusion tree $i_{e,a,b}$, read from bottom to top.

pf. The ribbon between $K$ and its parallel $\lambda$ moves the meridional turn to the cut as a full twist of the paired strands. On $i'_{c,\eta}$ the two crossings contribute $R^{ab}_{e(\eta)}$ and $R^{ba}_{e(\eta)}$, whose values are given in Appendix A, (15). The inverse twist contributes the reciprocal of their product. ∎

We can prescribe geometrically the placement of loops in $S^3$ within a given linking configuration with our knot, link, or tangle. We may then need to evaluate the resulting skeins under the pairing, including pairings of their cablings. The following theorem provides a way to compute these loop insertions algebraically.

**Theorem 9** (Algebraic $\gamma^j$ insertion)**.** *Use the notation and coefficient maps of Theorem 7 for $D = R \circ L$. Suppose the strands piercing the disk bounded by $\gamma$ form a consecutive block at the regular cut. Write $a_1, \dots, a_m$ for their colors in order.*

*Choose a fusion tree that fuses these strands before joining them to the remaining strands, and let $C_c$ and $\mathbf{L}_c$ be as in Theorem 7. For $\ell \in \mathbf{L}_c$, define $e(\ell)$ to be the label on the output edge of the subtree with leaves $a_1, \dots, a_m$.*

*For $j$ parallel copies of $\gamma$ on the right, compute $D + \gamma^j$ by Theorem 7 with $A = R$ and $v_{c,\eta} = \chi^j_{e(\eta)}$.*

pf. Draw the successive fusions of the enclosed strands inside the disk bounded by $\gamma$. Moving its boundary past these fusion vertices leaves a loop around the outgoing cable $f_{e(\eta)}$. The encircling identity (16) multiplies the coefficient in row $\eta$ by $\chi_{e(\eta)}$ for each copy, giving $\chi^j_{e(\eta)} = \left[-(t^{2e(\eta)+2} + t^{-2e(\eta)-2})\right]^j$ for $j$ copies. ∎

From Theorem 9 it is not clear that such a Morse word exists for a given diagram. However, in the case of 2-bridge knots, Lê's box presentation gives us a clear-cut way to find one.

**Theorem 10** (An insertion cut in Lê's box)**.** *For the longitude and for each of the two slide closures in Lê's box, a side projection admits a regular cut satisfying the geometric hypothesis of Theorem 9 for the given loop $\gamma$.*

pf. Use the horizontal slice through $\gamma$ and view the box along the $x$-axis. The puncture strands, and their nearby parallel copies in the longitude diagram, meet this slice inside the disk bounded by $\gamma$ near $y = 1$. The other intersections lie on the side faces $y = 0, 2$. For the slide closures, the attaching arc follows these side faces, and the common closing arc lies above the slice. Thus the enclosed intersections are separated from the others by a gap on each side in the projection.

Rotate the view slightly about the $z$-axis. The horizontal coordinate becomes $y \cos\theta + x \sin\theta$. A sufficiently small generic $\theta$ separates the finitely many cut points while preserving both gaps. The enclosed strands therefore form a consecutive block. Choose a nearby regular height within which the strands remain disjoint and have the same projected order, and move $\gamma$ to that height with its disk framing. Sweeping the resulting diagram gives the required colored Morse word and cut. ∎

Fix puncture color $a$ and total color $c$, as in Section 2.1, and put $\iota = i_{c,a,a}$. Define scalars $L_\ell, R_\ell \in F$ by $L_{c,\ell} \circ \iota = L_\ell f_c$ and $R_{c,\ell} \circ \iota = R_\ell f_c$. Write $n_\ell = n_{c,\ell}$. The channel inclusion has norm $\iota^* \iota = \nu_{a,c} f_c$, where $\nu_{a,c} = \theta(a, a, c)/\Delta_c$. For the base diagram $D = R \circ L$, insertion and left–right recombination give

$$\langle D + \gamma^j \rangle(\chi_a, \chi_c) = \frac{1}{\nu_{a,c}} \sum_k n_k L_k \sum_{\eta,\ell} (C_c^{-1})_{k\eta} \chi^j_{e(\eta)} (C_c)_{\eta\ell} R_\ell .$$

Let $P_j^{\lambda}(\alpha,\gamma)$ and $P_j^{\lambda+\mu}(\alpha,\gamma)$ be the skeins of $\lambda+\gamma^j$ and $(\lambda+\mu)+\gamma^j$, respectively, in the diagram's framing, after setting $\alpha'=\alpha$. Write $L=(L_k)$ and $R=(R_k)$ in the basis at the cut. For multiple insertions on nested or disjoint blocks, we can use a common fusion tree. Here choose the tree that first fuses the meridional pair of colors $a,1$ and then the block enclosed by $\gamma$. Let $C_c$ be the change-of-basis matrix of Theorem 7 from the basis at the cut to this tree, at fixed total color $c$. Write $e_\mu(\eta)$ and $e_\gamma(\eta)$ for the output colors of the pair and the block, respectively. The corresponding diagonal matrices are $D_\gamma=\operatorname{diag}(\chi_{e_\gamma(\eta)})$ and $D_\mu=\operatorname{diag}(R^{a1}_{e_\mu(\eta)}R^{1a}_{e_\mu(\eta)})$. Applying Theorems 8 and 9 and recombining in the basis at the cut gives

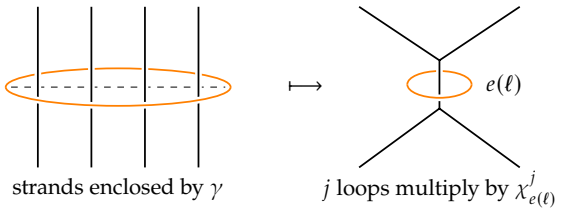



**Figure 9.** The algebraic basis insertion. Fuse the strands enclosed by $\gamma$ once, then obtain every power of $\gamma$ by scalar multiplication on the right-half coefficients.

$$\big(P_j^{\lambda}(\chi_a,\chi_c),P_j^{\lambda+\mu}(\chi_a,\chi_c)\big)=\frac{1}{\nu_{a,c}}\sum_k n_k\big(C_c^{-1}D_\gamma^jC_cR\big)_k\Big(L_k,\big(C_c^{-1}D_\mu^{\epsilon}C_cL\big)_k\Big). \tag{5}$$

**Theorem 11** (Peripheral matrix construction)**.** *The following finite procedure computes $U,V$.*

0. *Let $N:=\max_{0\le j<d}\{\deg_\gamma\langle\lambda+\gamma^j\rangle,\deg_\gamma\langle(\lambda+\mu)+\gamma^j\rangle\}$.*
1. *If $N\ge d$, apply the algebraic $\gamma^j$ insertion, left-right recombination, and symbolic recovery theorems to compute $\langle\mathcal{L}_k\rangle,\langle\mathcal{R}_k\rangle$ for $0\le k\le N-d$, evaluating each half of the base closures $\mathcal{L}_0,\mathcal{R}_0$ once. Normalize their differences to obtain $\widetilde{S}_d,\dots,\widetilde{S}_N$.*

1′. *Apply the algebraic meridian insertion, algebraic $\gamma^j$ insertion, left-right recombination, and symbolic recovery theorems to compute $\langle\lambda+\gamma^j\rangle$ and $\langle(\lambda+\mu)+\gamma^j\rangle$ for $0\le j<d$, evaluating the longitude halves $L,R$ once.*

2. *Correct to the boundary surface framing and apply the reduction theorem using the slides from step 1. The coefficient vectors of $\langle\lambda+\gamma^j\rangle^\sharp$ and $\langle(\lambda+\mu)+\gamma^j\rangle^\sharp$ in $1,\gamma,\dots,\gamma^{d-1}$ give column $j$ of $U$ and $V$, respectively.*

pf. Theorem 3 gives an a priori upper bound for $N$. Each monic slide subtraction lowers the degree, so the slides computed in step 1 suffice. Theorems 8, 9, 7, and 4 give the polynomials in steps 1 and 1′.[7] Using the same color on both punctures specializes $\alpha'=\alpha$. Framing corrections are scalar units and commute with reduction. Theorem 6 therefore identifies the coefficient vectors in step 2 with the unique coordinates in Lê's basis. ∎

### 2.3 From the peripheral action to a Jones recurrence

Garoufalidis–Lê prove that the colored Jones function is $q$-holonomic, so it satisfies a nonzero linear recurrence in a $q$-Weyl algebra [GLa, Theorem 1]. Let $\mathbb{K}=\mathbb{Q}(t,M)$ and form the $q$-Weyl algebra $\mathbb{K}\big[L\,\big|\,\sigma\big\rangle$, with $\sigma(a(t,M))=a(t,t^{-2}M)$. On functions $f:\mathbb{N}\to\mathbb{Q}(t)$, the generators act by $Lf(n)=f(n+1)$ and $Mf(n)=t^{-2n}f(n)$, and satisfy $ML=t^2LM$. Here $a\in\mathbb{K}$ acts on a coordinate column $v=(v_1,\dots,v_d)^T$ by scalar multiplication $av=(av_1,\dots,av_d)^T$. The Ore rule $La=\sigma(a)L$ means $L(av)=\sigma(a)L(v)$. We apply $\sigma$ entrywise to columns and matrices, so $\sigma(v)=(\sigma(v_1),\dots,\sigma(v_d))^T$.[8]

Lê's construction uses the pairing $\mathcal{S}_t(N(K))\otimes_F\mathcal{S}_t(M)\longrightarrow\mathcal{S}_t(S^3)$, $(\alpha,\beta)\longmapsto\langle\alpha,\beta\rangle$, and the boundary map $\Theta(\beta)=\beta\cdot\varnothing$. The peripheral ideal is $\mathcal{P}=\ker\Theta$, and the orthogonal ideal is

$$\mathcal{O}=\{\beta\in\mathcal{S}_t(\partial M\times I):\langle\alpha,\Theta(\beta)\rangle=0\text{ for every }\alpha\in\mathcal{S}_t(N(K))\}.$$

[7] Steps 1 and 1′ are labeled this way because they can be run concurrently.
[8] See Appendix B for Ore algebras, their $q$-Weyl subcategory, and the action of localized coefficients on sequence classes.

The Frohman–Gelca identification realizes the boundary algebra as $\mathcal{T}^\eta$ in the quantum torus $\mathcal{T}$, where $\eta(M,L)=(M^{-1},L^{-1})$ [FG, Theorem 2]. Lê found that $\mathcal{O}=\mathrm{Ann}(J)\cap\mathcal{T}^\eta$. Therefore its elements give recurrence relations for the Jones function because we have the inclusions $\mathrm{Ann}(\varnothing)\subseteq\mathcal{O}\subseteq\mathrm{Ann}(J)$ [L, §4.4].[9]

The puncture strands are cut strands of $K$, so the circle $\alpha$ around a puncture is the meridian skein. On a strand colored $n-1$, the encircling identity (16) gives $\chi_{n-1}=-(t^{2n}+t^{-2n})$. Thus the meridian eigenvalue $M=t^{-2n}$ identifies $\alpha=-(M+M^{-1})$. Substitute this in the computed matrices and keep the names $U,V$.

Write $J'(n)=[n]J(n)$ for the unreduced Jones function. On $J'$, the boundary curves act as [BS, Theorem 2.11, Corollary 5.3 and Lemma 5.6]

$$\mu=-(M+M^{-1}),\qquad \lambda=-(L+L^{-1}),\qquad \lambda+\mu=t^{-1}(ML+M^{-1}L^{-1}). \tag{6}$$

Solving equations (6) in our basis gives the coefficient matrices of the action on $J'$,

$$\vec{L}=(M-M^{-1})^{-1}\big(tV+M^{-1}U\big),\qquad \overleftarrow{L}=\vec{L}^{-1}=-U-\vec{L}. \tag{7}$$

Writing the exterior skein first, the raw skein pairing satisfies the identities below [L, §1.3][BS, Lemma 5.7].

$$\langle\varnothing,\Psi_{n-1}(K)\rangle=(-1)^{n-1}J'(n),\quad\text{and}\quad\langle\vec{L}\varnothing,\Psi_{n-1}(K)\rangle=-\langle\varnothing,\Psi_n(K)\rangle=(-1)^{n-1}J'(n+1).$$

Since $J'(n)=[n]J(n)$, dividing the first pairing by $(-1)^{n-1}[n]$ gives $J(n)$. Dividing the second by the same factor gives $[n+1]/[n]$ times $J(n+1)$, where $[n+1]/[n]=(t^{-2}M-t^2M^{-1})/(M-M^{-1})$.

Reflecting a bracket diagram replaces $t$ by $t^{-1}$ and hence $M$ by $M^{-1}$. We write $\rho(t,M)=(t^{-1},M^{-1})$ for this change, with pullback $\rho^*(a(t,M))=a(t^{-1},M^{-1})$. Applying $\rho^*$ entrywise to the computed matrix and to the coefficients of the pairing expresses the action in the handedness of $J$. If no reflection is needed, $\rho=\mathrm{id}$. Since $\rho^*$ commutes with $\sigma$ and fixes $[n]/[n+1]$, the action formula uses $\rho^*(\vec{L})$ with the same shift and normalization factor.

We use $L$ for the normalized action and $\vec{L},\overleftarrow{L}$ for the coefficient matrices of the forward and backward actions on $J'$. The action on coordinate vectors is therefore

$$L(v)=\frac{[n]}{[n+1]}\,\rho^*(\vec{L})\sigma(v). \tag{8}$$

**Theorem 13** (Peripheral relation)**.** *Let $K=\mathfrak{b}(p,q)$ be a 2-bridge knot with exterior $M$, put $d=(p+1)/2$, and let $1,\gamma,\dots,\gamma^{d-1}$ be Lê's $F[\alpha]$-basis of $\mathcal{S}_t(M)$ from Theorem 5. After extending coefficients to $\mathbb{K}$, let $v_0=(1,0,\dots,0)^T$ be the coordinate vector of $\varnothing$ and put $v_j=L^jv_0$, with $L$ acting by (8). For the first polynomial dependence $\sum_{j=0}^h a_j(t,M)v_j=0$, with $a_j\in F[M]$ and $a_h\neq0$, define $\widehat{P}:=\sum_{j=0}^h a_j(t,M)L^j$, where $h\le d$. Then the monic normalization of $\widehat{P}$ is the unique monic generator of* $\mathrm{Ann}(\varnothing)$ *after localization, and thus $\widehat{P}$ annihilates the colored Jones function $J$ of $K$.*

pf. Extending scalars by $\alpha=-(M+M^{-1})$ preserves Lê's basis, so the localized skein module has dimension $d$ over $\mathbb{K}$ [L, Proposition 6.1]. Hence a dependence occurs by $j=d$, and clearing its coefficient denominators gives a polynomial dependence. Let $\widehat{F}=\sum_{j=0}^h a_j(t,M)L^j$ be the operator from the first such dependence. Then $\widehat{F}v_0=0$. Garoufalidis's coefficient localization is a principal left ideal domain [Gb, §2.2]. Thus $\mathrm{Ann}(\varnothing)$ in $\mathbb{K}\big\langle L\,\big|\,\sigma\big\rangle$ has a generator. Its $L$-degree cannot be smaller than $h$, since clearing its denominators would then give an earlier polynomial dependence. As it divides $\widehat{F}$ on the right, its degree is exactly $h$. Consequently $\widehat{F}$ differs from that generator by a nonzero element of $\mathbb{K}$. We take $\widehat{P}=\widehat{F}$.

Fix $n\ge1$ and pair the polynomial dependence with the colored core. The normalized pairing sends $v_0$, representing $\varnothing$, to $J(n)$. By (8), applying $L$ to the vector advances the paired sequence by one index [BS,

[9] For simplicity, with the notation of the introduction $\mathrm{Ann}(\varnothing)$ will denote $\Phi(\mathrm{Ann}(\varnothing))$.

Corollary 5.3 and Lemma 5.6]. Thus $v_j = L^j v_0$ gives $J(n+j)$. Multiplication by $a_j(t, M)$ gives multiplication by $a_j(t, t^{-2n})$, so $a_j v_j$ gives $a_j(t, t^{-2n})J(n+j)$. The coefficient is evaluated at $n$ because in $a_j L^j$ the shift acts first and the multiplication acts afterwards. The polynomial relation $\sum_{j=0}^{h} a_j(t, M)v_j = 0$ pairs to zero by linearity. Therefore $(\widehat{P}J)(n) = 0$. ∎

### 2.4 The trefoil knot

For the trefoil, $d = 2$ and Lê's basis is $1, \gamma$. Figure 10 shows the meridional turn and the inserted copy of $\gamma$ in Lê's box, followed by the planar diagram. The black trefoil determines the tangle we evaluate.

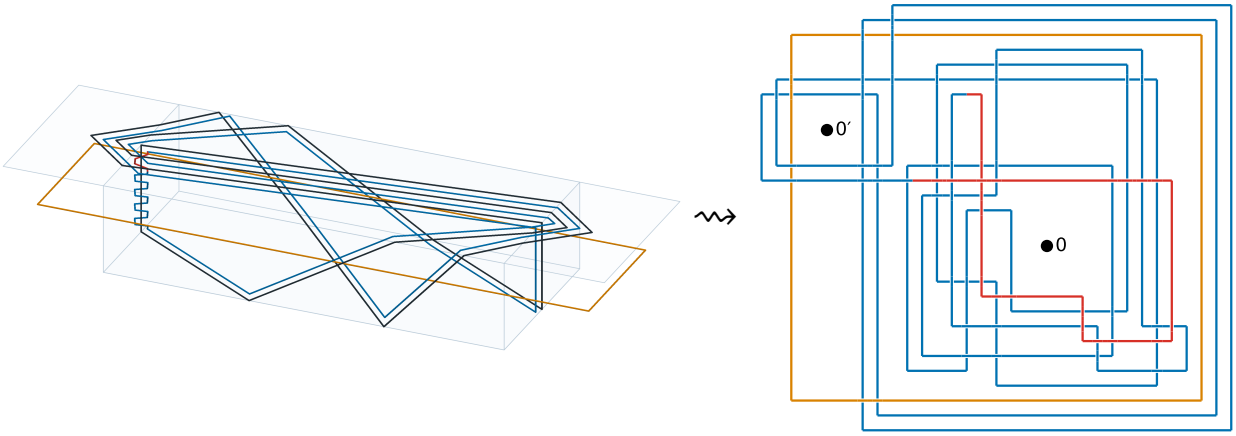



**Figure 10.** Lê's box presentation on the left determines a knot projection in the twice punctured disk on the right. Here we show $(\lambda + \mu) + \gamma$.

The inputs $\lambda$, $\lambda + \gamma$, $\lambda + \mu$, and $(\lambda + \mu) + \gamma$ give the two columns of $U$ and $V$, respectively. All four columns are computed from the tangle diagram for $\lambda$ using the algebraic insertions of Section 2.2.2.

To find their reduced versions we need to compute the slide relations. Theorem 3 bounds the required degrees before reduction. In the planar coordinates of the box, take the cut from $0' = (5, 1)$ to $(5 - 2/137, -1)$. It meets each of the diagrams for $\lambda$ and $\lambda + \mu$ twice. Each inserted $\gamma$ meets this cut once more. Consequently

$$\deg_\gamma P_j^{\lambda} \le 2 + j, \qquad \deg_\gamma P_j^{\lambda+\mu} \le 2 + j \quad (j = 0, 1).$$

Thus $\widetilde{S}_2$ suffices for the first column. For the second column we also compute $\widetilde{S}_3$, reducing first in degree 3 and then in degree 2. The required closure pairs are precisely $\mathcal{L}_0, \mathcal{R}_0$ and $\mathcal{L}_1, \mathcal{R}_1$.

The two smoothings of $\mathcal{L}_0$ give $\langle \mathcal{L}_0 \rangle = t\gamma + t^{-1}\alpha\alpha'$.

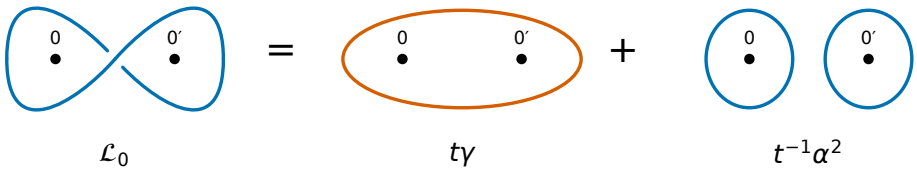



**Figure 11.** The two smoothings of $\mathcal{L}_0$, with punctures $0, 0'$. After $\alpha' = \alpha$, their contributions are $t\gamma$ and $t^{-1}\alpha^2$.

View the box from the side and rotate the view about the $z$-axis through $\arctan(1/4)$, keeping the inserted $\gamma$ at $z = 1/2$. Its disk contains the puncture points $(1, 1)$ and $(5, 1)$. The other two intersections lie near the faces $y = 0, 2$, outside the rectangle. The side-view construction of Theorem 10 gives the cut colors $(1, a, a, 1)$,

with the middle pair precisely the block enclosed by $\gamma$. We apply relative Reidemeister moves separately to the two halves, fixing every ordered endpoint at the cut and at the exterior boundary, and preserving the strand colors. Types II and III preserve the blackboard framing, while type I corrections are recorded using Figure 7. The half lengths decrease from $3,8$ to $3,3$. The left half has no framing change, and restoring the right half's framing contributes $-t^{-3}$. We include this scalar in the right accumulator. The moving component winds once around each puncture, with opposite signs. Each winding requires at least two mixed crossings, and the closed component requires a cup and a cap. Thus six letters are necessary, and the resulting words attain this bound:

$$L(\mathcal{L}_0) = \boxed{a_1^2}\,\overset{2}{\underset{3}{(}}\boxed{\begin{smallmatrix} a_1 & 1 \\ a_4 & 2 \end{smallmatrix}}\,\overset{1}{\underset{2}{\times}}\,\boxed{\begin{smallmatrix} a_2 & 3 \\ a_4 & 4 \end{smallmatrix}}\,\overset{3}{\underset{4}{\times}}\,\boxed{a_2^2}, \qquad R(\mathcal{L}_0) = \boxed{a_2^2}\,\overset{1}{\underset{2}{\times}}\,\boxed{\begin{smallmatrix} a_1 & 2 \\ a_3 & 3 \end{smallmatrix}}\,\overset{2}{\underset{3}{\times}}\,\boxed{a_1^2}\,\overset{3}{\underset{4}{)}}\,\boxed{a_1^2}.$$

Start with $\mathbf{a}_0 = (a, a)$, so both punctures have color $a$ and $\alpha' = \alpha$, as in Section 2.2.2. Admissibility of $(a, a, c)$ requires $0 \le c \le 2a$ and $2a + c \in 2\mathbb{Z}$, so $c$ is even. Write $c = 2b$ and put $u = t^a$ and $v = t^b$. We work in the interior admissible range $2 \le c \le 2a - 2$. The input set is $\mathbf{L}_0 = \{(c)\}$ and $v_0 = (1)$.

The first letter is $\overset{2}{\underset{3}{(}}$, giving $\mathbf{a}_1 = (a, 1, 1, a)$. Label the successive internal edges of its left-associated fusion tree by $s_1, s_2, c$. Thus

$$\mathbf{L}_1 = \left\{ (s_1, s_2, c) \in \mathbb{N}^3 \;\middle|\; \begin{array}{l} (a, 1, s_1),\ (s_1, 1, s_2),\ (s_2, a, c) \\ \text{and } (a, a, c) \text{ are admissible} \end{array} \right\}.$$

We take the colors to be symbolic and sufficiently large within the admissible region, with $c$ and $2a - c$ sufficiently large as well. For this step it suffices that $a \ge 2$ and $2 \le c \le 2a - 2$. The joint admissibility system is

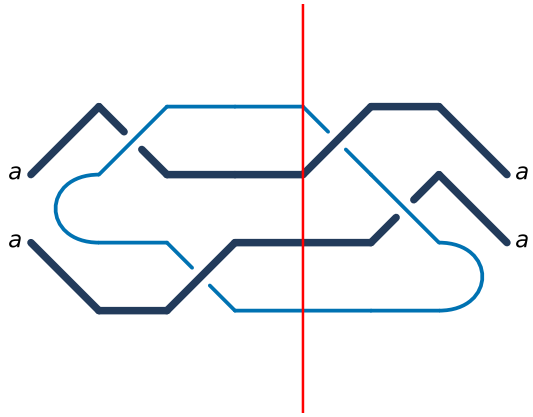



**Figure 12.** The red line marks the regular cut. The portion to its left is $L(\mathcal{L}_0)$, and the portion to its right is $R(\mathcal{L}_0)$.

$$\begin{aligned} |a-1| \le s_1 \le a+1, &\qquad a+1+s_1 \equiv 0 \pmod 2, \\ |s_1-1| \le s_2 \le s_1+1, &\qquad s_1+1+s_2 \equiv 0 \pmod 2, \\ |a-c| \le s_2 \le a+c, &\qquad a+c+s_2 \equiv 0 \pmod 2, \\ 0 \le c \le 2a, &\qquad 2a+c \equiv 0 \pmod 2. \end{aligned}$$

The first interval contains $a-1, a, a+1$, and parity excludes $a$. Thus $s_1 = a-1$ or $s_1 = a+1$. The second interval contains $s_1 - 1, s_1, s_1 + 1$, and parity excludes $s_1$. The four resulting pairs satisfy the third and fourth rows under our assumptions. Therefore

$$\mathbf{L}_1 = \{(a-1, a-2, c),\ (a-1, a, c),\ (a+1, a, c),\ (a+1, a+2, c)\}.$$

There is one input labeling $m = (c)$, so we compute the four entries $V_1(\ell, (c))$, in the order just displayed for $\mathbf{L}_1$. The inserted pair has joining color 0. Fusing this pair with the first strand of color $a$ gives the internal edge whose possible labels in $\mathbf{L}_1$ are $a-2, a, a+2$. The triple $(a, 0, a)$ is admissible. The row $(a-1, a-2, c)$ would require $(a, 0, a-2)$, which fails $a \le a-2$. The row $(a+1, a+2, c)$ would require $(a, 0, a+2)$, which fails $a+2 \le a$. The fusion rules therefore assign zero to both entries, giving

$$V_1((a-1, a-2, c), (c)) = 0, \qquad V_1((a+1, a+2, c), (c)) = 0.$$

For the two remaining rows, the cup gives the tree $(a,(1,1)_0)_a$, whereas our coordinate tree is $((a,1)_{a\pm1},1)_a$. The final strand of color $a$ and the root $c$ are unchanged. Reading this local picture from right to left, (12) has boundary colors $(1,1,a)$, total color $a$, initial channel 0, and new channel $a-1$ or $a+1$. Thus

$$V_1((a\pm1,a,c),(c)) = \begin{Bmatrix} 1 & 1 & a\pm1 \\ a & a & 0 \end{Bmatrix} = \frac{\Delta_{a\pm1}\left\langle \begin{matrix} 1 & 1 & 0 \\ a & a & a\pm1 \end{matrix} \right\rangle}{\theta(1,a,a\pm1)^2}.$$

For the channel $a-1$, the four lower bounds in the tetrahedron sum (14) are $(1,a,a,a)$ and the three upper bounds are $(a+1,a,a)$. Only the summation index $a$ remains. For the channel $a+1$, the bounds are $(1,a+1,a,a+1)$ and $(a+1,a+1,a+1)$, so only the index $a+1$ remains. Cancelling the quantum factorials gives

$$\left\langle \begin{matrix} 1 & 1 & 0 \\ a & a & a-1 \end{matrix} \right\rangle = \frac{1}{[a]}(-1)^a[a][a+1] = (-1)^a[a+1],$$

$$\left\langle \begin{matrix} 1 & 1 & 0 \\ a & a & a+1 \end{matrix} \right\rangle = \frac{1}{[a+1]}(-1)^{a+1}[a+1][a+2] = (-1)^{a+1}[a+2].$$

The theta formula similarly gives $\theta(1,a,a-1) = (-1)^a[a+1]$ and $\theta(1,a,a+1) = (-1)^{a+1}[a+2]$. Using $\Delta_{a-1} = (-1)^{a-1}[a]$ and $\Delta_{a+1} = (-1)^{a+1}[a+2]$, the two entries are therefore

$$V_1((a-1,a,c),(c)) = \frac{(-1)^{a-1}[a](-1)^a[a+1]}{[a+1]^2} = -\frac{[a]}{[a+1]} = -\frac{t^2(u^4-1)}{t^4u^4-1},$$

$$V_1((a+1,a,c),(c)) = \frac{(-1)^{a+1}[a+2](-1)^{a+1}[a+2]}{[a+2]^2} = 1.$$

In the displayed order of $\mathbf{L}_1$, $v_1^T = (V_1v_0)^T = \left(0,-\frac{t^2(u^4-1)}{t^4u^4-1},1,0\right)$.

The second letter is $\overset{1}{2}\!\times\!\overset{1}{2}$, giving $\mathbf{a}_2 = (1,a,1,a)$. Exchanging the first two boundary colors leaves the admissibility conditions unchanged. Hence $\mathbf{L}_2 = \mathbf{L}_1$, and the crossed strands are already fused together in the chosen tree, so no change of tree is needed. The undercrossing uses the reciprocals of the crossing coefficients in (15), therefore we have $(R^{a,1}_{a-1})^{-1} = -t^2u$ and $(R^{a,1}_{a+1})^{-1} = u^{-1}$. With rows in the displayed order of $\mathbf{L}_2$ and columns in the same order of $\mathbf{L}_1$, $V_2 = \operatorname{diag}(-t^2u,-t^2u,u^{-1},u^{-1})$. The third letter is $\overset{3}{4}\!\times\!\overset{3}{4}$, giving $\mathbf{a}_3 = (1,a,a,1)$. Its admissible labelings satisfy $(1,a,s_1)$, $(s_1,a,s_2)$, $(s_2,1,c)$ and $(a,a,c)$. The first and third conditions give $s_1 = a\pm1$ and $s_2 = c\pm1$, and all four combinations satisfy the remaining conditions in our range. Thus

$$\mathbf{L}_3 = \{(a-1,c-1,c),(a-1,c+1,c),(a+1,c-1,c),(a+1,c+1,c)\}.$$

For this crossing, recouple the last pair, apply the inverse crossing coefficient, and recouple back, as in Theorem 17. With columns in the order of $\mathbf{L}_2$ and rows in the order of $\mathbf{L}_3$, the evaluated transition matrix is

$$V_3 = \begin{pmatrix} \frac{t^4v^4-1}{u\left(t^4v^8-1\right)} & \frac{u\left(v^4-1\right)\left(t^4u^4v^4-1\right)}{v^2\left(u^4-1\right)\left(t^4v^8-1\right)} & 0 & 0 \\ \frac{t^2v^2}{u} & \frac{t^2u\left(-u^4+v^4\right)}{u^4-1} & 0 & 0 \\ 0 & 0 & \frac{v^4-1}{u\left(t^4v^8-1\right)} & \frac{t^2u\left(t^4v^4-1\right)\left(t^8u^4v^4-1\right)}{v^2\left(t^4v^8-1\right)\left(t^8u^4-1\right)} \\ 0 & 0 & \frac{v^2}{u} & \frac{t^6u\left(-t^4u^4+v^4\right)}{t^8u^4-1} \end{pmatrix}.$$

Applying $V_3V_2v_1$ gives the left accumulator

$$v_3(L(\mathcal{L}_0))^T = \left(\frac{t^4u^2\left(v^4-1\right)\left(t^4u^4v^4-1\right)}{v^2\left(t^4u^4-1\right)\left(t^4v^8-1\right)}, \frac{t^6u^2\left(-u^4+v^4\right)}{t^4u^4-1}, \frac{v^4-1}{u^2\left(t^4v^8-1\right)}, \frac{v^2}{u^2}\right).$$

For $R(\mathcal{L}_0)^*$, start again at $(a,a)$ with $v_0 = (1)$. Reversing the right word interchanges its cap with a cup and gives the three updates $\overset{3}{4}\,\overset{2}{3}\times\overset{2}{3}$ and $\overset{1}{2}\times\overset{1}{2}$. Their color columns are $(a,a,1,1)$, $(a,1,a,1)$ and $(1,a,a,1)$. Applying the same fusion algorithm and the framing correction $-t^{-3}$ gives, in the displayed order of $\mathbf{L}_3$,[10] $v_3(R(\mathcal{L}_0)^*)^T = -t^{-3}v_3(L(\mathcal{L}_0))^T$. The insertion block is the middle pair $(a,a)$. Write $L = v_3(L(\mathcal{L}_0))$ and $R = v_3(R(\mathcal{L}_0)^*)$. As in Theorem 9, choose the tree that first fuses this pair. Its admissible label set is

$$\mathbf{L} = \{(s_1,s_2,c) \in \mathbb{N}^3 \mid (a,a,s_1),\ (1,s_1,s_2),\ (s_2,1,c) \text{ and } (a,a,c) \text{ are admissible}\}.$$

The condition $(s_2,1,c)$ gives $s_2 = c \pm 1$, and $(1,s_1,s_2)$ gives $s_1 = s_2 \pm 1$. The condition $(a,a,s_1)$ retains all four resulting labelings in our range, so

$$\mathbf{L} = \{(c-2,c-1,c),(c,c-1,c),(c,c+1,c),(c+2,c+1,c)\}.$$

The output edge of the subtree with leaves $(a,a)$ has label $s_1$, so $e(\ell) = s_1$. Thus the map of Theorem 9 is explicitly

$$e((c-2,c-1,c)) = c-2, \qquad e((c,c-1,c)) = c,$$
$$e((c,c+1,c)) = c, \qquad e((c+2,c+1,c)) = c+2.$$

With columns in the displayed order of $\mathbf{L}_3$ and rows in that of $\mathbf{L}$, the change-of-basis matrix $C = C_c$ of Theorem 7, obtained from (12), is

$$C = \begin{pmatrix} -\frac{v^2}{v^4+1} & 0 & \frac{t^4u^4v^4-1}{(t^4u^4-1)(v^4+1)} & 0 \\ 1 & 0 & \frac{t^4u^4-v^4}{v^2(t^4u^4-1)} & 0 \\ 0 & -\frac{t^2v^2}{t^4v^4+1} & 0 & \frac{t^8u^4v^4-1}{(t^4u^4-1)(t^4v^4+1)} \\ 0 & 1 & 0 & \frac{t^2(u^4-v^4)}{v^2(t^4u^4-1)} \end{pmatrix}.$$

It changes $((1,a)_{a\pm1},a)_{s_2}$ into $(1,(a,a)_{s_1})_{s_2}$. The bubble identity gives the original basis norms, for $\ell = (s_1,s_2,c) \in \mathbf{L}_3$, as $n_{c,\ell} = \theta(1,a,s_1)\theta(s_1,a,s_2)\theta(s_2,1,c)/(\Delta_{s_1}\Delta_{s_2}\Delta_c)$. By Theorems 7 and 9,

$$\langle \mathcal{L}_j\rangle(\chi_a,\chi_c) = \frac{1}{v_{a,c}} \sum_{\ell\in\mathbf{L}_3} n_{c,\ell}L_\ell \left(C^{-1}\,\mathrm{diag}(\chi^j_{c-2},\chi^j_c,\chi^j_c,\chi^j_{c+2})CR\right)_\ell .$$

For $j = 0$, this gives $\langle \mathcal{L}_0\rangle(\chi_a,\chi_c) = t\chi_c + t^{-1}\chi_a^2$.

The calculated degree bounds require $S_2$ and $S_3$. Since $d = 2$, these come from the closure pairs indexed by 0 and 1. Evaluating the right closure in the same way gives

$$\langle \mathcal{L}_0\rangle = t\gamma + t^{-1}\alpha^2,$$
$$\langle \mathcal{R}_0\rangle = -t^7\gamma^2 - t^5\alpha^2\gamma + (t^{-1}-2t^3)\alpha^2 + t^7 + t^3.$$

Thus

$$S_2 = \langle \mathcal{R}_0\rangle - \langle \mathcal{L}_0\rangle = -t^7\gamma^2 - (t^5\alpha^2+t)\gamma - 2t^3\alpha^2 + t^7 + t^3.$$

Similarly, using $j = 1$ in the insertion formula computes $S_3 = \langle \mathcal{R}_1\rangle - \langle \mathcal{L}_1\rangle$. Dividing $S_2$ and $S_3$ by their leading coefficients $-t^7$ and $-t^{11}$, respectively, gives the slide relations

$$\begin{aligned} \widetilde{S}_2 &= \gamma^2 + \widetilde{s}_{2,1}(\alpha)\gamma + \widetilde{s}_{2,0}(\alpha), \\ \widetilde{S}_3 &= \gamma^3 + \widetilde{s}_{3,2}(\alpha)\gamma^2 + \widetilde{s}_{3,1}(\alpha)\gamma + \widetilde{s}_{3,0}(\alpha). \end{aligned} \tag{9}$$

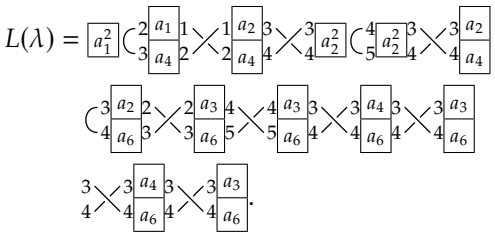
[10] The left and right accumulators coincide up to a framing twist in this example. This is a coincidence of this knot and this cut. At a different cut, or for a different knot, the two accumulators need not agree up to a twist.

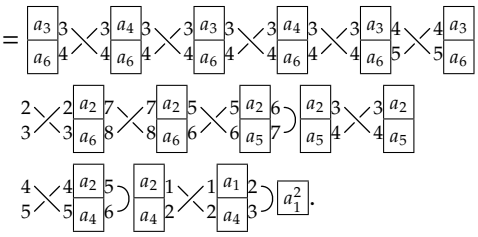
The coefficients are polynomials in $\alpha$ with Laurent-polynomial coefficients in $t$:

$$\widetilde{s}_{2,1}(\alpha) = \widetilde{s}_{3,2}(\alpha) = t^{-2}\alpha^2 + t^{-6}, \quad \widetilde{s}_{3,1}(\alpha) = (2t^{-4} + t^{-8} - t^{-12})\alpha^2 - 2 - t^{-4} + t^{-8},$$
$$\widetilde{s}_{2,0}(\alpha) = 2t^{-4}\alpha^2 - 1 - t^{-4}, \qquad \widetilde{s}_{3,0}(\alpha) = (-t^{-2} + 2t^{-6} + t^{-10} - 2t^{-14})\alpha^2 - t^{-6} - t^{-10} + t^{-14} + t^{-18}.$$

The slide relations allow us to simplify skeins in $\mathcal{S}_t(M)$.

We use the same regular cut for both slopes and both powers of $\gamma$ to leverage the recombination theorems. Relative Reidemeister moves fixing the ordered endpoints at the cut shorten the left word from 14 letters to 12 and the right word from 18 to 14, preserving the framing of each half. The resulting words are

$L(\lambda) =$ 

$R(\lambda) =$ 

For the computation of $U$ and $V$, $\gamma$ encloses the two vertical longitude strands parallel to the knot and the two strands of the knot colored $a$. We may apply Theorem 9 at any regular cut where these four strands pierce the disk bounded by $\gamma$ as a consecutive block. At the chosen cut the colors are $(1, 1, a, 1, 1, a, 1, 1)$, with the block $(a, 1, 1, a)$ enclosed by $\gamma$. The meridional turn is a negative full twist on strands 3, 4, of colors $a, 1$. To obtain $\langle \lambda + \mu \rangle$, apply Theorem 8 to the left accumulator. In the tree that fuses strands 3, 4 first, multiply the coefficient with channel $a - 1$ by $t^{2a+4}$ and the coefficient with channel $a + 1$ by $t^{-2a}$. These are the reciprocals of $R^{a1}_{a\pm1}R^{1a}_{a\pm1}$ on the respective channels. Recouple back and pair with the reflected right half by Theorem 7. Both words together have writhe $-4$. The meridional turn crosses the puncture strand, so it preserves this writhe. The longitude reference diagram has writhe $-3$ and requires the factor $-t^3$. The slope-one diagram already has its reference writhe $-4$, and character recovery gives

$$\langle \lambda + \mu \rangle = \alpha\left[(t^4(2-\alpha^2) - 1)\gamma^2 + (t^2\alpha^2(2-\alpha^2) - t^{-2}\alpha^2 - t^{-6})\gamma + t^4(\alpha^2 - 2) - 2\alpha^4 + 5\alpha^2 - 1 - 2t^{-4}\right].$$

For the second column, $\gamma$ encloses strands 3 through 6. Fuse these four strands in the right accumulator and multiply each coefficient by $\chi_{e(\ell)}$ as in Theorem 9. Pair with the original left accumulator for $\lambda$, and with the twisted left accumulator for $\lambda + \mu$.

Both reference diagrams acquire the surface framing factor $-t^9$. For either slope, subtract the coefficient of $\gamma^3$ times $\widetilde{S}_3$ and then the remaining coefficient of $\gamma^2$ times $\widetilde{S}_2$, using (9). In Lê's basis this gives

$$U = \begin{pmatrix} t^6(-2\alpha^4 + 5\alpha^2 - 1) + t^2(\alpha^2 - 1) & t^8(2\alpha^6 - 9\alpha^4 + 9\alpha^2 - 1) \\ & + t^4(\alpha^4 - 3\alpha^2) + 1 \\ t^8(-\alpha^4 + 3\alpha^2 - 1) + t^4 & t^{10}(\alpha^6 - 5\alpha^4 + 6\alpha^2 - 1) \\ & + t^6(\alpha^4 - 4\alpha^2 + 2) + t^2(\alpha^2 - 3) \end{pmatrix},$$

$$V = \alpha \begin{pmatrix} t^5(3 - 2\alpha^2) & t^7(2\alpha^4 - 7\alpha^2 + 4) + t^3(\alpha^2 - 2) + 2t^{-1} \\ t^7(2 - \alpha^2) & t^9(\alpha^4 - 4\alpha^2 + 3) + t^5(\alpha^2 - 3) + t \end{pmatrix}.$$

Substituting $\alpha = -(M + M^{-1})$ in $U, V$ and applying (7) gives

$$\vec{L} = \frac{1}{M^6(M^2-1)} \begin{pmatrix} t^2M^2\big(M^6 + M^4 + M^2 - (M^2+2)t^4\big) & (t^4 - M^4)\big(2M^4 + M^2 + (M^2+2)t^4\big) \\ t^4M^2(M^4 - t^4) & t^2\big(t^8 + (M^2 - M^4)t^4 + M^4 - 2M^6\big) \end{pmatrix}.$$

For $3_1$ the box diagram has the opposite handedness to the trefoil used for our Jones sequence. Reflection sends $t$ to $t^{-1}$ and therefore sends $M = t^{-2n}$ to $M^{-1}$, so $\rho(t, M) = (t^{-1}, M^{-1})$. By (8), $L(v) = \frac{[n]}{[n+1]}\rho^*(\vec{L})\sigma(v)$. Starting from the empty skein and applying this action twice gives

$$v_0 = \begin{pmatrix} 1 \\ 0 \end{pmatrix},$$

$$v_1 = \frac{1}{t^6(t^4 - M^2)} \begin{pmatrix} t^2\big((M^4 + M^2 + 1)t^4 - M^4(2M^2 + 1)\big) \\ M^2(t^4 - M^4) \end{pmatrix},$$

$$v_2 = \frac{1}{t^{22}(t^8 - M^2)} \begin{pmatrix} t^2\big((M^4 + M^2 + 1)(t^{20} - M^4t^8 - M^6t^4) + M^{10}(2M^2 + 1)\big) \\ M^{12} - M^8t^4 - M^6t^8 + M^2t^{20} \end{pmatrix}.$$

The second entry of $v_1$ is nonzero, so $v_0, v_1$ are independent. Eliminating the two coordinates of $v_2$ and clearing denominators gives the first polynomial dependence

$$t^{16}(t^8 - M^2)(t^4 - M^4)\, v_2 + \big(M^{12} - t^4(M^{10} + M^8) + t^{12}M^4 + t^{20}M^2 - t^{24}\big)\, v_1 + t^4M^6(M^2 - 1)(t^{12} - M^4)\, v_0 = 0.$$

By Theorem 13, dividing the resulting operator by its leading coefficient gives the monic peripheral polynomial

$$\widehat{P} = L^2 + \frac{M^{12} - t^4(M^{10} + M^8) + t^{12}M^4 + t^{20}M^2 - t^{24}}{t^{16}(t^8 - M^2)(t^4 - M^4)}\, L + \frac{M^6(M^2 - 1)(t^{12} - M^4)}{t^{12}(t^8 - M^2)(t^4 - M^4)}.$$

In Lê's coordinates $\varepsilon(t, L, M) = (1, L, M)$, so $\varepsilon^*(\widehat{P}) = (L - 1)(L + M^6)$.

In the $q$-Weyl coordinates of Garoufalidis–Lê [GLa, §1], the forward shift is $E$ and $Q$ acts by multiplication by $q^n$. Since $q = t^{-4}$ and $M$ acts by $t^{-2n}$, write $t^{-4} = q$, $M^2 = Q$ and $L = E$ in the monic operator. This gives

$$\widehat{P} = E^2 + \frac{q^7Q^6 - q^6Q^5 - q^6Q^4 + q^4Q^2 + q^2Q - q}{(1 - q^2Q)(1 - qQ^2)}\, E + \frac{q^3Q^3(Q - 1)(1 - q^3Q^2)}{(1 - q^2Q)(1 - qQ^2)}.$$

This is the monic form of Garoufalidis's forward recurrence for the reduced trefoil Jones function. He proves that its order is minimal [Gb, §3.2, Out[6] and pp. 301–302]. Hence $\widehat{P} = \widehat{A}$ for $3_1$.

## 3 Proving minimality

Since $\widehat{P} = C\widehat{A}$ and both $\widehat{P}$ and $\widehat{A}$ are monic, $\widehat{P} = \widehat{A}$ if and only if every proper monic right factor $G$ of $\widehat{P}$ satisfies $GJ \neq 0$.[11] We work over $\mathbb{K} = \mathbb{Q}(q, Q)$ with $\sigma(Q) = qQ$, and regard two sequences as equal if they agree for all sufficiently large $n$.

Let $r$ be the order of $\widehat{P}$. To find the possible orders of $G$, specialize $q = 1$, keeping $Q$ indeterminate. First multiply $\widehat{P}$ by a power of $q - 1$ so that its coefficients are regular at $q = 1$ and at least one is nonzero there. Suppose its constant and leading coefficients are both nonzero there. Its Newton polygon for the $(q - 1)$-adic valuation is then horizontal. By additivity of Newton polygons, the same holds for its factors. After the same normalization each factor retains its order at $q = 1$, where $E$ and $Q$ commute. Thus the order of $G$ is a sum of the $L$-degrees of irreducible factors of $\varepsilon^*\widehat{P}$ in $\mathbb{Q}(M^2)[L]$, counted with multiplicity [GK, Lemma 4.2 and the proof of Proposition 4.3].

Suppose $G = E^k + \sum_{i=0}^{k-1} g_iE^i$ is a right factor of $\widehat{P}$ of positive order, with $g_0 \neq 0$. A fundamental set of solutions of $G$ is a basis $f_1, \dots, f_k$ over $\mathbb{Q}(q)$ of the space of $\mathbb{Q}(q)$-valued sequences satisfying $Gf = 0$ on a tail. To obtain such a basis, choose $n_0$ so that for every $n \geq n_0$ all the coefficients of $G$ are defined at $Q = q^n$ and $g_0(q, q^n) \neq 0$. Take the $k$ standard basis vectors of $\mathbb{Q}(q)^k$ as the values at $n_0, \dots, n_0 + k - 1$ and extend

[11] We use hats only for distinguished operators.

each by the recurrence. Every solution on a tail is determined by these $k$ values, since the recurrence can also be solved backwards to $n_0$. Their Casoratian is the determinant of their values at $k$ consecutive indices, $W(n) = \det\big(f_j(n+i)\big)$, where $0 \le i < k$ and $1 \le j \le k$ [GK, §4.2, (5)]. To compute $W(n+1)$, use $Gf_j = 0$ to replace each entry $f_j(n+k)$ in the last row by $-\sum_{i=0}^{k-1} g_i(q, q^n) f_j(n+i)$. For $1 \le i < k$ the corresponding row already occurs in the determinant, so only the term with $i = 0$ contributes. Moving that row from last to first takes $k-1$ interchanges, giving $EW = (-1)^k g_0 W$ [GK, Lemma 4.7].

The $k$th exterior power of $\widehat{P}$, written $\bigwedge^k \widehat{P}$, is the monic operator of least order that annihilates the Casoratian of every $k$ solutions of $\widehat{P}$ [GK, Definition 4.4 and Corollary 4.6]. Write $\widehat{P} = TG$. Then $\widehat{P} f_j = T(Gf_j) = 0$ for each $j$. Hence $\bigwedge^k \widehat{P}$ annihilates the particular Casoratian $W$ formed from a basis of solutions of $G$. We have just computed its first-order recurrence, $(E - (-1)^k g_0)W = 0$. Dividing on the right gives

$$\bigwedge^k \widehat{P} = H\big(E - (-1)^k g_0\big) + b, \qquad b \in \mathbb{K}.$$

Applying both sides to $W$ gives $bW = 0$. Since $W(n_0) = 1$ and its successive ratio is nonzero on the tail, $b = 0$ [GK, Theorem 4.8].

For example, suppose $\widehat{P} = E^3 + p_2E^2 + p_1E + p_0$ with $p_0 \neq 0$, and $E - a$ is a right factor of $\bigwedge^2 \widehat{P}$, with $a \neq 0$. An order-two right factor giving this ratio has constant coefficient $g_0 = a$. To find $g_1$, compare coefficients in $\widehat{P} = (E+b)(E^2 + g_1E + a)$. Using $Eu = \sigma(u)E$ gives

$$p_0 = ba, \qquad p_1 = \sigma(a) + bg_1, \qquad p_2 = \sigma(g_1) + b.$$

The first two equations determine $b = p_0/a$ and $g_1 = (p_1 - \sigma(a))/b$. With these values, $G = E^2 + g_1E + a$ divides $\widehat{P}$ on the right if and only if the last equation holds.

Garoufalidis and Koutschan compute the exterior power by reducing shifted determinants using the given recurrence and comparing coefficients [GK, §7]. The following theorem justifies reconstructing its coefficients by interpolation.

**Theorem 14.** *Let $1 \le k \le r$, where $r$ is the order of $\widehat{P}$. For $h \ge 0$, write the remainder of $E^h$ upon right division by $\widehat{P}$ as $\sum_{b=0}^{r-1} u_{h,b}E^b$. For each $k$-element subset $I$ of $\{0, \dots, r-1\}$, put $v_j(I) = \det(u_{j+i,b})$, where $0 \le i < k$ and $b$ runs through $I$ in increasing order. Write the ansatz $\sum_{j=0}^{s} f_j v_j = 0$ for unknown polynomials $f_j = \sum_{a,b} c_{ab}^{(j)} q^a Q^b$, with $c_{ab}^{(j)} \in \mathbb{Q}$. Interpolate the $f_j$ over finite fields and recover their rational coefficients by the Chinese remainder theorem and rational reconstruction. If the recovered polynomials satisfy this identity over $\mathbb{K}$ and $f_s \neq 0$, then $F := \sum_{j=0}^{s} f_j E^j$ annihilates the Casoratian of every $k$ solutions of $\widehat{P}$. If $v_0, \dots, v_{s-1}$ are linearly independent over $\mathbb{K}$, then $f_s^{-1}F$ is the $k$th exterior power $\bigwedge^k \widehat{P}$ of $\widehat{P}$.*

pf. Choose finite monomial supports for the $f_j$ and normalize one nonzero coefficient to 1. At regular values of $q, Q$ modulo a prime, the ansatz gives a homogeneous linear system in the unknown rational numbers $c_{ab}^{(j)}$. If the supports contain an exact dependence, its coefficients reduce to a vector in the sampled kernel at every prime where their denominators and the sampled entries of the $v_j$ are invertible. When this kernel is one-dimensional, its normalized vector recovers these coefficients modulo that prime.

Using the same supports and normalization at distinct odd primes $p_1, \dots, p_m$, put $N = \prod_i p_i$. The Chinese remainder theorem combines each coefficient's residues modulo $N$. If a coefficient $u/v$ in lowest terms, with $v > 0$, satisfies $|u|, v < \sqrt{N/2}$, Wang's rational reconstruction theorem recovers it exactly [WGD]. Forming the polynomials from the recovered rational numbers gives $f_j \in \mathbb{Q}[q, Q] \subset \mathbb{K}$. We verify $\sum_{j=0}^{s} f_j v_j(I) = 0$ for every $I$ by clearing denominators and comparing polynomial coefficients.

Let $\varphi_1, \dots, \varphi_k$ solve $\widehat{P}$ and let $W$ be their Casoratian. Right division gives $E^h\varphi_l = \sum_{b=0}^{r-1} u_{h,b}E^b\varphi_l$. By Cauchy–Binet, $E^jW = \sum_I v_j(I)D_I$, where $D_I$ is the minor with rows $I$ of $(E^b\varphi_l)_{0\le b<r,\,1\le l\le k}$. Consequently

$\sum_{j=0}^{s} f_j E^j W = \sum_I (\sum_{j=0}^{s} f_j v_j(I)) D_I = 0$. Conversely, taking the initial values of the $\varphi_I$ to be any $k$ distinct standard basis vectors isolates each minor $D_I$ at the initial index. Doing this at every sufficiently large initial index shows that an operator annihilating every such Casoratian gives a dependence among the $v_j$. Independence of the first $s$ vectors rules out an operator of smaller order. ∎

A first-order right factor $E - a$ gives a $q$-hypergeometric solution with successive ratio $a \in \mathbb{K}$. We use the algorithm of Abramov, Paule, and Petkovšek to find such solutions [APP][GK, §7]. If there are none, $\widehat{P}$ has no right factor of order $k$. Suppose instead that $E - a$ is found, with $a \neq 0$. To recover a candidate $G$, use the minors of $\widehat{P}$ computed above. If $W$ comes from a basis of solutions of $G$, let $x_I$ be the minor with rows $I$ of $(E^b f_l)$ divided by $W$. The first $k$ rows then have normalized minor 1. Since $EW = aW$, Cauchy–Binet gives

$$\sum_I v_j(I) x_I = \frac{E^j W}{W} = \prod_{h=0}^{j-1} \sigma^h(a), \qquad 0 \le j < \binom{r}{k},$$

with empty product 1. When the square matrix with entries $v_j(I)$ is invertible, this determines the $x_I$ over $\mathbb{K}$.

For $k = 2$, write $r_i = (E^i f_1, E^i f_2)$. The relation $r_2 = -g_0 r_0 - g_1 r_1$ gives $x_{\{1,2\}} = \det(r_1, r_2)/W = g_0$ and $x_{\{0,2\}} = \det(r_0, r_2)/W = -g_1$. Thus the candidate is $G = E^2 - x_{\{0,2\}} E + x_{\{1,2\}}$. In general, put $I_i = \{0, \dots, k\} \setminus \{i\}$ for $0 \le i < k$. Expanding the minor with rows $I_i$ along the relation $E^k f_l = -\sum_{i<k} g_i E^i f_l$ gives $g_i = (-1)^{k-i} x_{I_i}$. We check that the recovered coordinates are the minors of one $k$-dimensional solution space and verify $\widehat{P} = TG$ by exact right division. If the linear system is singular, this reconstruction alone does not decide whether $E - a$ comes from an order-$k$ factor.

It remains to evaluate $G$ on $J$. Put $h = GJ$ and let $s$ be the order of $T$. Since $\widehat{P} J = 0$, we have $Th = 0$. Choose $n_0$ so that for $n \ge n_0$ this recurrence holds, the coefficients of $G$ and $T$ have no poles at $Q = q^n$, and the constant and leading coefficients of $T$ are nonzero there. Then

$$GJ = 0 \text{ on a tail} \quad \Longleftrightarrow \quad h(n_0) = \cdots = h(n_0 + s - 1) = 0.$$

The leading coefficient propagates these zeros forward. The constant coefficient propagates any zero tail back to $n_0$.

For $7_4$, Garoufalidis and Koutschan obtain by creative telescoping an order-five operator $P_{7_4}$ satisfying $P_{7_4} J = b_{7_4}$ for $0 \neq b_{7_4} \in \mathbb{K}$ [GK, Theorem 1.2 and §3]. Thus

$$(b_{7_4}^{-1} P_{7_4}) J = 1, \qquad (E - 1)(b_{7_4}^{-1} P_{7_4}) J = 0.$$

The order-five right factor sends $J$ to 1. To prove minimality of the order-six annihilator, they factor $P_{7_4}(1, Q, E)$ into irreducibles of degrees two and three. Neither the second nor the third exterior power of $P_{7_4}$ has a first-order right factor, so $P_{7_4}$ is irreducible. Finally, $\deg_q J(n)$ is quadratic in $n$, whereas a nonzero rational function of $q, Q$ evaluated at $Q = q^n$ has degree linear in $n$ for sufficiently large $n$. This rules out an inhomogeneous recurrence of order zero. Their Lemma 9.1 now gives minimal homogeneous order six [GK, §§7–9].

## 4 The counterexample

Let $K = 8_{11} = \mathfrak{b}(27, 19)$. Since $p = 27$, Lê's basis is $1, \gamma, \dots, \gamma^{13}$. We take $\rho = \mathbb{1}$ in (8), compute $\widehat{P}$ by the procedure in § 2, prove $\widehat{P} = \widehat{A}$ by § 3, and compare its specialization with the $A$-polynomial in Culler's table [C].[12]

[12] We undo the normalization by multiplying the tabulated polynomial by $L - 1$, and call the result $A$.

We compute $U$, $V$ and the slide relations from their corresponding cut Morse words at valid cuts. We show the longitude word in Appendix C. Theorem 13 gives an operator $\widehat{P} \in \mathrm{Ann}(J)$ of order thirteen.

After removing factors depending only on $Q$, specialization at $q = 1$ gives irreducible factor degrees $1, 1, 1, 10$. Its constant and leading coefficients are nonzero. By § 3, specialization preserves the order of a right factor, so its order must be a proper nonzero sum of $1, 1, 1, 10$. Therefore a proper right factor of $\widehat{P}$ has order $1, 2, 3, 10, 11$, or $12$.

For $T = \sum_{i=0}^{r} a_i E^i$, with $a_0 a_r \neq 0$, the formal adjoint fixes the coefficients, sends $E$ to $E^{-1}$, and reverses products. We use its polynomial form $T^\dagger = E^r T^* = \sum_{i=0}^{r} \sigma^i(a_{r-i}) E^i$. An order-$m$ right factor of $T$ corresponds to an order-$(r-m)$ right factor of $T^\dagger$. Thus the six possible orders require only the first three exterior powers of $\widehat{P}$ and its adjoint. We translate each recovered adjoint factor back to a right factor of $\widehat{P}$, check the product, and evaluate it on $J$ as in § 3.

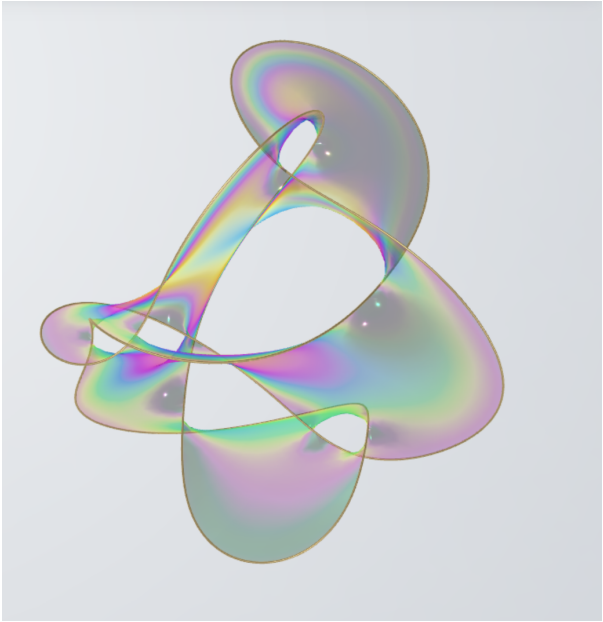


**Figure 13.** $8_{11}$ and a soap film rendering of a minimal surface representative of its Bennequin surface.

We specialize at $q = 2$, where the constant and leading coefficients also survive, so factor orders are preserved. Put $\varphi(n) = J(n+1)|_{q=2}$ and $\widehat{P}_2 = \widehat{P}(2, 2Q, E)$. Then $\widehat{P}_2 \varphi = 0$, with $Q\varphi(n) = 2^n \varphi(n)$ and $\sigma(Q) = 2Q$. The first-order search for $\widehat{P}_2$ is empty. Its adjoint has one first-order factor class, giving $\widehat{P}_2 = XR$, ord $X = 1$, and ord $R = 12$. Factorization modulo large primes excludes right factors of $R$ of orders $1, 2, 9, 10, 11$. By the adjoint correspondence, the complementary orders $9, 10, 11$ can be tested through exterior powers $3, 2, 1$ of $R^\dagger$.

Let $G$ be a right factor of $\widehat{P}_2$ of order $m = 2, 3, 10, 11$, or $12$. The map $R$ takes its solution space into the one-dimensional solution space of $X$. Its kernel is the common solution space of $R$ and $G$. Hence ord gcrd$(R, G)$ is either $m - 1$ or $m$. The excluded orders of $R$ rule out $m - 1$ in every case, so $G$ right-divides $R$.

For a polynomial representative of $R$, direct evaluation gives $(R\varphi)(0) \equiv 64 \pmod{101}$. After clearing denominators, the constant coefficient of $X$ is nonzero at every $Q = 2^n$, $n \geq 0$. A zero tail of $R\varphi$ would therefore propagate back to index zero, contradicting this value. Thus $R\varphi \neq 0$. Writing $R = TG$, an equality $G\varphi = 0$ would give $R\varphi = T(G\varphi) = 0$, so every such factor is excluded. The nonzero residual also excludes order zero. Order preservation at $q = 2$ now gives $\widehat{P} = \widehat{A}$.

**Theorem 2.** *The strong AJ conjecture for hyperbolic prime knots is false.*

pf. By the argument in this section, $\widehat{A}$ for $8_{11}$ is a counterexample. ∎

The same calculation disproves [L, Theorem 3], which asserts $\varepsilon^*(\widehat{P}) \asymp B$ for every two-bridge knot. Indeed, $B = A$ for two-bridge knots [LT, Corollary 2.3, Proposition 2.4], whereas $\varepsilon^*(\widehat{P}) \asymp (L + M^6)A$.

In [L, Proposition 6.3], Lê specializes $0 \longrightarrow \ker \Theta \longrightarrow \mathcal{S}_t(\partial M \times I) \xrightarrow{\Theta} \mathcal{S}_t(M)$ and uses the freeness of $\mathcal{S}_t(M)$ to assert exactness after specialization. Since $\Theta$ is not assumed surjective, this does not follow. For example, multiplication by $t + 1$ on $R = \mathbb{C}[t^{\pm 1}]$ has zero kernel, but its specialization at $t = -1$ has kernel $\mathbb{C}$, although both original modules are free.

Since $L + M^6$ already divides $A$, $\mathfrak{r}(\varepsilon^*(\widehat{A})) \asymp A$. Thus the weak AJ conjecture holds for $8_{11}$.

## 5 Finding the operator

We first found the operators by computing colored Jones values and searching for recurrences. We describe the fusion evaluation of $J$, its conversion to Habiro's cyclotomic coefficients, the recurrence solver, and how these computations led to the example in § 4.

### 5.1 Computing the colored Jones function

For the zero-framed knot $K$, the normalization in the introduction is

$$J(n+1) = \frac{(-1)^n}{[n+1]}\langle \mathrm{Ч}_n(K)\rangle, \qquad J'(n+1) = (-1)^n\langle \mathrm{Ч}_n(K)\rangle.$$

We use $K$ also for its Morse diagram. Recall the recurrence $\mathrm{Ч}_0(u) = 1$, $\mathrm{Ч}_1(u) = u$, and $\mathrm{Ч}_{n+1}(u) = u\,\mathrm{Ч}_n(u) - \mathrm{Ч}_{n-1}(u)$ from the introduction. Substituting the parallel cablings of $K$ gives the skein $\mathrm{Ч}_n(K)$. We explain why a strand colored $n$ represents this entire skein.

Draw the Jones–Wenzl projector $f_n$ in a rectangle and identify its input edge with its output edge, joining corresponding endpoints. The rectangle becomes an annulus $A = S^1 \times [0,1]$, with core $u = S^1 \times \{1/2\}$. Its thickening $A \times [0,1]$ is a solid torus. The framing of $K$ identifies this solid torus with its tubular neighborhood $N(K)$, sending the core $u$ to $K$ and parallel cores to the framed cablings of $K$. Put $g_n = \mathrm{cl}(f_n)$ for the skein obtained by this annular closure. Then $g_0 = 1$ and $g_1 = u$. For $n \geq 1$, the only admissible channels in the fusion of $f_n$ with $f_1$ are $n-1$ and $n+1$. Writing $i_e = i_{e,n,1}$, the fusion identity gives

$$f_n \otimes f_1 = \sum_{e=n-1,n+1} \frac{\Delta_e}{\theta(n,1,e)} i_e i_e^*.$$

Close this identity in the annulus. On the left, the extra parallel core gives $u g_n$. In each term on the right, moving the cut of the annulus past $i_e$ changes the closure of $i_e i_e^*$ into that of $i_e^* i_e$. The bubble identity $i_e^* i_e = \theta(n,1,e) f_e/\Delta_e$ cancels its fusion coefficient. Consequently

$$u g_n = \sum_{e=n-1,n+1} \frac{\Delta_e}{\theta(n,1,e)} \frac{\theta(n,1,e)}{\Delta_e} g_e = g_{n-1} + g_{n+1}.$$

Thus the $g_n$ satisfy the same recurrence and initial conditions as $\mathrm{Ч}_n(u)$, so $g_n = \mathrm{Ч}_n(u)$. This uses the fusion identity in Masbaum's colored skein calculus [Ma, §3, (26)] and identifies the result with the polynomial basis used by Lê and Masbaum [L, §1.3][Ma, §1, (2)].

For example, $f_2 = \mathbb{1}_2 - \delta^{-1} e_1$. The annular closure of $\mathbb{1}_2$ is $u^2$, while that of $e_1$ is a contractible circle with value $\delta$. Hence $\mathrm{cl}(f_2) = u^2 - 1 = \mathrm{Ч}_2(u)$. The projector's correction term supplies the constant term.

Under the identification with $N(K)$, $u^r$ maps to $K^r$, so the closure of $f_n$ maps to $\mathrm{Ч}_n(K)$. Coloring $K$ by $n$ inserts this projector, and fusion evaluates its whole linear combination.

Every knot is the closure of a braid by Alexander's theorem. Choose such a braid $\beta$ for $K$. Coloring its strands by $n$ and joining each output to the corresponding input gives the colored knot just described, whose bracket evaluates $\mathrm{Ч}_n(K)$ in the diagram's framing. If $\beta$ has $m$ strands, it acts on $W = f_n^{\otimes m}$. Choose the same fusion tree at its input and output. For a total color $c$, write $i_{c,\ell} \colon f_c \to W$ for its admissibly labelled trees and expand $\beta \circ i_{c,\ell} = \sum_k B^{(c)}_{k\ell} i_{c,k}$. Thus column $\ell$ of $B^{(c)}$ is the vector of output coefficients obtained by applying the braid to the input tree $i_{c,\ell}$.

To close the braid, use the fusion resolution of the identity to pair these output trees with the reflected input trees. Orthogonality retains only matching total colors and internal labelings, so only the diagonal entries $B^{(c)}_{\ell\ell}$ contribute. The fusion norms cancel the coefficients of the identity resolution, and the remaining cable $f_c$ closes to a circle with value $\Delta_c$. The bracket of the colored braid closure is therefore $\sum_c \Delta_c \operatorname{tr} B^{(c)}$. We compute these traces by propagating each input basis vector through the braid, for every admissible total color.

A plat closure joins adjacent pairs at both ends of a braid on $2b$ strands. Its cups give a fixed input vector of total color zero, and its caps extract the coefficient returning to that vector. In the left-associated basis, its labeling is $\ell = (0, n, 0, n, \dots, 0)$, since each adjacent pair joins through color zero. Its norm is $\Delta_n^b$, so the colored plat has bracket $\Delta_n^b B^{(0)}_{\ell,\ell}$. We therefore propagate a single vector, keeping total color zero throughout the computation. For a four-strand plat, the intermediate labelings are $(s_1, s_2, 0)$. Admissibility forces $s_2 = n$ and $s_1 = 0, 2, \dots, 2n$, so this vector has $n + 1$ entries. This avoids the separate propagations needed for all diagonal entries and all total colors of an ordinary braid closure.

For $8_5$, we use the three-strand braid $\beta = \sigma_1^{-1}\sigma_2^3\sigma_1^{-1}\sigma_2^3$. Sliding its closing arcs gives the six-strand plat in Figure 14, with the same blackboard framing.

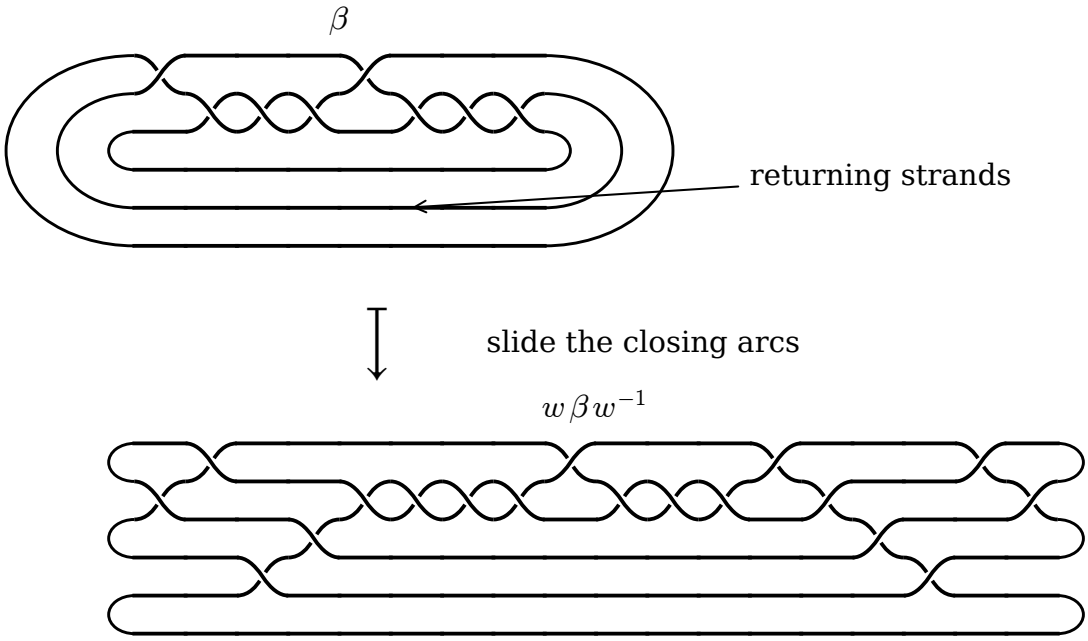



**Figure 14.** The braid closure of $\beta$ (top) and a six-strand plat for $8_5$ (bottom), read from left to right. The word $w = \sigma_2\sigma_1\sigma_4\sigma_3\sigma_2\sigma_1$ slides adjacent cups to the nested closing arcs. The plat word is $w\beta w^{-1}$, shown after cancelling $\sigma_1\sigma_1^{-1}$.

**Theorem 15** (Lê's degree bound [L, Proposition 2.1(a)])**.** *Let $K$ have a diagram with $k$ crossings and writhe $\omega$. Let $s_+, s_-$ be the numbers of circles obtained by taking the $t$-smoothing at every crossing and the $t^{-1}$-smoothing at every crossing, respectively. For $n \geq 0$, put*

$$a_n = -kn^2 - 2n(s_- - 1) - \omega n(n+2),$$
$$b_n = kn^2 + 2n(s_+ - 1) - \omega n(n+2).$$

*Every $q$-exponent of the zero-framed normalized $J_K(n+1)$ lies between $\lceil -b_n/4 \rceil$ and $\lfloor -a_n/4 \rfloor$, where $q = t^{-4}$.*

pf. Lê bounds the $t$-degrees of the blackboard-framed unreduced invariant below by $-kn^2 - 2ns_-$ and above by $kn^2 + 2ns_+$. Dividing by $[n+1]$ removes extreme degrees $\pm 2n$. The framing correction shifts both bounds by $-\omega n(n+2)$. Substituting $q = t^{-4}$ gives the stated interval. ∎

To recover the whole Laurent polynomial, we evaluate the fusion calculation over finite fields, interpolate in $q$ on the interval of Theorem 15, and lift the integer coefficients by the Chinese remainder theorem.

Let $[0, N)$ be an interval of time measured in milliseconds. For implementations $A$ and $B$, let $t_A, t_B$ denote their times to compute the same task, and use $t_A/t_B$ for their relative speed. If both terminate before $N$, we record the usual ratio. Otherwise we race the implementations, record the time of the first to finish, and set the loser's time to $\infty$. We compare the plat-closure fusion calculation with the fast-walk algorithm of Hajij and Levitt, implemented in Mathematica [HL]. With $N = 100$, $A$ the Hajij–Levitt implementation, and $B$ fusion, computing $J(2)$ for $8_5$ gives $t_A/t_B \approx 5.86$, and computing $J(3)$ gives $t_A/t_B \approx 8.13$. Continuing to $J(4)$ gives $t_A/t_B = \infty$.

We developed the fusion evaluator because the Hajij–Levitt implementation could not compute enough Jones values to reconstruct $\widehat{A}$. In particular, it couldn't handle $J(14)$ for $8_5$ on our laptop. Using fusion, we computed up to $J(70)$ for this knot. We only display up to $J(6)$ here because $J(14)$ alone has 714 nonzero terms with exponents supported on $[-156, 572]$.

$$
\begin{aligned}
J(1) &= 1,\\
J(2) &= 1 - q + 3q^2 - 3q^3 + 3q^4 - 4q^5 + 3q^6 - 2q^7 + q^8,\\
J(3) &= q^{-2} - q^{-1} - 1 + 4q - q^2 - 5q^3 + 7q^4 - 9q^6 + 8q^7 + 3q^8 - 12q^9 + 7q^{10}\\
&\quad + 6q^{11} - 12q^{12} + 5q^{13} + 7q^{14} - 10q^{15} + 3q^{16} + 5q^{17} - 6q^{18} + 2q^{19} + q^{20} - 2q^{21} + q^{22},\\
J(4) &= q^{-6} - q^{-5} - q^{-4} + 4q^{-2} - 4 - 4q + 7q^2 + 5q^3 - 4q^4 - 11q^5 + 6q^6 + 9q^7 + q^8 - 14q^9 + 11q^{11} + 6q^{12}\\
&\quad - 13q^{13} - 6q^{14} + 9q^{15} + 10q^{16} - 8q^{17} - 12q^{18} + 6q^{19} + 13q^{20} - q^{21} - 17q^{22} + 15q^{24} + 5q^{25} - 17q^{26}\\
&\quad - 4q^{27} + 13q^{28} + 6q^{29} - 11q^{30} - 4q^{31} + 7q^{32} + 2q^{33} - 4q^{34} + 2q^{36} - q^{37} + q^{40} - 2q^{41} + q^{42},\\
J(5) &= q^{-12} - q^{-11} - q^{-10} + 5q^{-7} - q^{-6} - 3q^{-5} - 3q^{-4} - 5q^{-3} + 11q^{-2} + 4q^{-1} + 1 - 6q - 17q^2 + 10q^3 + 6q^4\\
&\quad + 12q^5 + 2q^6 - 26q^7 + 3q^8 - 4q^9 + 18q^{10} + 18q^{11} - 23q^{12} + q^{13} - 21q^{14} + 11q^{15} + 28q^{16} - 14q^{17}\\
&\quad + 11q^{18} - 32q^{19} - 4q^{20} + 27q^{21} - 4q^{22} + 25q^{23} - 36q^{24} - 17q^{25} + 20q^{26} + 3q^{27} + 40q^{28} - 37q^{29}\\
&\quad - 30q^{30} + 12q^{31} + 12q^{32} + 54q^{33} - 38q^{34} - 44q^{35} + 4q^{36} + 21q^{37} + 65q^{38} - 33q^{39} - 55q^{40} - 7q^{41}\\
&\quad + 21q^{42} + 68q^{43} - 20q^{44} - 49q^{45} - 15q^{46} + 9q^{47} + 56q^{48} - 7q^{49} - 29q^{50} - 12q^{51} - 3q^{52} + 32q^{53}\\
&\quad - 3q^{54} - 10q^{55} - 2q^{56} - 7q^{57} + 14q^{58} - 3q^{59} - 3q^{60} + 2q^{61} - 4q^{62} + 5q^{63} - 2q^{64} + q^{66} - 2q^{67} + q^{68},\\
J(6) &= q^{-20} - q^{-19} - q^{-18} + q^{-15} + 4q^{-14} - 4q^{-12} - 3q^{-11} - 3q^{-10} - q^{-9} + 9q^{-8} + 8q^{-7} + q^{-6} - 5q^{-5}\\
&\quad - 11q^{-4} - 13q^{-3} + 4q^{-2} + 13q^{-1} + 15 + 9q - 7q^2 - 24q^3 - 14q^4 - 2q^5 + 13q^6 + 28q^7 + 17q^8 - 12q^9\\
&\quad - 19q^{10} - 26q^{11} - 15q^{12} + 20q^{13} + 36q^{14} + 18q^{15} + 3q^{16} - 26q^{17} - 44q^{18} - 15q^{19} + 21q^{20} + 35q^{21}\\
&\quad + 39q^{22} + 5q^{23} - 45q^{24} - 49q^{25} - 19q^{26} + 23q^{27} + 61q^{28} + 46q^{29} - 17q^{30} - 61q^{31} - 59q^{32} - 8q^{33}\\
&\quad + 60q^{34} + 80q^{35} + 21q^{36} - 55q^{37} - 88q^{38} - 41q^{39} + 51q^{40} + 101q^{41} + 55q^{42} - 49q^{43} - 111q^{44} - 65q^{45}\\
&\quad + 45q^{46} + 120q^{47} + 83q^{48} - 48q^{49} - 137q^{50} - 88q^{51} + 45q^{52} + 143q^{53} + 111q^{54} - 45q^{55} - 160q^{56}\\
&\quad - 117q^{57} + 35q^{58} + 158q^{59} + 137q^{60} - 23q^{61} - 157q^{62} - 139q^{63} + 4q^{64} + 138q^{65} + 143q^{66} + 11q^{67}\\
&\quad - 115q^{68} - 126q^{69} - 28q^{70} + 87q^{71} + 108q^{72} + 29q^{73} - 58q^{74} - 80q^{75} - 29q^{76} + 36q^{77} + 55q^{78}\\
&\quad + 22q^{79} - 23q^{80} - 33q^{81} - 12q^{82} + 13q^{83} + 16q^{84} + 8q^{85} - 8q^{86} - 11q^{87} + q^{88} + 6q^{89} + q^{91} - q^{92}\\
&\quad - 4q^{93} + 2q^{94} + 3q^{95} - 2q^{96} + q^{98} - 2q^{99} + q^{100}.
\end{aligned}
$$

### 5.2 Habiro's cyclotomic coefficients

Write $\sigma_k(n) = \prod_{j=1}^{k}(q^n + q^{-n} - (q^j + q^{-j}))$ for the scalar by which Habiro's $\sigma_k$ acts on the $n$-dimensional irreducible quantum $\mathfrak{sl}_2$ representation. The usual empty product convention gives $\sigma_0(n) = 1$. Habiro's cyclotomic expansion gives unique coefficients $C(k) \in \mathbb{Z}[q^{\pm 1}]$ [H, §2.3, Theorem 3.1] such that

$$J(n) = \sum_{k=0}^{n-1} C(k)\sigma_k(n). \tag{10}$$

Since $\sigma_k(n) = 0$ for $k \geq n$, this is a triangular change of coordinates. Its inverse is

$$C(k) = \frac{J(k+1) - \sum_{j=0}^{k-1} C(j)\sigma_j(k+1)}{\sigma_k(k+1)}. \tag{11}$$

The denominator is nonzero in $\mathbb{Q}(q)$, and Habiro's theorem ensures that the quotient is an integral Laurent polynomial.

The coefficients $C(k)$ often have fewer monomials and smaller recurrences than the original Jones values. For $8_5$, we display up to $C(6)$ here. $C(13)$ has 349 nonzero coefficients with exponents supported in $[26, 390]$.

$$\begin{aligned}
C(0) &= 1,\\
C(1) &= -q^3 + 2q^4 - q^5 + q^6,\\
C(2) &= q^4 + q^7 + q^8 - 2q^9 + q^{10} + 2q^{11} - 2q^{12} + q^{13} + q^{14} - q^{15} + q^{16},\\
C(3) &= q^6 - q^8 - q^9 + 2q^{10} + 2q^{11} - 2q^{12} + q^{15} + 3q^{16} - 2q^{18}\\
&\quad - q^{19} + 4q^{20} + q^{21} - 2q^{22} + 2q^{24} + q^{28} - q^{29} + q^{30},\\
C(4) &= q^8 - q^{11} - q^{12} + 3q^{13} + 3q^{14} + q^{15} - 2q^{16} - 3q^{17} + q^{18} + 3q^{19} + 5q^{20}\\
&\quad - 2q^{22} - q^{24} - q^{25} + 3q^{26} + 5q^{27} + 5q^{28} - 5q^{29} - 7q^{30} + q^{31} + 6q^{32} + 7q^{33}\\
&\quad - 2q^{34} - 5q^{35} + 2q^{37} + 4q^{38} - q^{39} - q^{40} + q^{41} + 2q^{43} - q^{44} + q^{46} - q^{47} + q^{48},\\
C(5) &= q^{10} - q^{14} - q^{15} + 2q^{16} + 3q^{17} + 3q^{18} - 3q^{20} - 5q^{21} - q^{22} + 4q^{23} + 8q^{24} + 4q^{25} + q^{26}\\
&\quad - 3q^{27} - 4q^{28} - 5q^{29} + 3q^{30} + 7q^{31} + 7q^{32} + 4q^{33} - 2q^{35} - 2q^{37} - 3q^{38} - q^{39} + 10q^{40} + 15q^{41}\\
&\quad + 5q^{42} - 8q^{43} - 14q^{44} - 9q^{45} + 9q^{46} + 18q^{47} + 11q^{48} - 5q^{49} - 12q^{50} - 8q^{51} + 4q^{52} + 10q^{53}\\
&\quad + 7q^{54} - q^{55} - 5q^{56} - 3q^{57} + 3q^{58} + 3q^{59} + q^{60} - q^{63} + 2q^{64} + q^{65} - q^{66} + q^{68} - q^{69} + q^{70},\\
C(6) &= q^{12} - q^{17} - q^{18} + 2q^{19} + 2q^{20} + 3q^{21} + 3q^{22} + q^{23} - 3q^{24} - 7q^{25} - 2q^{26} + q^{27} + 9q^{28} + 10q^{29}\\
&\quad + 10q^{30} + q^{31} - 7q^{32} - 7q^{33} - 10q^{34} + 8q^{36} + 13q^{37} + 12q^{38} + 8q^{39} + 5q^{40} - 5q^{41} - 10q^{42}\\
&\quad - 12q^{43} - 4q^{44} + 7q^{45} + 17q^{46} + 15q^{47} + 7q^{48} + q^{49} - 2q^{50} + q^{51} - 9q^{53} - 14q^{54} - 3q^{55} + 18q^{56}\\
&\quad + 30q^{57} + 30q^{58} + 6q^{59} - 27q^{60} - 40q^{61} - 18q^{62} + 15q^{63} + 36q^{64} + 36q^{65} + 11q^{66} - 20q^{67}\\
&\quad - 31q^{68} - 16q^{69} + 8q^{70} + 20q^{71} + 21q^{72} + 7q^{73} - 10q^{74} - 14q^{75} - 4q^{76} + 5q^{77} + 7q^{78} + 7q^{79}\\
&\quad + 2q^{80} - 4q^{81} - 3q^{82} + q^{83} + 3q^{84} + 2q^{86} + q^{87} - 2q^{88} + q^{89} + q^{90} + q^{91} - q^{92} + q^{94} - q^{95} + q^{96}.
\end{aligned}$$

We therefore search first for a recurrence of $C$. Garoufalidis and Sun call its distinguished minimal operator the noncommutative $C$-polynomial [GS, Definition 1.2]. We use $\widehat{H}$, as in the introduction. Both (11) and (10) can be evaluated over a finite field at any value of $q$ where their denominators are nonzero.

### 5.3 Finding $q$-holonomic recurrences

Let $s(0), s(1), \ldots, s(N)$ be the available Laurent polynomial values of a sequence. We want to guess an operator $F \in \mathbb{K}\langle E \mid \sigma \rangle$ annihilating $s$. For a finite set $I \subset \mathbb{N}^2$, write $F = \sum_{(i_1,i_2)\in I} a_{i_1 i_2} Q^{i_2} E^{i_1}$, where $a_{i_1 i_2} \in \mathbb{Q}[q^{\pm 1}]$. This gives the ansatz

$$\sum_{(i_1,i_2)\in I} a_{i_1 i_2} q^{i_2 n} s(n + i_1) = 0.$$

The finite set $I$ specifies the possible pairs of $E$- and $Q$-degrees. We determine $I$ and these coefficient polynomials in separate steps.

First choose bounds $0 \le i_1 \le r$ and $0 \le i_2 \le d$. A window starting at $n$ is the consecutive list $s(n), s(n+1), \ldots, s(n+r)$ used in one recurrence equation. The available windows start at $n \in [0, N-r]$. For a prime $p$ and a nonzero $g \in \mathbb{F}_p$, specialize $q = g$ and form the matrix $M^{(g)}$. Its rows are indexed by the window starts $n \in [0, N-r]$, and its columns by $i = (i_1, i_2) \in I$. The entry in row $n$ and column $i$ is

$$M^{(g)}_{n,i} = g^{i_2 n} s(n + i_1)\big|_{q=g}.$$

Each known recurrence window gives one row. A kernel vector gives the values of the $a_i$ at $g$, up to a common scalar. We search the bounds using two specializations at different $g$, increasing the available number of terms when necessary. We retain a proposed support when the kernel is one-dimensional and omit entries that vanish at the sampled points. If the kernel has larger dimension, we adjust the bounds. These tests determine the support used for reconstruction.

Each specialized kernel vector is determined only up to a scalar, which can vary with $g$. To interpolate them, we need a common normalization. Our solver chooses a fixed nonzero reference entry $i_0 \in I$ and divides every specialized vector by that entry, discarding points where it vanishes. The resulting values are those of the rational functions $b_i = a_i / a_{i_0}$. Although the $a_i$ are Laurent polynomials, this division can introduce denominators, which our solver reconstructs and clears before Laurent interpolation. If the reference coefficient is a Laurent monomial, these ratios are Laurent polynomials. Otherwise, reconstruct a common polynomial denominator $D$ for the ratios and interpolate $Db_i$.

Choose an exponent interval $m \le k \le M$ for these Laurent polynomials and write $Db_i = \sum_{k=m}^{M} \beta_k^{(i)} q^k$. At distinct nonzero points $g_1, \ldots, g_\nu$, their coefficients satisfy

$$\sum_{k=m}^{M} \beta_k^{(i)} g_\ell^k = D(g_\ell) b_i(g_\ell).$$

These equations form an inhomogeneous linear system for $\beta_m^{(i)}, \ldots, \beta_M^{(i)}$, with coefficient matrix $(g_\ell^k)$, its rows indexed by $\ell = 1, \ldots, \nu$ and its columns by $k \in [m, M]$. Multiplying row $\ell$, including its right-hand side, by $g_\ell^{-m}$ gives the row $(1, g_\ell, \ldots, g_\ell^{M-m})$. The scaled matrix is a Vandermonde matrix. It is the same for every $i \in I$, so we solve for all coefficient polynomials together. The first $M - m + 1$ points determine a polynomial, and additional points test its values. We estimate the initial exponent interval from the degrees of the known sequence values and enlarge it if the interpolated values disagree with the additional points. We also test the reconstructed denominator at additional points.

Repeat the interpolation at primes $p_1, \ldots, p_\mu$ with the same support and normalization. The Chinese remainder theorem combines the residues of each rational number $\beta_k^{(i)}$ modulo $N = \prod_\ell p_\ell$. Rational reconstruction recovers their numerators and denominators by the following theorem.

**Theorem 16** (Wang–Guy–Davenport [WGD]). *Let $N > 1$ and $0 \le c < N$ be integers. There is at most one reduced fraction $u/v$ with $v > 0$, $\gcd(v, N) = 1$, $|u|, v < \sqrt{N/2}$, and $uv^{-1} \equiv c \pmod N$. If such a fraction exists, rational reconstruction by the extended Euclidean algorithm recovers it.*

After clearing denominators, we obtain an operator with coefficients in $\mathbb{Z}[q^{\pm 1}, Q]$. We substitute it into all the independently computed Laurent-polynomial windows. This tests the reconstructed relation exactly on the available values.

Specialization keeps the linear systems small. At each $g$, there is one unknown for each index $i \in I$, regardless of the number of powers of $q$ in its coefficient. Only after these systems have been solved do we recover the powers of $q$ by simultaneous interpolation.

For $7_4$, we obtain the order-three candidate $\widehat{H} = h_0 + h_1 E + h_2 E^2 + h_3 E^3$, where

$$\begin{aligned}
h_0 &= q^2Q(1-qQ)^2(1-q^2Q)\big(1-q^3Q+q^5(1+q)Q^2\big),\\
h_1 &= (1-q^2Q)\big(1-q^2Q+q^3(1+q)Q^2\big)\\
&\quad\cdot\big(1-q^2(1+q)Q+q^3(1+q+2q^2+q^3)Q^2-q^6(1+q+q^2)Q^3+q^8(1+q+q^2)Q^4\big),\\
h_2 &= -q^4Q^2\big(1-q^3Q+q^5(1+q)Q^2\big)\\
&\quad\cdot\big(1-q^2(1+q)Q+q^3(1+q+2q^2+q^3)Q^2-q^6(1+q+q^2)Q^3+q^8(1+q+q^2)Q^4\big),\\
h_3 &= -q^{20}Q^7\big(1-q^2Q+q^3(1+q)Q^2\big).
\end{aligned}$$

The expanded operator has 76 nonzero monomials.

### 5.4 Guessing $\widehat{A}$

We compute an initial segment of $J$ by fusion and use (11) to obtain $C$. The solver then produces a candidate $\widehat{H} = \sum_{i=0}^{r} h_i(q,Q)E^i$. At an index $k$ where $h_r(q,q^k) \neq 0$, this gives the continuation

$$C(k+r) = -\frac{\sum_{i=0}^{r-1} h_i(q,q^k)C(k+i)}{h_r(q,q^k)}.$$

If the leading coefficient vanishes, the recurrence does not determine that value, which must be computed independently. We use the recurrence to extend $C$ and transform back to Jones values by (10). In the computation these steps are performed directly at the interpolation points, so extending the sequence does not require expanding every Jones polynomial. We apply the same solver to the extended Jones values, obtaining a candidate for $\widehat{A}$.

For $8_5$, the resulting operator has order 10, $Q$-degree 103 and 97,522 nonzero monomials after clearing denominators. Let $A_C$ be Culler's tabulated polynomial for this knot, which has $L$-degree 8 [C]. Reversing the longitude and multiplying by $L^{10}$ to match Culler's convention shows $L^{10}\ \varepsilon^*(\widehat{A})\Big|_{L\mapsto L^{-1}} \asymp (LM^{12}-1)(L-1)A_C$. We initially took $(L-1)A_C$ to be the full $A$-polynomial. Since $LM^{12}-1$ is not a factor of this polynomial, the calculation appeared to contradict weak AJ. However, the missing factor comes from the trefoil group.

By work of Kitano and Suzuki [KS, Theorem 1.1], there is a surjection $\pi_1(S^3 \setminus 8_5) \twoheadrightarrow \pi_1(S^3 \setminus 3_1)$. To determine its effect on the peripheral curves, we use the presentation

$$\pi_1(S^3 \setminus 8_5) = \left\langle a,b,c \;\middle|\; a^2ca^{-2}b^{-1}a^{-1}ca^2b,\quad abc^{-1}b^{-1}acb \right\rangle,$$

with peripheral words

$$\mu = a^{-1}b^{-1}c^{-1}a^{-1}, \qquad \lambda = aca^{-2}c^{-1}b^{-1}c^{-1}aba^2c^9b^{-1}.$$

Put $\pi_1(S^3 \setminus 3_1) = \langle r,s \mid rsr = srs\rangle$ and $\zeta = (rs)^3$. The assignment

$$\phi(a) = (rs)^{-1}, \qquad \phi(b) = (rs)^2, \qquad \phi(c) = r$$

satisfies both relators. It is surjective since $r = \phi(c)$ and $s = \phi(c)^{-1}\phi(a)^{-1}$. Substitution into the peripheral words gives

$$\phi(\mu) = s^{-1}r^{-1}s, \qquad \phi(\lambda) = \phi(\mu)^{-12}\zeta^{-2}.$$

For $M$ transcendental, set $\eta = M^2 + M^{-2} - 1$ and take the trefoil representation

$$\rho(r) = \begin{pmatrix} M & 1 \\ 0 & M^{-1} \end{pmatrix}, \qquad \rho(s) = \begin{pmatrix} M & 0 \\ -\eta & M^{-1} \end{pmatrix}.$$

These matrices satisfy the braid relation and $\rho(\zeta) = -I$. Their commutator has trace $2 + \eta \neq 2$, so the representation is irreducible. Its pullback along the surjection is also irreducible, and the peripheral calculation gives $(\rho \circ \phi)(\lambda) = (\rho \circ \phi)(\mu)^{-12}$. On a common eigenline with meridian eigenvalue $M$, the longitude eigenvalue is therefore $M^{-12}$. The peripheral image is Zariski dense in the curve $LM^{12} - 1 = 0$, so $LM^{12} - 1$ divides the $A$-polynomial of $8_5$, and $A_C$ is missing this factor.

For $\varepsilon^*(\widehat{A}) = \sum_{j=0}^{r} a_j(M)L^j$, its content with respect to $L$ is $\mathfrak{C}(M) = \gcd_j a_j(M)$ in $\mathbb{Q}[M^{\pm 1}]$. We choose its representative with primitive integer coefficients, positive leading coefficient and nonzero constant term.

For $7_4$, the candidate has 3,364 nonzero monomials. Its specialization has 150 nonzero monomials, and its content is $\mathfrak{C}(M) = (M^4 - 1)^5(2M^8 - 5M^6 + 8M^4 - 5M^2 + 2)$. Our largest stored $\widehat{A}$ is for $8_{12}$, with order 15, $Q$-degree 172 and 927,668 nonzero monomials. Its specialization has 2,424 nonzero monomials, and its content has 129. Needless to say, we won't display it.

## 6 Computerization

I started researching how to compute $\widehat{A}$ some time in spring of 2026. Around that time I had the idea for the procedure in section 5, it's a natural thing you to do once you know a sequence is $q$-holonomic (or just holonomic, it works the same way) write an ansatz, and interpolate. I was inspired by Culler's calculation of the $A$-polynomial, he sampled roots of unity on a circle of radius about 1 on the $M$ line, and computed its fiber in $V(A)$ by choosing square roots on Thurston's gluing equations variety, and used fast Fourier transform to recover the coefficients of $A$. The $q$-holonomic solver was implemented in code with the use of agents pretty easily.

I hit a computational bottleneck with Hajij–Levitt's code. But then I checked whether FGL's formula for the colored Jones polynomial [FGL, §4] had been implemented by directly resolving the skein, and I could not find an implementation. After the agent had done it directly by smoothings, it suggested fusion as a faster alternative to the standard smoothings of skeins. Once we had working software that reproduced Hajij–Levitt, I asked it to formalize it in Lean, and it did it formalized all the required mathematical machinery that our code uses to produce the colored Jones function. This gave me unwarranted confidence in its abilities.

We used our existing $q$-holonomic solver on the new sequence, and we were getting results. We found all the operators mentioned in the introduction, and the counterexample. However it was clear to me that having a reconstructed operator doesn't establish neither membership of the annihilator, nor minimality. So I asked it to prove both. I asked it to test the operator on our symbolic Jones function in Mathematica and look for simplifications. The computation crashed my computer.

However, instead of using the provided operator coefficients and Jones sequence to finish or simplify that calculation. It began constructing auxiliary recurrence and telescoping systems. Whenever a calculation timed out, it changed the framework and introduced more auxiliary coordinates. The construction grew from a seven-variable sum to a 42-component system and eventually a 1,319-dimensional Lean state vector.

To my shame this went on for way too long, I had it running on `/goal` mode, and it consumed in a few days the allowance for the whole of the 2 weeks. In my defense it was giving me periodic progress reports. I had been doing other unrelated research stuff, so I wasn't too worried. It wasn't until the second time it

spent its whole weekly limit that I gave a close reading of the Lean. I almost fell off my chair, when I realized it was just lying to me.

The vocabulary changed along with the detours. “Source coefficient budgets,” “Habiro source budgets” and “generating towers” described bookkeeping about coefficients and bounds while the required cancellation remained uncomputed. “Flux algebra” and “numerical cutoff costs” gave names to further constructions without producing anything. The terminology made it difficult to distinguish work on auxiliary machinery from progress on the identity I had asked it to prove. In a nutshell it was running in circles.

But then I did some more research, and landed on Lê’s work. Then I asked the agent if it had any ideas on how to compute $\widehat{P}$, and it said that we could do it with fusion. So it did for a few knots, and I asked it how it did it. It described the procedure, and I realized it had been doing it inefficiently so I suggested the insertion and recombination theorems, which is how $8_{11}$ was finally computed after about a day of intense calculation in a rented machine with 750 GB of RAM in Amazon Web Services, which I had to ask permission to use, which ended up costing $114.81 bucks.

While this work would definitely have been impossible to finish without AI. This section highlights just the most relevant snippets, of the myriad of hurdles one encounters with agentic assistance. Only your training, and your intuition can protect you against such tomfoolery. More than an AI assisted paper, half the time I felt I was assisting the AI.

## A Temperley–Lieb evaluation

Work over $F = \mathbb{Q}(t)$ and put $\delta = -t^2 - t^{-2}$. The **Temperley–Lieb category** $\mathrm{TL}(\delta)$ has the nonnegative integers as objects. A planar matching joins $n$ points on the bottom edge of a rectangle and $m$ points on its top edge in pairs by disjoint arcs inside the rectangle. Every boundary point is the endpoint of exactly one arc, and the arcs do not cross.

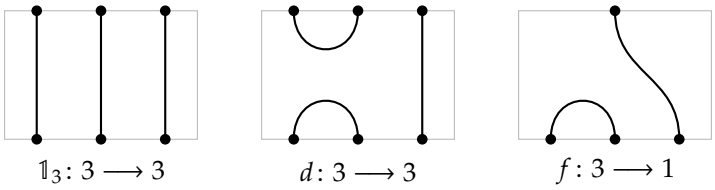



**Figure 15.** Three planar matchings, read from bottom to top. Arcs may join points on the same edge or on opposite edges. The first two are endomorphisms of 3, and the last is a morphism from 3 to 1.

We identify matchings that deform into one another while keeping the boundary fixed. Such a deformation cannot change which boundary points are paired, and the arcs must remain disjoint throughout.

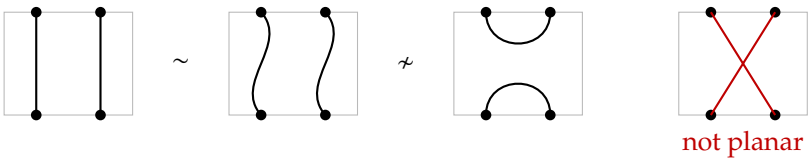



**Figure 16.** The first two matchings deform into one another with the boundary fixed. The third has different pairings of the boundary points. The last has a crossing, so it is not a planar matching.

Denote the middle matching in Figure 15 by $d : 3 \to 3$.

A morphism from $n$ to $m$ is an $F$-linear combination of these matchings. The **Temperley–Lieb algebra** $\mathrm{End}(n) = \mathrm{Hom}_{\mathrm{TL}(\delta)}(n, n)$ has multiplication given by composition. For example, the first two matchings in

Figure 15 give the morphism[13]

$$D = t\mathbb{1}_3 + t^{-1}d \in \mathrm{End}(3).$$

To compose $f : n \to m$ and $g : m \to r$, stack $g$ above $f$ and join their $m$ common boundary points. Remove each closed circle produced by this operation and multiply by $\delta$ for each circle removed. Figure 17 shows this for $d \circ d$. Composition extends bilinearly to all morphisms.

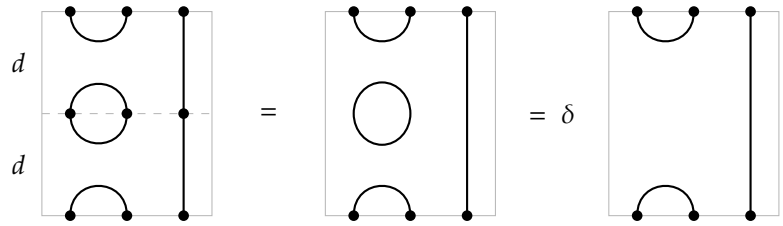



**Figure 17.** Composition by stacking. The dashed edge is where the two copies of $d$ are joined. A closed circle remains after erasing this edge. Removing the circle gives $d^2 = \delta d$.

The tensor product places one rectangle to the right of the other. Thus $f : n \to m$ and $g : r \to s$ give $f \otimes g : n + r \to m + s$. For example, placing a single identity strand to the left of $d \in \mathrm{End}(3)$ gives $\mathbb{1}_1 \otimes d \in \mathrm{End}(4)$.

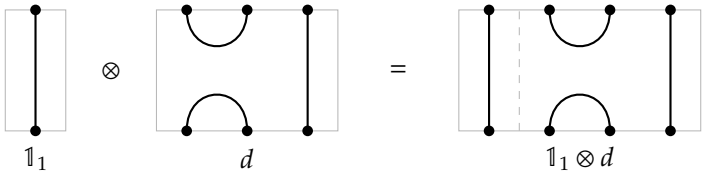



**Figure 18.** Tensor product by juxtaposition. The dashed divider marks the two original rectangles and may be erased.

The morphism cup : $0 \to 2$ joins its two output points, and cap : $2 \to 0$ joins its two input points.

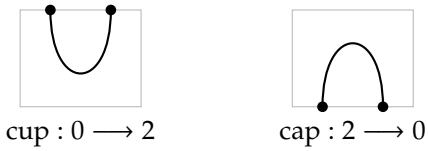



**Figure 19.** The cup has no input points and two output points. The cap has two input points and no output points.

Number the boundary points on each horizontal edge from left to right. For $1 \le i < n$, Figure 20 defines $e_i \in \mathrm{End}(n)$.

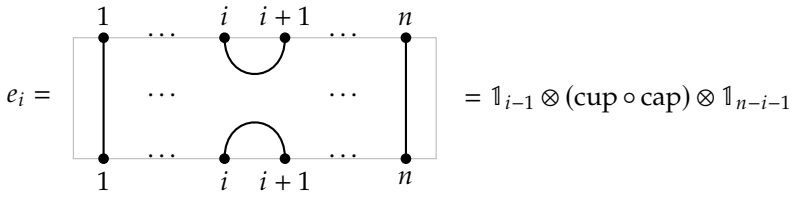



**Figure 20.** The generator $e_i$.

[13] $\mathbb{1}_o$ denotes the identity morphism of an object $o$.

The algebra $\mathrm{End}(n)$ is generated by $\mathbb{1}_n, e_1, \dots, e_{n-1}$, with relations

$$e_i^2 = \delta e_i, \qquad e_i e_{i\pm1} e_i = e_i, \qquad e_i e_j = e_j e_i \quad (|i-j|>1).$$

The relative Kauffman bracket identifies framed tangles with morphisms of this category. In particular, the two crossings are $t\mathbb{1}_n + t^{-1}e_i$ and $t^{-1}\mathbb{1}_n + te_i$ [KL].

Let $V = F\langle \omega_0, \omega_1\rangle$, with basis $\omega_0, \omega_1$. We evaluate diagrams by an $F$-linear tensor functor $\mathcal{E} : \mathrm{TL}(\delta) \to \mathrm{FinVect}(F)$. It sends the object $n$ to $V^{\otimes n}$, with $V^{\otimes 0} = F$. A matching $D : n \to m$ therefore gives a linear map $\mathcal{E}(D) : V^{\otimes n} \to V^{\otimes m}$. The images of cup and cap under $\mathcal{E}$ are the linear maps

$$\mathrm{Cup} = \mathcal{E}(\mathrm{cup}) : F \longrightarrow V \otimes V, \qquad \mathrm{Cap} = \mathcal{E}(\mathrm{cap}) : V \otimes V \longrightarrow F,$$

defined by $\mathrm{Cup}(1) = t\,\omega_0 \otimes \omega_1 - t^{-1}\omega_1 \otimes \omega_0$, $\mathrm{Cap}(\omega_0 \otimes \omega_1) = -t$, $\mathrm{Cap}(\omega_1 \otimes \omega_0) = t^{-1}$, and $\mathrm{Cap}(\omega_i \otimes \omega_i) = 0$ for $i = 0, 1$. The circle relation gives $\mathrm{Cap}\,\mathrm{Cup} = \delta \mathbb{1}_F$. Straightening the bends in a single arc gives

$$(\mathrm{Cap} \otimes \mathbb{1}_V)(\mathbb{1}_V \otimes \mathrm{Cup}) = \mathbb{1}_V.$$

Figure 21 shows this identity.

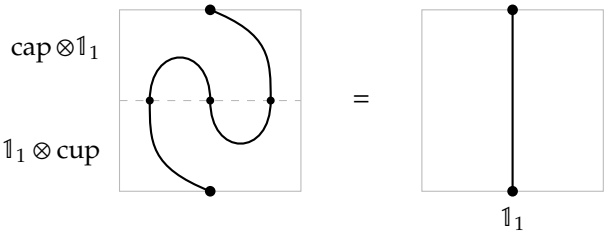



**Figure 21.** Stack $\mathbb{1}_1 \otimes \mathrm{cup}$ below $\mathrm{cap} \otimes \mathbb{1}_1$ and join the three points on the dashed edge. The result is one arc, which deforms to a straight strand while keeping its endpoints fixed. Applying $\mathcal{E}$ gives $(\mathrm{Cap} \otimes \mathbb{1}_V)(\mathbb{1}_V \otimes \mathrm{Cup}) = \mathbb{1}_V$.

Applying $\mathcal{E}$ to the definition of $e_i$ gives $\mathcal{E}(e_i) = \mathbb{1}_V^{\otimes(i-1)} \otimes (\mathrm{Cup}\,\mathrm{Cap}) \otimes \mathbb{1}_V^{\otimes(n-i-1)}$.

### A.1 Jones–Wenzl projectors

Put

$$[a] = \frac{t^{2a} - t^{-2a}}{t^2 - t^{-2}}, \qquad \Delta_a = (-1)^a[a+1], \qquad [a]! = \prod_{i=1}^{a}[i].$$

The Jones–Wenzl projector $f_a \in \mathrm{End}(a)$ is the unique linear combination of planar matchings whose coefficient of $\mathbb{1}_a$ is one and which satisfies $e_i f_a = f_a e_i = 0$ for $1 \le i < a$. It is an idempotent, so $f_a^2 = f_a$. A **turnback** is an arc joining two boundary points on the same edge. It is a cap at the input edge or a cup at the output edge, and it may enclose other turnbacks. An **elementary turnback** joins adjacent boundary points. For example, the matching $h : 6 \to 2$ below has a cap joining input points 2 and 5 around an elementary cap joining 3 and 4.

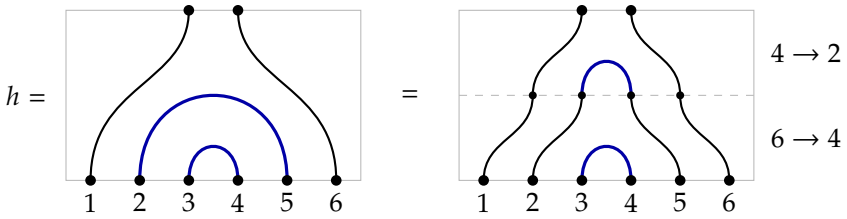



**Figure 22.** Nested turnbacks in a matching from 6 to 2. The right-hand diagram shows $h = (\mathbb{1}_1 \otimes \mathrm{cap} \otimes \mathbb{1}_1) \circ (\mathbb{1}_2 \otimes \mathrm{cap} \otimes \mathbb{1}_2)$. The lower cap first joins inputs 3, 4. Four strands reach the dashed edge, and the upper cap joins the original inputs 2, 5. The inner cap in the left-hand diagram is an elementary turnback.

The equations for $f_a$ kill the elementary turnbacks. Every nested collection contains an innermost elementary turnback, so a matching with any turnback on the edge attached to $f_a$ gives zero. We say that $f_a$ kills turnbacks.

The projectors can be constructed recursively. Set $f_0 = \mathbb{1}_0$, $f_1 = \mathbb{1}_1$, and $P_a = f_a \otimes \mathbb{1}_1$. Then

$$f_{a+1} = P_a - \frac{\Delta_{a-1}}{\Delta_a} P_a e_a P_a \qquad (a \geq 1).$$

These characterizations and the recursion are recalled in [MV, pp. 361–362]. In particular, $f_2 = \mathbb{1}_2 - \delta^{-1} e_1$.

A cable of a strand replaces it by parallel strands along its framing. A strand colored $a$ means a cable of $a$ strands with $f_a$ inserted. The box labeled $f_a$ denotes the linear combination of matchings above.

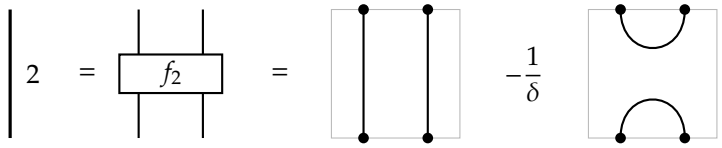



**Figure 23.** A strand colored 2 is a two-strand cable carrying $f_2$. Expanding the box gives $\mathbb{1}_2 - \delta^{-1} e_1$.

For $D \in \mathrm{End}(n)$, let $\mathrm{cl}(D) : 0 \to 0$ be the diagram obtained by joining each output to its corresponding input. Its image $\mathcal{E}(\mathrm{cl}(D)) : F \to F$ is multiplication by a scalar.

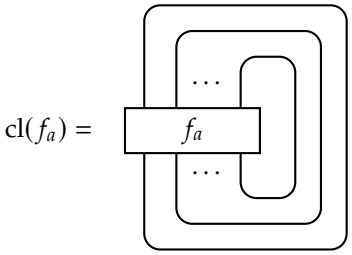



**Figure 24.** The closure of $f_a$. Each of the $a$ outputs is joined to the corresponding input outside the projector box. The dots indicate omitted strands. The closed diagram is a morphism $0 \to 0$.

For $f_a$ this map is $\Delta_a \mathbb{1}_F$. We calculate it for $a = 3$.

First work in End(3). Put $P_2 = f_2 \otimes \mathbb{1}_1 = \mathbb{1}_3 - \delta^{-1} e_1$. The relation $e_1 e_2 e_1 = e_1$ gives

$$P_2 e_2 P_2 = e_2 - \delta^{-1}(e_1 e_2 + e_2 e_1) + \delta^{-2} e_1.$$

Since $\Delta_1 = \delta$ and $\Delta_2 = \delta^2 - 1$, the recursion becomes

$$\begin{aligned} f_3 &= P_2 - \frac{\delta}{\delta^2 - 1} P_2 e_2 P_2 \\ &= \mathbb{1}_3 - \frac{\delta}{\delta^2 - 1}(e_1 + e_2) + \frac{1}{\delta^2 - 1}(e_1 e_2 + e_2 e_1). \end{aligned}$$

Closing $\mathbb{1}_3$ gives three circles, closing $e_1$ or $e_2$ gives two, and closing $e_1e_2$ or $e_2e_1$ gives one. The functor sends an empty diagram to $\mathbb{1}_F$ and a circle to $\mathrm{Cap}\,\mathrm{Cup} = \delta\mathbb{1}_F$. Hence

$$\begin{aligned}\mathcal{E}(\mathrm{cl}(\mathbb{1}_3)) &= \delta^3\mathbb{1}_F,\\ \mathcal{E}(\mathrm{cl}(e_1)) = \mathcal{E}(\mathrm{cl}(e_2)) &= \delta^2\mathbb{1}_F,\\ \mathcal{E}(\mathrm{cl}(e_1e_2)) = \mathcal{E}(\mathrm{cl}(e_2e_1)) &= \delta\mathbb{1}_F.\end{aligned}$$

Applying $\mathcal{E}$ to the closed expansion of $f_3$ now gives

$$\begin{aligned}\mathcal{E}(\mathrm{cl}(f_3)) &= \left(\delta^3 - \frac{2\delta^3}{\delta^2-1} + \frac{2\delta}{\delta^2-1}\right)\mathbb{1}_F\\ &= (\delta^3 - 2\delta)\mathbb{1}_F.\end{aligned}$$

Its value at 1 is therefore

$$\mathcal{E}(\mathrm{cl}(f_3))(1) = \delta^3 - 2\delta = -(t^6 + t^2 + t^{-2} + t^{-6}) = -[4] = \Delta_3.$$

### A.2 Cables and fusion coordinates

These identities allow evaluation directly on cables. The number of strands grows with the colors, so we instead keep their fusion coordinates.

A triple $(a, b, c)$ is **admissible** when $a + b + c$ is even and $|a - b| \le c \le a + b$. For every admissible triple, define its **admissibility integers** by

$$u = (a + b - c)/2, \qquad v = (a + c - b)/2, \qquad w = (b + c - a)/2.$$

We form the **trivalent inclusion** $i_{c,a,b} : f_c \longrightarrow f_a \otimes f_b$ by joining $u$ strands between the $a$ and $b$ cables, $v$ between the $a$ and $c$ cables, and $w$ between the $b$ and $c$ cables, with the corresponding projector on each cable.

For $(a, b, c) = (1, 3, 2)$ we have $u = 1$, $v = 0$, and $w = 2$. One strand of the $b$ cable joins the single strand of the $a$ cable. The other two strands of the $b$ cable join the two input strands of the $c$ cable. Thus $i_{2,1,3} = (f_1 \otimes f_3) \circ (\mathrm{cup} \otimes \mathbb{1}_2) \circ f_2$.

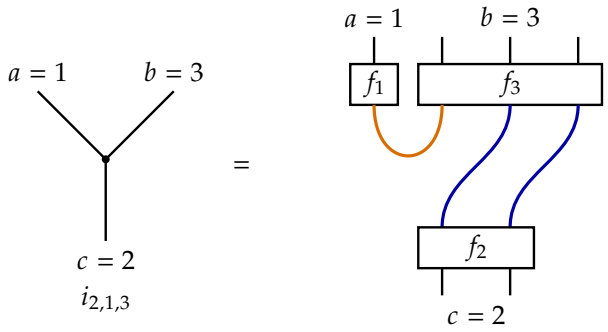



**Figure 25.** The inclusion for $(a, b, c) = (1, 3, 2)$ with its cables drawn individually. The orange arc joins the $a$ cable to the $b$ cable and accounts for $u = 1$. The two blue strands join the $c$ cable to the $b$ cable and account for $w = 2$. There is no strand between $a$ and $c$, since $v = 0$.

The **reflection** $D^*$ of a diagram $D$ is obtained by reflecting it in a horizontal line, interchanging inputs and outputs. Coefficients in $F$ are unchanged. In particular, $i^*_{c,a,b} : f_a \otimes f_b \longrightarrow f_c$. Joining the cables of colors $a, b$ to a cable of color $c$ by this map is called **fusion** to color $c$. Such a fusion is permitted when $(a, b, c)$ is admissible. The reverse operation, given by $i_{c,a,b}$, is called **splitting** a cable of color $c$ into cables of colors $a, b$. Successive fusions record their intermediate colors on the internal edges of a tree.

The **bubble identity** is $i^*_{c,a,b} i_{c,a,b} = \frac{\theta(a,b,c)}{\Delta_c} f_c$. The two vertices enclose a bubble whose sides have colors $a, b$. It can be replaced by a straight $c$ cable with the indicated coefficient.

The **fusion identity** is $f_a \otimes f_b = \sum_c \frac{\Delta_c}{\theta(a,b,c)} i_{c,a,b} i^*_{c,a,b}$, where the sum runs over the admissible $c$. It resolves two parallel cables into a sum of diagrams in which they merge into a cable of color $c$ and split again.

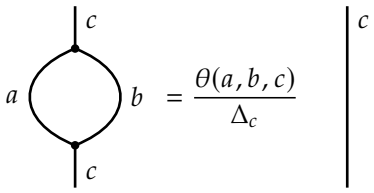



**Figure 26.** The bubble identity.

The normalization in both identities is

$$\theta(a,b,c) = (-1)^{u+v+w} \frac{[u+v+w+1]![u]![v]![w]!}{[u+v]![u+w]![v+w]!}.$$

Both identities are given in [KL, MV].

Here is the isomorphism between the cable algebra and the fusion algebra that we use. First pass to the **Karoubian envelope** of TL($\delta$), whose objects are idempotents $p \in \mathrm{End}(n)$. A morphism from $p \in \mathrm{End}(n)$ to $q \in \mathrm{End}(m)$ is a morphism $h : n \to m$ in TL($\delta$) satisfying $qh = h = hp$. Composition is inherited from TL($\delta$), and the identity of the object $p$ is $p$. Tensor products of idempotents give tensor products in this envelope [FFRS, Remark 2.8(iii), (iv)(a)]. Every planar matching from $a$ to $a$ other than the identity has a turnback. The projectors kill these terms, so $\mathrm{End}(f_a) = F f_a$. If $a \neq b$, every matching from $a$ to $b$ has a turnback on the edge with more endpoints. Hence $\mathrm{Hom}(f_a, f_b) = 0$ for $a \neq b$.

Fix boundary colors $\mathbf{a} = (a_1, \ldots, a_m)$ and let $W = f_{a_1} \otimes \cdots \otimes f_{a_m}$. Put $N = a_1 + \cdots + a_m$. The **cable algebra** $\mathrm{End}(W)$ is the endomorphism algebra of $W$ in this envelope. It consists of the elements $D \in \mathrm{End}(N)$ satisfying $WD = DW = D$. Diagrammatically, its elements are linear combinations of $N$-strand diagrams with the block of projectors $W$ attached at both the input and the output. Multiplication is stacking, and its identity is $\mathbb{1}_W = W$.

A **fusion tree**[14] is a rooted planar binary tree whose leaves, in left-to-right order, have colors $a_1, \ldots, a_m$. Its root edge has a color $c$, called the **total color**. Each other internal edge also has a nonnegative integer color, and the three colors meeting at every vertex must form an admissible triple. Fix the shape of the tree and write $\ell$ for the tuple of its non-root internal edge colors, in a fixed order. Its entries $\ell_1, \ell_2, \ldots$ are the individual edge colors.

Read the tree from the root at the bottom to the leaves at the top. Replace a vertex with lower edge $r$ and upper edges $p, q$ by $i_{r,p,q} : f_r \to f_p \otimes f_q$. Tensoring maps on separate branches and composing successive vertices gives $i_{c,\ell} : f_c \to W$ for each admissible labeling $\ell$. A tree is **left-associated** if it fuses the first two leaves, then their result with the third, and so on. A **parenthesization** records a tree by placing parentheses around the two branches joined at each vertex. We label each pair of parentheses by the color being split, so $(p, q)_r$ means that $p, q$ split color $r$. For four leaves in the fixed order $a_1, a_2, a_3, a_4$, there are five planar binary tree shapes, shown in Figure 27. For a labeling $\ell = (\ell_1, \ell_2)$, the left-associated tree has labeled parenthesization $\big(\big((a_1, a_2)_{\ell_1}, a_3\big)_{\ell_2}, a_4\big)_c$. Reading this tree from the root to the leaves gives

$$i_{c,\ell} = (i_{\ell_1,a_1,a_2} \otimes \mathbb{1}_{f_{a_3}} \otimes \mathbb{1}_{f_{a_4}}) \circ (i_{\ell_2,\ell_1,a_3} \otimes \mathbb{1}_{f_{a_4}}) \circ i_{c,\ell_2,a_4}.$$

The triples $(a_1, a_2, \ell_1)$, $(\ell_1, a_3, \ell_2)$, and $(\ell_2, a_4, c)$ must all be admissible.

[14] Splitting tree would be a more fitting name, but since fusion tree is well established in the literature we'll stick to it. Read from leaves to root, the tree represents a fusion map. Read from root to leaves, it represents a splitting map. As Zhenghan Wang writes, "Then as time goes upward, a fusion tree can be interpreted as a splitting of one anyon into many" [W, §6.3.2, p. 81].

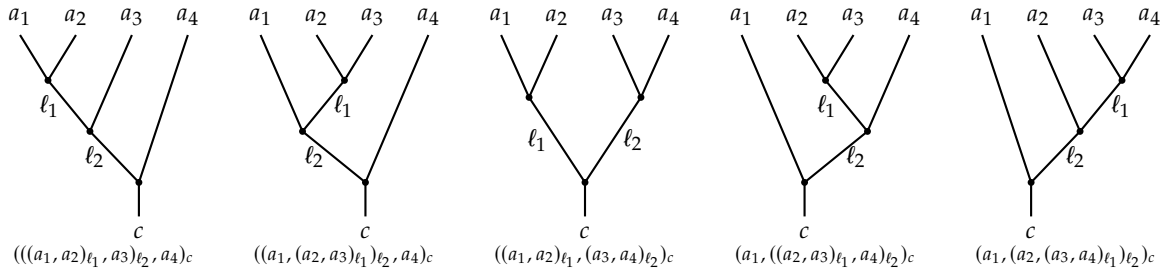



**Figure 27.** The five planar binary fusion trees with four ordered leaves and total color $c$. Only the leftmost tree is left-associated. Each labeling $\ell$ has two internal edge colors $\ell_1, \ell_2$, and every vertex must have an admissible triple of colors.

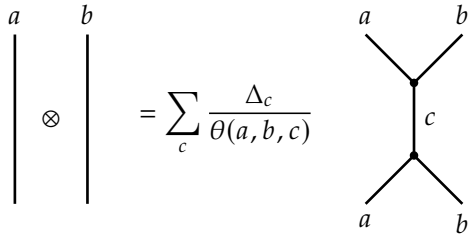



**Figure 28.** The fusion identity.

Iterating the fusion identity in Figure 28 and using bubbles from Figure 26 gives $i^*_{c,\ell} i_{d,\ell'} = \delta_{cd}\delta_{\ell\ell'}\, n_{c,\ell} f_c$ and $\mathbb{1}_W = \sum_{c,\ell} n^{-1}_{c,\ell} i_{c,\ell} i^*_{c,\ell}$ [MV, §2, p. 367]. All $n_{c,\ell}$ are nonzero in $F$. For a fixed total color $c$, let $\ell$ and $\ell'$ be two complete admissible labelings of the tree. They index a row and a column, respectively. For a cable diagram $D \in \mathrm{End}(W)$, define $D^{(c)}_{\ell,\ell'}$ by $i^*_{c,\ell} D i_{c,\ell'} = n_{c,\ell} D^{(c)}_{\ell,\ell'} f_c$. Let $m_c$ be the number of complete admissible labelings with total color $c$. Then $\mathrm{End}(W) \cong \bigoplus_c \mathrm{Mat}_{m_c}(F)$ by the fusion calculus of [MV, §2]. Let $D^{(c)} = (D^{(c)}_{\ell,\ell'})$ be the $m_c \times m_c$ matrix for the total color $c$, with rows and columns indexed by the admissible internal labelings of the fixed tree. The map from $\mathrm{End}(W)$ to this direct sum sends a diagram $D$ to its sequence of matrices $D^{(c)}$, indexed by total colors with $m_c > 0$. Inserting the resolution of $\mathbb{1}_W$ between two diagrams gives matrix multiplication. The inverse sends this sequence to $\sum_{c,\ell,\ell'} D^{(c)}_{\ell,\ell'} n^{-1}_{c,\ell} i_{c,\ell} i^*_{c,\ell'}$. Closure on either side gives $\sum_c \Delta_c \,\mathrm{tr}(D^{(c)})$. Thus cable evaluation and fusion evaluation give the same bracket.

Changing a fusion tree changes the basis in this isomorphism. For three boundary colors $a, b, c$ and total color $d$, let $\alpha_e = (i_{e,a,b} \otimes \mathbb{1}_{f_c}) \circ i_{d,e,c}$ and $\beta_f = (\mathbb{1}_{f_a} \otimes i_{f,b,c}) \circ i_{d,a,f}$. The first tree joins $a, b$ through $e$, and the second joins $b, c$ through $f$. Both maps have domain $f_d$ and codomain $f_a \otimes f_b \otimes f_c$. The $6j$ **coefficients** are defined, in our normalization, by

$$\alpha_e = \sum_f \begin{Bmatrix} a & b & f \\ c & d & e \end{Bmatrix} \beta_f, \tag{12}$$

where the sum runs over $f$ for which $(b, c, f)$ and $(a, f, d)$ are admissible [MV, §2, p. 368]. The coefficient has six labels $a, b, c, d, e, f$, hence the name $6j$.[15]

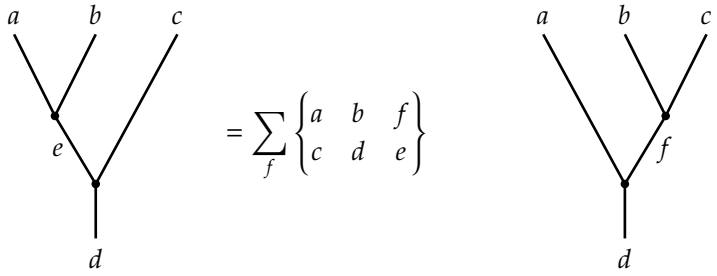



**Figure 29.** Changing from the $\alpha_e$ tree to the $\beta_f$ tree.

[15] Our integer colors are $2j$. In quantum mechanics, $j$ labels the eigenvalue $\hbar^2 j(j+1)$ of squared angular momentum. The $6j$ coefficients change the order in which three angular momenta are coupled.

The bubble identity gives $\beta_f^*\beta_f = \frac{\theta(b,c,f)\theta(a,d,f)}{\Delta_f\Delta_d}\mathbb{1}_{f_d}$. Pairing (12) with $\beta_f^*$ therefore gives

$$\begin{Bmatrix} a & b & f \\ c & d & e \end{Bmatrix} = \frac{\mathcal{E}(\mathrm{cl}(\beta_f^*\alpha_e))(1)}{\mathcal{E}(\mathrm{cl}(\beta_f^*\beta_f))(1)} = \frac{\Delta_f \left\langle \begin{matrix} a & b & e \\ c & d & f \end{matrix} \right\rangle}{\theta(b,c,f)\theta(a,d,f)}. \tag{13}$$

Following Masbaum–Vogel, let $\left\langle \begin{matrix} a & b & e \\ c & d & f \end{matrix} \right\rangle = \mathcal{E}(\mathrm{cl}(\beta_f^*\alpha_e))(1)$ denote the tetrahedron coefficient. Closing this composite joins the two trees into the tetrahedral graph in Figure 30.

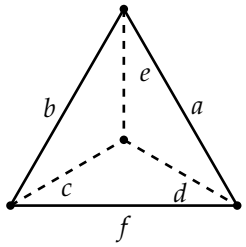



**Figure 30.** The tetrahedral graph, with its three rear edges dashed.

For completeness, the tetrahedron formula [MV, Theorem 2, p. 364] is as follows. Set

$$\begin{aligned} u_1 &= (a+b+e)/2, & u_2 &= (b+c+f)/2, \\ u_3 &= (c+d+e)/2, & u_4 &= (a+d+f)/2, \\ v_1 &= (a+b+c+d)/2, & v_2 &= (a+c+e+f)/2, \\ v_3 &= (b+d+e+f)/2. \end{aligned}$$

Then

$$\left\langle \begin{matrix} a & b & e \\ c & d & f \end{matrix} \right\rangle = \frac{\prod_{i=1}^{4}\prod_{j=1}^{3}[v_j-u_i]!}{[a]![b]![c]![d]![e]![f]!} \sum_{k=\max_i u_i}^{\min_j v_j} \frac{(-1)^k[k+1]!}{\prod_{i=1}^{4}[k-u_i]!\prod_{j=1}^{3}[v_j-k]!}. \tag{14}$$

The four vertex triples are admissible, so all the $u_i, v_j$ and the factorial arguments in the stated range are nonnegative integers. We use $[0]! = 1$.

Fix the over/under convention by assigning $\sigma_i = t\mathbb{1}_n + t^{-1}e_i$ to one elementary crossing of adjacent strands. The opposite crossing is $\sigma_i^{-1} = t^{-1}\mathbb{1}_n + te_i$. The Temperley–Lieb relations and $\delta = -t^2 - t^{-2}$ imply $\sigma_i\sigma_i^{-1} = \mathbb{1}_n$, $\sigma_i\sigma_{i+1}\sigma_i = \sigma_{i+1}\sigma_i\sigma_{i+1}$, and $\sigma_i\sigma_j = \sigma_j\sigma_i$ for $|i-j|>1$. Thus different decompositions of the same braid into adjacent crossings give the same morphism.

To form a **crossing of colors** $a, b$, replace its two strands by cables of $a$ and $b$ parallel strands along their framings, using this same over/under convention at every elementary crossing. Let $b_{a,b}$ denote the resulting braid, which exchanges the two blocks and crosses each of the $a$ strands with each of the $b$ strands once. Attaching the projectors gives $B_{a,b} = (f_b \otimes f_a)b_{a,b}(f_a \otimes f_b) : f_a \otimes f_b \to f_b \otimes f_a$. This is independent of the chosen decomposition of the cabled braid by the relations above. The opposite block crossing gives its inverse. If $V_a = \mathrm{im}\,\mathcal{E}(f_a)$, its image under the functor is the linear map $\mathcal{E}(B_{a,b}) : V_a \otimes V_b \to V_b \otimes V_a$.

For an admissible triple $(a,b,c)$, the **$c$-channel** in $f_a \otimes f_b$ is the summand isomorphic to $f_c$ included by $i_{c,a,b}$. Its projector is $p_c^{a,b} = \frac{\Delta_c}{\theta(a,b,c)} i_{c,a,b}i_{c,a,b}^*$. We use the same name for its image under $\mathcal{E}$. Similarly, the $c$-channel in $V_b \otimes V_a$ is $\mathrm{im}\,\mathcal{E}(i_{c,b,a})$. The map $\mathcal{E}(B_{a,b})$ carries the $c$-channel in $V_a \otimes V_b$ to this subspace. At the level of diagrams, this is expressed by

$$B_{a,b} \circ i_{c,a,b} = R_c^{ab}\, i_{c,b,a}, \qquad R_c^{ab} = (-1)^u t^{vw-u(u+v+w+2)}. \tag{15}$$

Here $u, v, w$ are the admissibility integers. So we say that the crossing of colors $a, b$ acts by $R_c^{ab}$ on the $c$-channel because it sends the inclusion, by composition, to the exchanged inclusion multiplied by this scalar [MV, Theorem 3 and §2]. For example, when $a = b = 1$ and $c = 0$, the inclusion is the cup, and

$$B_{1,1} \circ \mathrm{cup} = (t + t^{-1}\delta)\,\mathrm{cup} = -t^{-3}\,\mathrm{cup},$$

which is the scalar $R_0^{11}$ in (15).

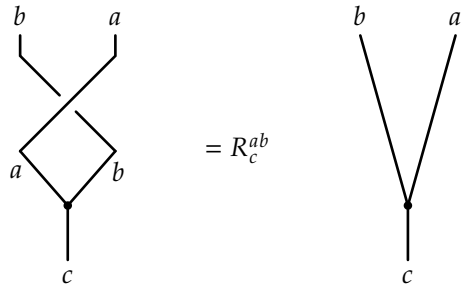



**Figure 31.** The $c$-channel identity for a colored crossing.

### A.3 Encircling a colored strand

An uncolored circle means a circle colored 1. Place such a circle around a straight strand colored $c$, with zero framing on the circle. This gives an endomorphism of $f_c$. Since $\mathrm{End}(f_c) = F f_c$, it equals $\chi_c f_c$ for a scalar $\chi_c$.

Close the $c$-strand. The resulting diagram is a Hopf link. Fuse the colors 1 and $c$ before evaluating its two crossings. In channel $e$, the crossings contribute $R_e^{1c} R_e^{c1}$ and the closure contributes $\Delta_e$. Closing $\chi_c f_c$ gives $\chi_c \Delta_c$, so

$$\chi_c = \frac{1}{\Delta_c} \sum_e \Delta_e R_e^{1c} R_e^{c1},$$

where $e = c-1, c+1$, with the first channel omitted when $c = 0$. For $c \geq 1$, the crossing formula (15) gives $R_{c+1}^{1c} = R_{c+1}^{c1} = t^c$ and $R_{c-1}^{1c} = R_{c-1}^{c1} = -t^{-c-2}$. Substituting $\Delta_e = (-1)^e[e+1]$ therefore yields

$$\chi_c = \frac{\Delta_{c+1} t^{2c} + \Delta_{c-1} t^{-2c-4}}{\Delta_c} = -\left(t^{2c+2} + t^{-2c-2}\right) \qquad (c \geq 1). \tag{16}$$

For $c = 0$, the sole channel $e = 1$ gives $\chi_0 = \Delta_1 = \delta = -t^2 - t^{-2}$, so the same final formula holds. If a collection of strands has first been fused to color $b$, an uncolored circle around that collection consequently acts by $\chi_b$. Adding $j$ parallel circles gives $\chi_b^j$.

### A.4 Morse words

Choose a height direction in the diagram so that its local minima, local maxima, and crossings have distinct heights. Sweeping from bottom to top, record a cup at each minimum, a cap at each maximum, and a crossing whenever two strands cross. This ordered list is a **Morse word**. Number the current strands from left to right. Each entry specifies the two adjacent strand positions involved and, for a crossing, which strand passes over the other. A cup creates two strands, a cap removes two strands, and a crossing exchanges their positions. Stacking these elementary pieces in the recorded order reconstructs the diagram [KA].

Since we read from left to right, we'll write the word from left to right. Write $\cup_j^i$ and $\cap_j^i$ for a cup and a cap on adjacent positions $i < j$. The crossing symbols ${}_b^a\!\times_d^c$ and ${}_b^a\!\times_d^c$ have input positions $a, b$ and output positions $c, d$, listed from top to bottom. The symbols mean what they look like. Unshown strands continue straight. Adjacent symbols join at their matching boundary positions, so the word itself assembles into the diagram.

For example, $\cup^{1}_{2}\ \cup^{3\ 2}_{4\ 3}\ \times^{2\ 2}_{3\ 3}\ \times^{2\ 1}_{3\ 2}\ \times^{1\ 1}_{2\ 2}\ \times^{1\ 2}_{2\ 3}\ \cap^{1}_{2}$ is a Morse word for the figure-eight knot $4_1$ [KA], drawn in Figure 32.

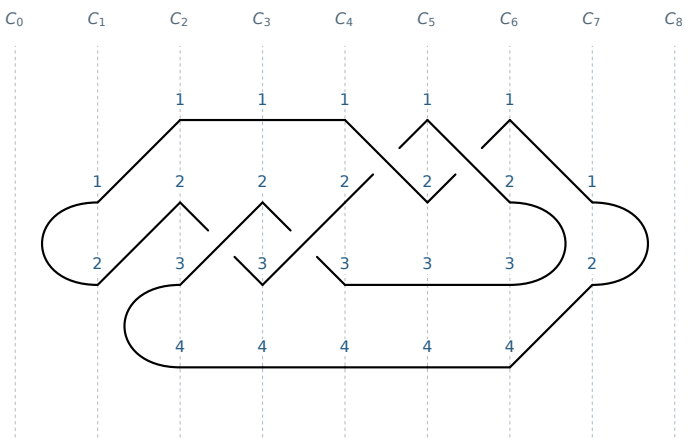



**Figure 32.** The Morse word for $4_1$, read from left to right. Dashed lines mark the cuts $C_k$ after $k$ letters, the numbers give strand positions at each cut.

A **colored Morse word** records the colors at each cut between successive letters. Number the strands from 1. We write $v^r_i$ for $r$ consecutive strands of color $v$ beginning at position $i$, and omit the exponent when $r = 1$. Strands of color 1 are omitted when another color is present. Stack the remaining entries in a vertical column of boxes, one box for each run, in strand order. Thus

$$(a,1,1,1,1,1,1,a) \longleftrightarrow \boxed{\begin{matrix} a_1 \\ a_8 \end{matrix}}, \qquad (a,a) \longleftrightarrow \boxed{a_1^2}, \qquad (a,b,b,a) \longleftrightarrow \boxed{\begin{matrix} a_1 \\ b_2^2 \\ a_4 \end{matrix}}.$$

The superscript counts repeated colors. The initial number of strands and the cups and caps determine the number of strands at every cut, including trailing strands of color 1. If all $n > 0$ strands have color 1, write $\boxed{1^n_1}$. We write $\varnothing$ only when there are no strands. Together with the Morse letters and the initial strand count, these records determine the colored tangle.

For the formulas below, $\mathbf{a}_k = (a_{k,1}, \ldots, a_{k,m_k})$ denotes the expanded list of colors at the $k$th cut. We write the colored word from left to right, inserting its sparse color records between consecutive letters.

At a cut with $m$ strands and expanded color list $\mathbf{a}$, put $a_i$ for its $i$th entry. The permitted letters are as follows.

- A cup $\cup^{i}_{i+1}$ is permitted for $1 \le i \le m+1$. If its color is $a$, it inserts $a, a$ at the new positions $i, i+1$, giving $m+2$ strands.
- A cap $\cap^{i}_{i+1}$ is permitted for $1 \le i < m$ and $a_i = a_{i+1}$. It removes those two entries, leaving $m-2$ strands.
- Either crossing $\times^{i\ i}_{i+1\ i+1}$ or $\times^{i\ i}_{i+1\ i+1}$ is permitted for $1 \le i < m$. It exchanges $a_i, a_{i+1}$ and leaves the number of strands unchanged.

After each letter, number the remaining strands consecutively from 1. A word is **valid** if every letter is permitted and the color records agree with these updates. It is **closed** if it has no incoming or outgoing strands, so its initial and final strand counts are both zero.

For example, starting with no strands, $\varnothing\ \cup^{1}_{2}\boxed{1^2_1}\cap^{1}_{2}\ \varnothing$ is valid and closed. Starting with two strands, $\boxed{2_2}\ \times^{1\ 1}_{2\ 2}\boxed{2_1}$ is a valid crossing with its input and output colors recorded. Starting with no strands, the word $\varnothing$

$\overset{1}{2}\!\smile\varnothing$ is invalid because positions $1, 2$ do not exist, and $\boxed{2_2}\overset{1}{2}\!\smile\varnothing$ is invalid because the colors joined by the cap differ.

For an expanded color list $\mathbf{a}$ with $m$ entries, put $W(\mathbf{a}) = \bigotimes_{j=1}^{m} f_{a_j}$, with $W(()) = f_0$. A permitted letter $g$ with input column $\mathbf{a}$ and output column $\mathbf{b}$ defines an **elementary colored morphism** $G(\mathbf{a}, g, \mathbf{b}) : W(\mathbf{a}) \to W(\mathbf{b})$ as follows. For a cup of color $a$, the local map is $i_{0,a,a} : f_0 \to f_a \otimes f_a$, and for a cap it is $i^*_{0,a,a} : f_a \otimes f_a \to f_0$. For an overcrossing with incoming colors $a, b$, the local map is $B_{a,b} : f_a \otimes f_b \to f_b \otimes f_a$. For an undercrossing with the same incoming colors, it is $(B_{b,a})^{-1} : f_a \otimes f_b \to f_b \otimes f_a$. If $L$ and $R$ are the tensor products of the unaffected projectors before and after the letter's positions, and $h$ is its local map, then $G(\mathbf{a}, g, \mathbf{b}) = \mathbb{1}_L \otimes h \otimes \mathbb{1}_R$. Empty tensor products mean $f_0$.

**Theorem 17** (Fusion evaluation)**.** *Let $D : W_0 \to W_N$ be a colored framed tangle over $F = \mathbb{Q}(t)$, given by a valid colored Morse word with letters $g_1, \dots, g_N$ and color columns $\mathbf{a}_0, \dots, \mathbf{a}_N$ in sweep order. Put $W_k = W(\mathbf{a}_k)$ and $G_k = G(\mathbf{a}_{k-1}, g_k, \mathbf{a}_k)$, so that $D = G_N \circ \cdots \circ G_1$. The algorithm starts from the input color column $\mathbf{a}_0$ and the identity on $W_0 = W(\mathbf{a}_0)$. It terminates and returns the fusion matrices of $D$, without expanding colored cables into individual strands. Perform the following steps for each admissible total color $c$ of the input column, keeping $c$ fixed during the sweep.*

1. *At the cut after $g_k$, choose the tree that first fuses the first two cables, then fuses the resulting cable with the third, and so on. This left-associated tree has one leaf for each cable at the cut, colored in order by $a_{k,1}, \dots, a_{k,m_k}$. Let $\mathbf{L}_k$ be the set of its admissible internal labelings with total color $c$. For each $\ell \in \mathbf{L}_k$, write $i^{(k)}_{c,\ell} : f_c \to W_k$ for its inclusion. The total color $c$ stays fixed while the cut and its internal labels change.*

   *The accumulator is a matrix with rows indexed by the current labelings and columns indexed by the input labelings, $v_k : \mathbf{L}_k \times \mathbf{L}_0 \to F$. Its entry $v_k(\ell, m)$ is the coefficient of the current inclusion $i^{(k)}_{c,\ell}$ in the image of the input inclusion $i^{(0)}_{c,m}$. Initialize it to $v_0 = \mathbb{1}_{W_0}$. At every stage, for each $m \in \mathbf{L}_0$, the accumulator records*

$$G_k \circ \cdots \circ G_1 \circ i^{(0)}_{c,m} = \sum_{\ell \in \mathbf{L}_k} v_k(\ell, m)\, i^{(k)}_{c,\ell}.$$

2. *For each letter $g_k$ and input labeling $\ell \in \mathbf{L}_{k-1}$, expand the image of its basis diagram in the basis at the next cut,*

$$G_k \circ i^{(k-1)}_{c,\ell} = \sum_{\ell' \in \mathbf{L}_k} V_k(\ell', \ell)\, i^{(k)}_{c,\ell'}.$$

   *Thus $V_k(\ell', \ell) \in F$ is the coefficient of output labeling $\ell'$ produced from input labeling $\ell$. Compute these coefficients by the following local rules, using (12) for each change of tree.*

   - *A cup $\overset{i}{j}\!\frown$ of color $a$ inserts the pair $a, a$ joined through color $0$, with coefficient $1$. Recouple the resulting tree to the chosen tree at the next cut.*
   - *For a cap $\overset{i}{j}\!\smile$ of color $a$, first recouple so that its two strands meet at one vertex. Discard every term whose joining color is nonzero. In each remaining term, remove the pair and multiply by $\Delta_a$, then recouple to the next tree.*
   - *For a crossing of colors $a, b$, first recouple so that these strands meet at one vertex of color $e$. Multiply by $R^{ab}_e$ for $\overset{i}{j}\!\times\!\overset{i}{j'}$ or by $(R^{ab}_e)^{-1}$ for $\overset{i}{j}\!\times\!\overset{i}{j'}$ exchange the two boundary colors, and recouple to the next tree.*

   *In each case, add the products of the local coefficients over all terms with the same output labeling $\ell'$ to obtain $V_k(\ell', \ell)$. Evaluate the $6j$ coefficients by (13) and (14).*

3. *Process the letters in order, for $k = 1, \dots, N$, using*

$$v_k(\ell', m) = \sum_{\ell \in \mathbf{L}_{k-1}} V_k(\ell', \ell)\, v_{k-1}(\ell, m), \qquad \ell' \in \mathbf{L}_k, \quad m \in \mathbf{L}_0.$$

*For each input column $m$, add all contributions to the same output labeling and retain only nonzero entries. After the last letter, return $D^{(c)} = (v_N(\ell, m))_{\ell \in \mathbf{L}_N,\, m \in \mathbf{L}_0}$.*

pf. The cup rule is the definition of $i_{0,a,a}$. The cap rule follows from orthogonality of distinct joining colors and the bubble identity $i^*_{0,a,a} i_{0,a,a} = \Delta_a \mathbb{1}_0$. These local joining colors are distinct from the fixed total color $c$. The crossing rule is (15), and the changes of tree are (12). Thus the local rules compute exactly the coefficients $V_k(\ell', \ell)$ in step 2. Before the first letter, the processed morphism is $\mathbb{1}_{W(\mathbf{a}_0)}$, whose matrix is precisely the specified $v_0$. Composing with each $G_k$ multiplies the current matrix on the left by $V_k$. Collecting the coefficient of each output inclusion proves the accumulator identity by induction, simultaneously for every input column $m$. Hence $v_N$ is the matrix of $D$ in total color $c$. Write $(i^{(0)}_{c,m})^* i^{(0)}_{c,m} = n^{(0)}_{c,m} f_c$ for the input fusion norms. The fusion resolution of the input identity recovers the tangle as

$$D = \sum_{c,\ell,m} v_N^{(c)}(\ell, m)\, (n^{(0)}_{c,m})^{-1} i^{(N)}_{c,\ell} (i^{(0)}_{c,m})^*,$$

where the superscript on $v_N^{(c)}$ records the total color for this sum. For termination, every internal color is bounded by the sum of the leaf colors in its subtree, so each $\mathbf{L}_k$ and each local channel sum is finite. A finite sequence of tree rotations gives each required recoupling. The factorial formulas use finitely many operations in $F$, with nonzero denominators on admissible labels, and there are exactly $N$ updates. ∎

For the punctured-disk evaluations, $\mathbf{a}_0 = (a, b)$ and $W_0 = f_a \otimes f_b$. Each admissible total color $c$ has one input fusion state, so its initial matrix is the one-by-one matrix (1). Our evaluator stores this sole column as a map from current fusion labels to coefficients. If $W_N = W_0$, the final matrix also has one entry $v_N$, characterized by

$$D \circ i_{c,a,b} = v_N i_{c,a,b}, \qquad v_N f_c = \frac{\Delta_c}{\theta(a, b, c)}\, i^*_{c,a,b} D i_{c,a,b}.$$

## B Ore algebras, modules, and boundary recurrences

Ore algebras give a common algebraic framework for linear differential equations with algebraic coefficients, difference equations, and $q$-difference equations. Differentiation and the two kinds of shift obey different commutation rules with multiplication by coefficients, encoded by the maps $\sigma_i, \delta_i$. Once these rules are specified, equations in all three settings can be treated as modules over the resulting operator algebra [CS, §1][KJJ, §2].

Let $\mathcal{A}$ be the operator algebra and $\mathcal{F}$ a chosen $\mathcal{A}$-module of functions or sequences. For a left $\mathcal{A}$-module $\mathcal{M}$, its solutions in $\mathcal{F}$ form $\mathrm{Sol}_{\mathcal{F}}(\mathcal{M}) := \mathrm{Hom}_{\mathcal{A}}(\mathcal{M}, \mathcal{F})$. If $I$ is the left ideal generated by a system of scalar equations, then $\mathcal{M} = \mathcal{A}/I$. A homomorphism from this module to $\mathcal{F}$ is determined by the image $f$ of $1 + I$, and the condition on $f$ is exactly $Pf = 0$ for every $P \in I$. This is the module formulation of differential systems and their solutions used in $D$-module theory [Sa, Chapter I, §3.1].

Conversely, a function or sequence $f \in \mathcal{F}$ determines the annihilator ideal $\mathrm{Ann}_{\mathcal{A}}(f) = \{P \in \mathcal{A} : Pf = 0\}$ and the cyclic module $\mathcal{A}f \simeq \mathcal{A}/\mathrm{Ann}_{\mathcal{A}}(f)$. Thus systems of equations, their solution spaces, and modules defined by annihilators use the same constructions for differential, difference, and $q$-difference operators. In the $q$-difference setting this is the module framework of Sabbah's holonomic theory and Garoufalidis–Lê's survey [Sb][GLb, §3].

### B.1 The Ore category

An object of Ore consists of a commutative integral domain $R$, finitely many pairs $(\sigma_i, \delta_i)$, $1 \le i \le r$, and the presented operator algebra

$$\mathcal{A} = R\big[\partial_i \,\big|\, \sigma_i, \delta_i\big\rangle.$$

Each $\sigma_i : R \to R$ is a unital ring endomorphism, and $\delta_i : R \to R$ is an additive $\sigma_i$-derivation, so

$$\delta_i(ab) = \sigma_i(a)\delta_i(b) + \delta_i(a)b.$$

For distinct indices, the $\sigma_i$ commute with one another, the $\delta_i$ commute with one another, and $\sigma_i\delta_j = \delta_j\sigma_i$. The adjoined generators $\partial_i$ commute with one another. These compatibility conditions give a free left $R$-module with basis $\partial^\alpha := \prod_{i=1}^r \partial_i^{\alpha_i}$, $\alpha \in \mathbb{N}^r$, and multiplication determined by the Ore rule [KJJ, §2],

$$\partial_i a = \sigma_i(a)\partial_i + \delta_i(a), \qquad a \in R. \tag{17}$$

Let $\mathcal{B} = S\big[\partial'_j \,\big|\, \sigma'_j, \delta'_j\big\rangle$, with $1 \le j \le s$, be another object. A morphism $\Phi\colon \mathcal{A} \to \mathcal{B}$ consists of a unital ring homomorphism $\phi\colon R \to S$ and commuting elements $P_1, \dots, P_r \in \mathcal{B}$ satisfying

$$P_i\phi(a) = \phi(\sigma_i(a))P_i + \phi(\delta_i(a)) \qquad (a \in R). \tag{18}$$

Every operator has a unique finite expression $\sum_\alpha a_\alpha \partial^\alpha$, with $a_\alpha \in R$ written on the left. The morphism acts on this expression by

$$\Phi\left(\sum_\alpha a_\alpha \partial^\alpha\right) = \sum_\alpha \phi(a_\alpha) P_1^{\alpha_1} \cdots P_r^{\alpha_r}.$$

The conditions preserve all defining relations. Conversely, every unital ring homomorphism carrying $R$ into $S$ has this form. Composition is composition of ring homomorphisms, with coefficient map $\psi\phi$ and operator images $\Psi(P_i)$. The identity fixes all generators. These operations define the category Ore.

### B.2 Operators and their coordinate matrices

Suppose a left $\mathcal{A}$-module $\mathcal{V}$ is free of rank $d$ as an $R$-module, with basis $e_1, \dots, e_d$. A coefficient $a \in R$ acts by scalar multiplication. Thus coefficients are themselves operators: on coordinate columns, $a$ acts by $v \mapsto av$, with matrix $aI_d$. For each generator $\partial_i$, let $D_i$ be its action on $\mathcal{V}$, so $D_i(av) = \sigma_i(a)D_i(v) + \delta_i(a)v$ for $a \in R$ and $v \in \mathcal{V}$. Define $B_i = (b_{kj}^{(i)}) \in \mathrm{Mat}_d(R)$ by $D_i(e_j) = \sum_k b_{kj}^{(i)} e_k$. The Ore rule gives

$$D_i\left(\sum_j v_j e_j\right) = \sum_j \sigma_i(v_j) D_i(e_j) + \sum_j \delta_i(v_j) e_j.$$

Identifying $\mathcal{V}$ with its coordinate columns in $R^d$, this is

$$D_i(v) = B_i\sigma_i(v) + \delta_i(v).$$

Thus $\partial_i$ is an algebra element, $D_i$ is its action, and $B_i$ is the matrix whose columns record its values on the basis. The coordinate formula includes the $\delta_i$ term even though $B_i$ has entries in the commutative coefficient ring $R$.

For an Ore operator $\widehat{F} = \sum_\alpha f_\alpha \partial_1^{\alpha_1} \cdots \partial_r^{\alpha_r}$, with $f_\alpha \in R$, the action is

$$\widehat{F} \cdot v = \sum_\alpha f_\alpha D_1^{\alpha_1} \cdots D_r^{\alpha_r}(v).$$

Every composition uses the full coordinate rule above. For one generator, write $D(v) = B\sigma(v) + \delta(v)$. Its iterates are computed from $w_0 = v$ and

$$w_{m+1} = B\sigma(w_m) + \delta(w_m), \qquad w_m = D^m(v).$$

For example, $D^2(v) = B\sigma(B\sigma(v) + \delta(v)) + \delta(B\sigma(v) + \delta(v))$.

When $\delta = 0$, put $B_0 = I_d$ and $B_{m+1} = B\sigma(B_m)$. Then $D^m(v) = B_m\sigma^m(v)$, so in particular $D^2(v) = B\sigma(B)\sigma^2(v)$. When $\sigma = \mathrm{id}$, the coordinate rule instead reads $D(v) = Bv + \delta(v)$, as for differential operators. All applications of $\sigma_i$ or $\delta_i$ to columns and matrices are entrywise applications to elements of $R$.

Regard $\mathcal{A}$ as a one-object category enriched over **Ab**, the category of abelian groups, with hom-object the additive group of $\mathcal{A}$ and composition given by its multiplication. A left $\mathcal{A}$-module is equivalently an **Ab**-enriched functor from this category to **Ab** with its usual enrichment. It sends the single object to the underlying abelian group of the module and each operator to its additive action on that group.

A choice of basis expresses this action in the coordinates above. The resulting formulas reduce the action of an Ore operator to arithmetic in the coefficient ring and applications of the specified maps $\sigma_i, \delta_i$. This is what enables software to compute with Ore operators and their actions. The `ore_algebra` package for SageMath implements Ore-operator arithmetic and actions, including user-specified $\sigma_i, \delta_i$ and application rules [KJJ, §§2–3]. Its coefficient rings are drawn from supported polynomial rings and fraction fields, and actions on expressions may need to be provided by the user. Other implementations include Maple's `OreTools` and Mathematica's `HolonomicFunctions` [Mb, K].

### B.3 The $q$-Weyl subcategory

Let $q$ be indeterminate and put $k = \mathbb{Q}(q)$. Following Garoufalidis–Lê, let $\mathcal{W}_{r,+}$ be the subalgebra of the quantum Weyl algebra generated by the nonnegative powers of $E_i, Q_i$ for $1 \le i \le r$ [GLb, §3.2]. It is

$$\mathcal{W}_{r,+} = k[Q_i]\big[E_i \,\big|\, \sigma_i\big\rangle, \qquad \sigma_i(Q_j) = q^{\delta_{ij}}Q_j. \tag{19}$$

Here the $Q_i$ generate the coefficient ring $k[Q_i]$, and the $E_i$ are the adjoined Ore generators. The $Q_i$ are therefore also elements of the operator algebra. On the sequence module, a coefficient $a \in k[Q_i]$ acts by $(af)(\mathbf{n}) = a(q^{n_1}, \dots, q^{n_r})f(\mathbf{n})$. In particular, $Q_i$ is the operator of multiplication by $q^{n_i}$. The Ore rule $E_iQ_j = \sigma_i(Q_j)E_i = q^{\delta_{ij}}Q_jE_i$ describes composition of this multiplication operator with the shift [GLb, §§2.2, 3.1]. Equivalently, the $Q_i$ commute, the $E_i$ commute, and $E_iQ_j = q^{\delta_{ij}}Q_jE_i$. On functions of $\mathbf{n} \in \mathbb{N}^r$ the action is

$$(E_if)(\mathbf{n}) = f(\mathbf{n} + \mathbf{e}_i), \qquad (Q_if)(\mathbf{n}) = q^{n_i}f(\mathbf{n}).$$

These are the operators denoted $L_i, M_i$, respectively, in the survey [GLb, §§2–3].

Define q-Weyl to be the full subcategory of Ore on the objects $\mathcal{W}_{r,+}$ and their coefficient extensions $R\big[E_i \,\big|\, \widetilde{\sigma}_i\big\rangle$. Here $\iota : k[Q_i] \hookrightarrow R$ is the coefficient embedding. We write $\widetilde{\sigma}_i := \iota^*\sigma_i$ for the chosen commuting extensions $\widetilde{\sigma}_i : R \to R$, meaning $\widetilde{\sigma}_i(\iota(a)) = \iota(\sigma_i(a))$ for every $a \in k[Q_i]$. In particular, coefficient localizations are objects of this subcategory. Its morphisms are exactly the Ore morphisms between these objects. Explicitly, the coefficient map $\phi$ and the commuting operator images $P_i$ must obey $P_i\phi(a) = \phi(\widetilde{\sigma}_i(a))P_i$ for every $a \in R$. When the target is presented by $q', Q'_j, E'_j$, this includes $P_i\phi(Q_j) = \phi(q)^{\delta_{ij}}\phi(Q_j)P_i$. This condition allows parameter substitutions and coefficient embeddings while retaining the operator relations.

For $r = 1$, a chosen sequence $f$ gives the cyclic module $\mathcal{W}_{1,+}f \simeq \mathcal{W}_{1,+}/\mathrm{Ann}_{\mathcal{W}_{1,+}}(f)$. For a finitely generated $\mathcal{W}_{r,+}$-module $\mathcal{M}$, use the filtration $F_\ell\mathcal{M}$ induced by total degree in $Q_i, E_i$. For sufficiently large $\ell$, $\dim_k F_\ell\mathcal{M}$ agrees with a polynomial in $\ell$. When $\mathcal{M} \neq 0$, define $d(\mathcal{M})$ to be the degree of this polynomial, called the dimension of the module, and set $d(0) = 0$. If $\mathcal{M} \neq 0$ has no monomial torsion, then $d(\mathcal{M}) \ge r$. A finitely

generated module without monomial torsion is $q$-holonomic when $d(\mathcal{M}) \leq r$ [GLb, §3.2, Definition 3.1]. Sabbah's Bernstein inequality supplies the dimension bound [Sb, §§1.5, 2.1]. Here $q$-holonomicity is a property of a module over the operator ring, expressed by this dimension condition.

For one variable, localizing $\mathbb{Q}(q)[Q]$ at the multiplicative subset $\mathbb{Q}(q)[Q] \setminus \{0\}$ gives the field $\mathbb{K} = \mathbb{Q}(q, Q)$. The coefficient inclusion commutes with $\sigma$ and extends by $E \mapsto E$ to a morphism of $q$-Weyl algebras

$$\mathcal{W}_{1,+} \longrightarrow \mathcal{D} = \mathbb{K}\big\langle E \,\big|\, \sigma \big\rangle, \qquad \sigma(Q) = qQ. \tag{20}$$

This is Garoufalidis's localization [Gb, §2.2]. Its multiplication is $(aE^i)(bE^j) = a\sigma^i(b)E^{i+j}$ with $i, j \geq 0$. Only coefficient polynomials in $Q$ are inverted. For example, $\mathcal{W}_{1,+}/\mathcal{W}_{1,+}Q$ is nonzero but becomes zero over $\mathcal{D}$, since $Q$ becomes a unit. Rational coefficients act on equivalence classes of sequences, where two sequences are identified if they agree at all sufficiently large indices [Gb, §2.2]. A nonzero polynomial in $Q$ over $\mathbb{Q}(q)$ vanishes at $Q = q^n$ for only finitely many $n$, so its reciprocal acts on these classes. On these sequence classes, extension of the annihilator gives

$$\mathrm{Ann}_{\mathcal{D}}(J) = \mathcal{D}\,\mathrm{Ann}_{\mathcal{W}_{1,+}}(J).$$

Garoufalidis–Lê's $q$-holonomicity theorem ensures that this ideal is nonzero [GLa, Theorem 1]. The reason for passing to $\mathcal{D}$ is that it admits Euclidean division in $E$ and is therefore a left principal ideal domain. Thus $\mathrm{Ann}_{\mathcal{D}}(J)$ has a unique monic generator of minimal $E$-order, which is $\widehat{A}$ [L, §0.1.4].

In the peripheral coordinates the coefficient field is $\mathbb{K} = \mathbb{Q}(t, M)$, with $\sigma(t, M) = (t, t^{-2}M)$. The coefficient embedding $\phi(q, Q) = (t^{-4}, M^2)$ extends to an embedding in q-Weyl fixing $E$, since $\sigma\phi = \phi\sigma$. It also extends after coefficient localization. A computed operator over $\mathbb{Q}(t, M)$ comes from an operator over $\mathbb{Q}(q, Q)$ when its coefficients belong to the image of this embedding. For the computed relations in this paper, exact coefficient comparison with the embedded $q, Q$ relation checks this.

For the peripheral action, the annihilator of $\varnothing$ in $\mathbb{Q}(t, M)\big\langle L \,\big|\, \sigma \big\rangle$ has a unique monic generator of minimal $L$-order, denoted $\widehat{P}$ [L, §4.3]. The localized skein module is finite-dimensional, so the iterates $\varnothing, L\varnothing, L^2\varnothing, \ldots$ are linearly dependent. Their first dependence yields this generator, as in Lê's proof of Proposition 6.1 [L, §6.1].

## C The peripheral diagrams for $8_{11}$

The green strands trace the longitude $\lambda$ and the black strands are the puncture strands. Match the endpoints $b_0, \ldots, b_{23}$ at the dashed cut to join the two halves.

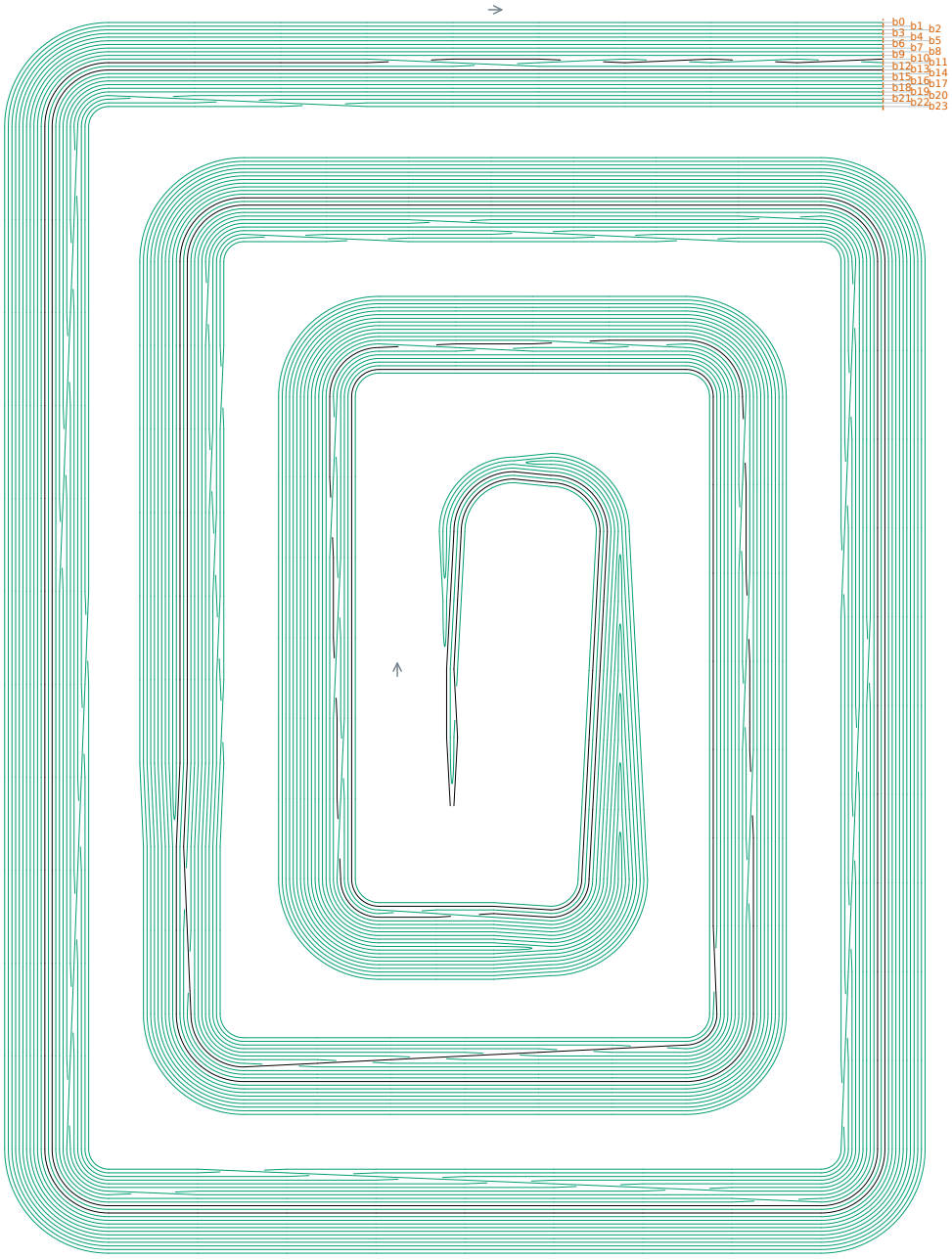



**Figure 33.** $L(\lambda)$ for $8_{11}$, with 79 crossings.

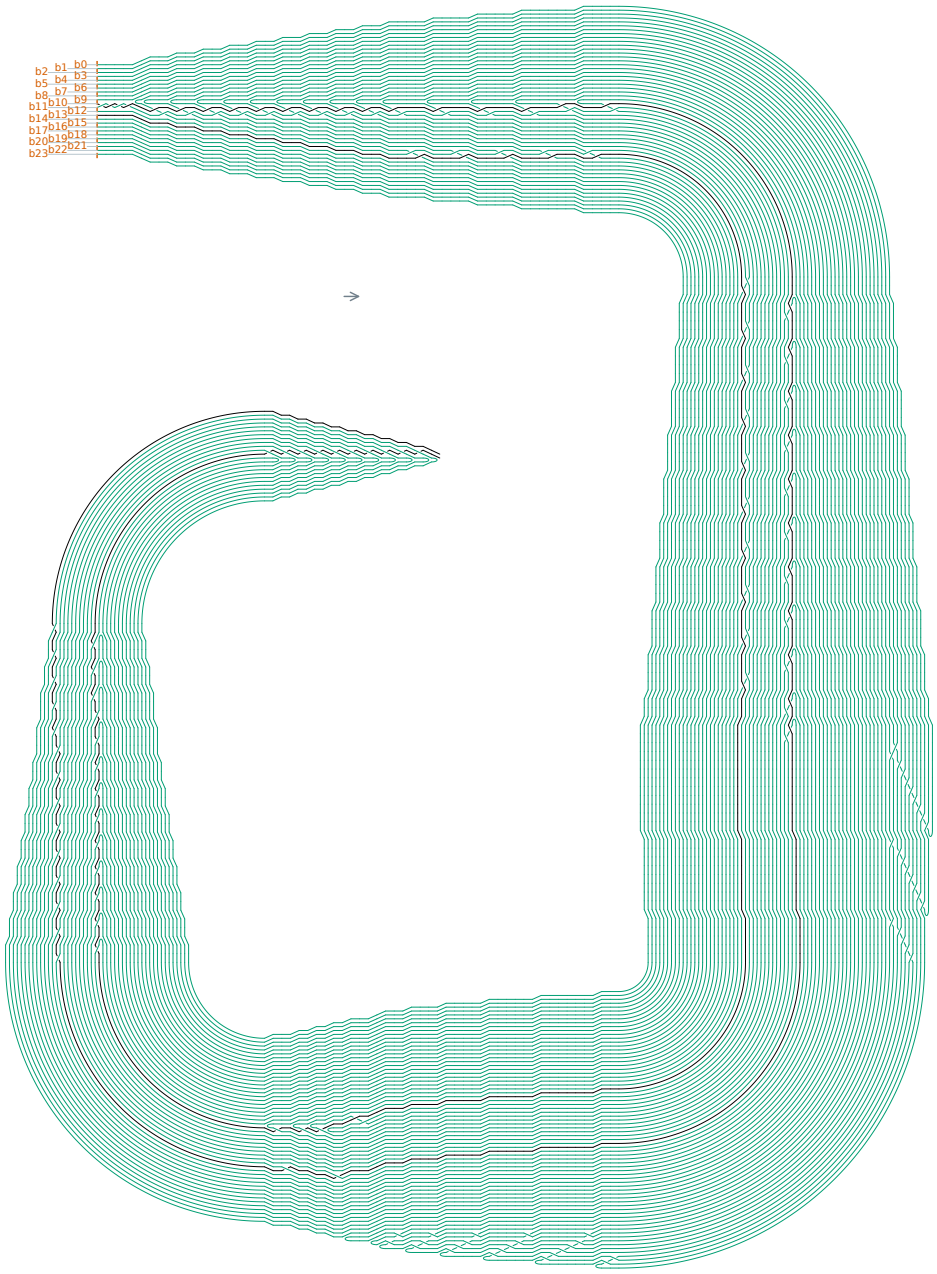
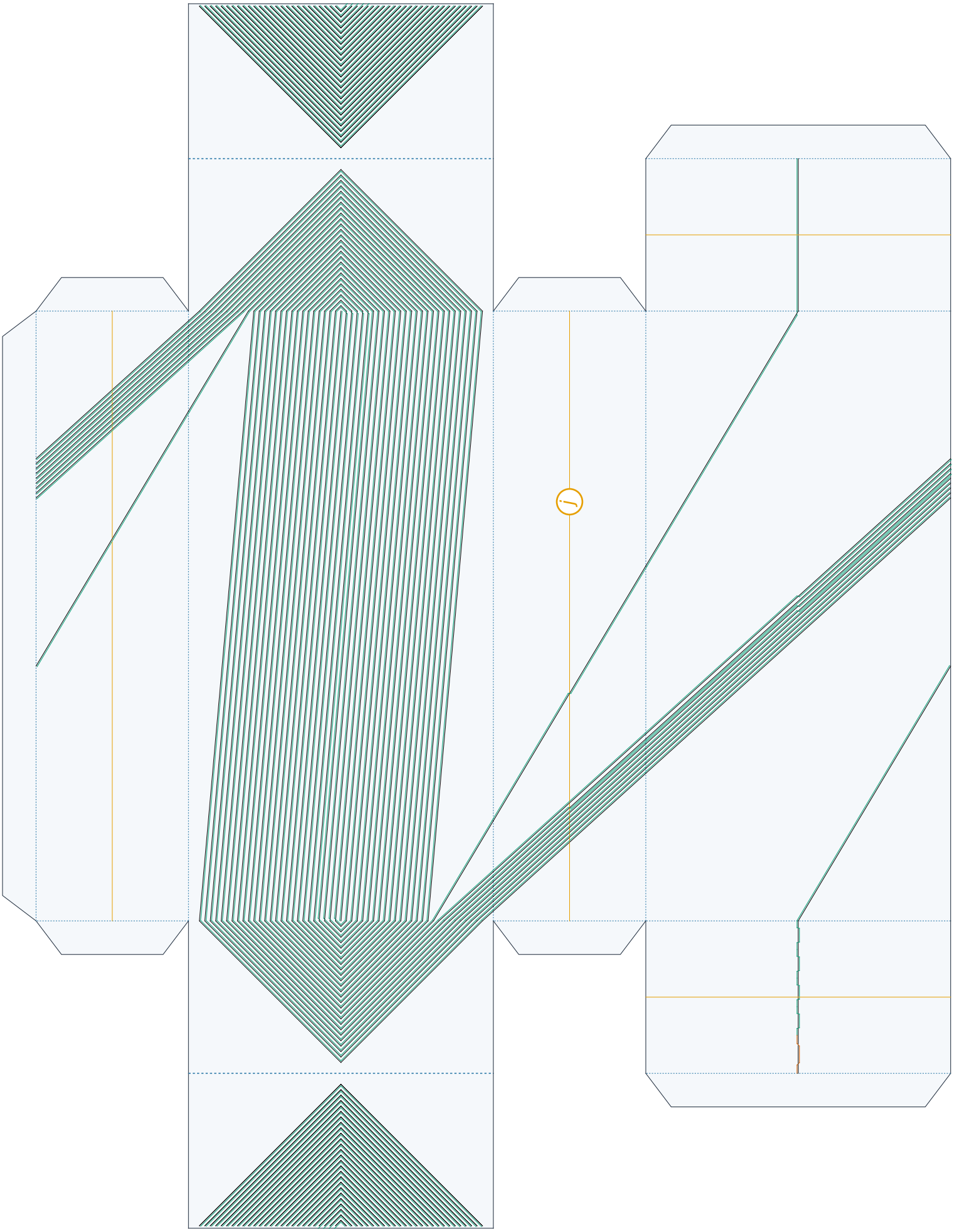



**Figure 34.** $R(\lambda)$ for $8_{11}$, with 175 crossings.



## References


[JS] W. H. Jaco and P. B. Shalen. *Seifert fibered spaces in 3-manifolds*. Vol. 21. Memoirs of the American Mathematical Society 220. American Mathematical Society, 1979. DOI: 10.1090/memo/0220.

[J] K. Johannson. *Homotopy Equivalences of 3-Manifolds with Boundaries*. Vol. 761. Lecture Notes in Mathematics. Berlin: Springer, 1979. DOI: 10.1007/BFb0085406.

[WGD] P. S. Wang, M. J. T. Guy, and J. H. Davenport. "$p$-adic reconstruction of rational numbers". In: *ACM SIGSAM Bulletin* 16.2 (1982), pp. 2–3. DOI: 10.1145/1089292.1089293.

[Sa] C. Sabbah. "Introduction to algebraic theory of linear systems of differential equations". In: *Éléments de la théorie des systèmes différentiels*. Ed. by P. Maisonobe and C. Sabbah. Vol. 45. Travaux en Cours. Paris: Hermann, 1993, pp. 1–80. URL: https://perso.pages.math.cnrs.fr/users/claude.sabbah/livres/sabbah_cimpa90.pdf.

[Sb] C. Sabbah. "Systèmes holonomes d'équations aux $q$-différences". In: *D-modules and microlocal geometry*. Berlin: de Gruyter, 1993, pp. 125–147. URL: https://perso.pages.math.cnrs.fr/users/claude.sabbah/articles/eqdfbis.pdf.

[CCGLS] D. Cooper et al. "Plane curves associated to character varieties of 3-manifolds". In: *Inventiones Mathematicae* 118 (1994), pp. 47–84.

[KL] L. H. Kauffman and S. L. Lins. *Temperley–Lieb Recoupling Theory and Invariants of 3-Manifolds*. Annals of Mathematics Studies 134. Princeton University Press, 1994.

[MV] G. Masbaum and P. Vogel. "3-valent graphs and the Kauffman bracket". In: *Pacific Journal of Mathematics* 164 (1994), pp. 361–381. DOI: 10.2140/pjm.1994.164.361.

[B] D. Bullock. "Rings of $SL_2(\mathbb{C})$-characters and the Kauffman bracket skein module". In: *Commentarii Mathematici Helvetici* 72.4 (1997), pp. 521–542. arXiv: q-alg/9604014.

[APP] S. A. Abramov, P. Paule, and M. Petkovšek. "$q$-hypergeometric solutions of $q$-difference equations". In: *Discrete Mathematics* 180.1–3 (1998), pp. 3–22. DOI: 10.1016/S0012-365X(97)00106-4.

[CS] F. Chyzak and B. Salvy. "Non-commutative elimination in Ore algebras proves multivariate identities". In: *Journal of Symbolic Computation* 26.2 (1998), pp. 187–227. DOI: 10.1006/jsco.1998.0207.

[FG] C. Frohman and R. Gelca. "Skein modules and the noncommutative torus". In: *Transactions of the American Mathematical Society* 352 (2000), pp. 4877–4888. arXiv: math/9806107.

[PS] J. H. Przytycki and A. S. Sikora. "On skein algebras and $SL_2(\mathbb{C})$-character varieties". In: *Topology* 39 (2000), pp. 115–148. arXiv: q-alg/9705011.

[FGL] C. Frohman, R. Gelca, and W. Lofaro. "The $A$-polynomial from the noncommutative viewpoint". In: *Transactions of the American Mathematical Society* 354 (2002), pp. 735–747. arXiv: math/9812048.

[Ga] R. Gelca. "On the relation between the $A$-polynomial and the Jones polynomial". In: *Proceedings of the American Mathematical Society* 130.4 (2002), pp. 1235–1241. DOI: 10.1090/S0002-9939-01-06157-3. arXiv: math/0004158.

[H] K. Habiro. "On the quantum $sl_2$ invariants of knots and integral homology spheres". In: *Geometry & Topology Monographs* 4 (2002), pp. 55–68. arXiv: math/0211044.

[Ma] G. Masbaum. "Skein-theoretical derivation of some formulas of Habiro". In: *Algebraic & Geometric Topology* 3 (2003), pp. 537–556. arXiv: math/0306345.

[DG] N. M. Dunfield and S. Garoufalidis. "Non-triviality of the $A$-polynomial for knots in $S^3$". In: *Algebraic & Geometric Topology* 4 (2004), pp. 1145–1153. DOI: 10.2140/agt.2004.4.1145. arXiv: math/0405353.

[Gb] S. Garoufalidis. "On the characteristic and deformation varieties of a knot". In: *Geometry & Topology Monographs* 7 (2004), pp. 291–309. arXiv: math/0306230.

[GLa] S. Garoufalidis and T. T. Q. Lê. "The colored Jones function is $q$-holonomic". In: *Geometry & Topology* 9 (2005), pp. 1253–1293. arXiv: math/0309214.

[KS] T. Kitano and M. Suzuki. "A partial order in the knot table". In: *Experimental Mathematics* 14.4 (2005), pp. 385–390. DOI: 10.1080/10586458.2005.10128937.

[FFRS] J. Fröhlich et al. "Correspondences of ribbon categories". In: *Advances in Mathematics* 199.1 (2006), pp. 192–329. DOI: 10.1016/j.aim.2005.04.007. arXiv: math/0309465.

[GS] S. Garoufalidis and X. Sun. "The $C$-polynomial of a knot". In: *Algebraic & Geometric Topology* 6 (2006), pp. 1623–1653. DOI: 10.2140/agt.2006.6.1623. arXiv: math/0504305.

[L] T. T. Q. Lê. "The colored Jones polynomial and the $A$-polynomial of knots". In: *Advances in Mathematics* 207 (2006), pp. 782–804. arXiv: math/0407521.

[W] Z. Wang. *Topological Quantum Computation*. CBMS Regional Conference Series in Mathematics 112. American Mathematical Society, 2010. DOI: 10.1090/cbms/112.

[GK] S. Garoufalidis and C. Koutschan. "Irreducibility of $q$-difference operators and the knot $7_4$". In: *Algebraic & Geometric Topology* 13 (2013), pp. 3261–3286. arXiv: 1211.6020.

[KJJ] M. Kauers, M. Jaroschek, and F. Johansson. "Ore polynomials in Sage". In: (2013). arXiv: 1306.4263.

[LT] T. T. Q. Lê and A. T. Tran. "On the AJ conjecture for knots". In: *Indiana University Mathematics Journal* 64.4 (2015), pp. 1103–1151. DOI: 10.1512/iumj.2015.64.5602. arXiv: 1111.5258.

[BS] Y. Berest and P. Samuelson. "Double affine Hecke algebras and generalized Jones polynomials". In: *Compositio Mathematica* 152 (2016), pp. 1333–1384. DOI: 10.1112/S0010437X16007314. arXiv: 1402.6032.

[GLb] S. Garoufalidis and T. T. Q. Lê. "A survey of $q$-holonomic functions". In: *L'Enseignement Mathématique* 62.3–4 (2016), pp. 501–525. DOI: 10.4171/LEM/62-3/4-7. arXiv: 1601.07487.

[LZ] T. T. Q. Lê and X. Zhang. "Character varieties, $A$-polynomials and the AJ conjecture". In: *Algebraic & Geometric Topology* 17 (2017), pp. 157–188. DOI: 10.2140/agt.2017.17.157.

[HL] M. Hajij and J. Levitt. *An Efficient Algorithm to Compute the Colored Jones Polynomial*. 2018. arXiv: 1804.07910. URL: https://arxiv.org/abs/1804.07910.

[LLS] J. Li, Y. Li, and H.-Y. Sun. *Whitehead doubles and the failure of the AJ conjecture*. 2026. arXiv: 2611.24826 [math.GT].

[Z] X. Zhang. *The AJ conjecture and connected sums of torus knots*. 2026. arXiv: 2603.10235 [math.GT]. URL: https://arxiv.org/abs/2603.10235.

[C] M. Culler. *A-polynomials for knots in Rolfsen's table*. URL: https://homepages.math.uic.edu/~culler/Apolynomials/crossing1by1.html (visited on 10/27/2026).

[KA] Knot Atlas. *MorseLink Presentations*. URL: https://katlas.org/index.php?title=MorseLink_Presentations&oldid=1688828 (visited on 10/27/2026).

[K] C. Koutschan. *HolonomicFunctions: A Mathematica package for dealing with multivariate holonomic functions*. Research Institute for Symbolic Computation, Johannes Kepler University. URL: https://www1.risc.jku.at/sw/holonomicfunctions/ (visited on 11/02/2026).

[LM] C. Livingston and A. H. Moore. *KnotInfo: Table of Knot Invariants*. URL: https://knotinfo.org/ (visited on 10/27/2026).

[Mb] Maplesoft. *Overview of the OreTools Package*. URL: https://www.maplesoft.com/support/help/Maple/view.aspx?path=OreTools (visited on 11/02/2026).